Clinical Pharmacokinetics

Comprehensive parent-metabolite PBPK/PD modeling insights into nicotine replacement therapy strategies

Electronic Supplementary Material

Lukas Kovar[1], Dominik Selzer[1], Hannah Britz[1], Neal Benowitz[2], Gideon St.Helen[2], Yvonne Kohl[3], Robert Bals[4] and Thorsten Lehr[1]

[1] Clinical Pharmacy, Saarland University, Saarbrücken, Germany
[2] Department of Medicine, University of California, San Francisco, CA, USA
[3] Fraunhofer Institute for Biomedical Engineering IBMT, Sulzbach, Germany
[4] Department of Internal Medicine V, Saarland University, Homburg, Germany

Running Heading

A PBPK/PD model of nicotine including brain concentration patterns during smoking and smoking cessation strategies.

Funding

This project has received funding from the German Federal Ministry of Education and Research (BMBF), 031L0153, «Alternativmethoden zum Tierversuch» and 03XP0196, «NanoCare4.0 – Anwendungssichere Materialinnovationen». Data used for model development were collected in part with the support of grants DA039264 and DA012393 from the National Institute on Drug Abuse, U.S.A.

Conflict of Interest

Neal Benowitz has been a consultant to Pfizer and Achieve Life Sciences, companies that market or are developing smoking cessation medications. He has also been a paid witness in litigation against tobacco companies. No potential conflicts of interest were disclosed by the other authors (Lukas Kovar, Dominik Selzer, Hannah Britz, Gideon St.Helen, Yvonne Kohl, Robert Bals and Thorsten Lehr).

Corresponding Author

Prof. Dr. Thorsten Lehr
Clinical Pharmacy, Saarland University, Campus C2 2, 66123 Saarbrücken.
Phone: +49 681 302 70255
Fax: +49 681 302 70258
Email: thorsten.lehr@mx.uni-saarland.de

Contents

1 PBPK/PD model development

In this study, a physiologically based pharmacokinetic/pharmacodynamic (PBPK/PD) parent-metabolite model of nicotine and cotinine was developed. 90 reported observed plasma concentration-time profiles after intravenous (iv), oral, transdermal and pulmonary administration, a brain tissue concentration-time profile and 11 heart rate profiles were digitized from 34 clinical studies and split into an internal training and an external test dataset.

The training dataset was selected in a way to inform all the physiological processes implemented in the model. Hence, for cotinine PBPK model building three plasma profiles of cotinine administered intravenously were used which covered a broad dosing range and included information on urinary excretion of cotinine. For the nicotine PBPK model building plasma profiles of nonsmokers and smokers after intravenous administration were included in the training dataset with a broad dosing range including studies with cotinine metabolite data, information on fraction of nicotine excreted unchanged to urine and fraction of nicotine metabolized to cotinine. Moreover, a study with plasma concentrations of cytochrome P450 (CYP) 2A6 poor metabolizer (PM) and a study with brain tissue concentrations after nicotine intake were included in the training dataset in order to inform model input parameters for CYP2B6 and brain transporters.
For the PD heart rate model, three studies with intravenous administration were used for model training which covered the largest timeframe of heart rate measurements and the highest nicotine plasma concentrations.

A tabular overview of all clinical studies and the division into test and training datasets are shown in Tables S2.6.1 to S2.6.3.

2 PBPK/PD model building

2.1 General PBPK model building

Drug-specific model input parameters for nicotine and cotinine were obtained from published *in vitro* and human phramacokinetic (PK) data (see Table S2.7.1). Cotinine and nicotine model input parameters which could not be adequately informed from literature were estimated using the *parameter identification* function in PK-Sim®.

Parameter estimation was performed by

1. fitting the cotinine model to
    - cotinine observed intraveneous data
    - published fractions of cotinine dose excreted unchanged to urine
2. fitting the nicotine model to
    - nicotine and cotinine observed intraveneous data
    - nicotine and cotinine observed oral data
    - nicotine brain tissue concentrations after pulmonary nicotine intake
    - published fractions of nicotine dose excreted unchanged to urine
    - published fraction of nicotine dose metabolized to cotinine [1]

of the training dataset with the Monte Carlo algorithm.

For the simulation of different studies, the reported mean values for age, weight, height and ethnic and genetic background of each study protocol were used to create representative virtual individuals. If no information on these demographics was available, a standard 30-year-old male European was assumed with weight and height values according to the PK-Sim® database. Distribution and elimination processes including CYP enzymes and transporters were implemented according to literature [1–3]. The nicotine model incorporates (1) metabolism of nicotine to its major metabolite cotinine via two CYP enzymes, (2) unspecific metabolic hepatic clearance (responsible for the remaining hepatic metabolism of nicotine including metabolism via UGT2B10 (uridine 5'-diphosphoglucuronosyltransferase 2B10) and FMO3 (flavin-containing monooxygenase 3)) and (3) influx and efflux transport of nicotine over the blood-brain-barrier (BBB). For cotinine, an unspecific metabolic hepatic clearance was implemented in the model. Additionally, renal excretion through glomerular filtration was implemented as an elimination pathway for both compounds, as they are subject to glomerular filtration under physiological conditions [2, 4].

To model the metabolic clearance of nicotine to cotinine, which accounts for about three quarters of nicotine elimination, nicotine metabolism via CYP2A6 and CYP2B6 was implemented in accordance with literature [1, 2]. Nicotine is primarily metabolized via CYP2A6. However, in CYP2A6-PM that lack CYP2A6 metabolism, and thus cotinine production diminishes, CYP2B6 is responsible for a modest nicotine conversion to cotinine [2]. A PM plasma-concentration time profile was included in the training dataset to estimate CYP2B6 metabolism in the model [5]. Relative CYP enzyme expression in different organs of the body was implemented using PK-Sim® expression database reverse transcription-polymerase chain reaction profile (CYP2A6) [6] and protein tissue data from the ProteomicsDB database (CYP2B6) [7].

The Michaelis-Menten constant (K_m) value for CYP2A6 was fitted with bounds obtained from literature [8–11]. According to published data, nicotine clearance in smokers is about 15 % lower compared to nonsmokers [12]. To account for this difference, the catalytic rate constant (k_{cat}) of CYP2A6 was estimated seperately for the smoker subpopulation leading to a lower k_{cat} in comparison to the nonsmoker subpopulation. Since PM show no CYP2A6 activity, k_{cat} for PM was set to 0 [5]. Moreover, since nicotine is metabolized not solely to cotinine, an unspecific first-order hepatic clearance was implemented and was fitted during parameter optimization.

As published literature suggests, influx and efflux of nicotine over the BBB play an important role for nicotine brain tissue concentration kinetics [3]. Hence, an influx and an efflux transporter with nicotine specific transport and Michaelis-Menten kinetics were added to the BBB in PK-Sim®. The k_{cat} value for the BBB nicotine influx transporter and K_m and k_{cat} values for the BBB efflux transporter were fitted to nicotine brain tissue concentrations from literature [13], the K_m value for the BBB influx transporter was obtained from literature [3]. Subsequently, this implementation yielded to a reasonable description of experimental nicotine brain tissue concentrations (see Figures S3.5.1r and S3.5.2r). A summary of all drug-dependent PBPK model parameters is shown in Table S2.7.1.

2.2 Nicotine gum PBPK model building

To model and simulate nicotine gum consumption, nicotine was administered via the oral route in PK-Sim®. The corresponding nicotine release from the gum was implemented according to an empirical release function (PK-Sim® table release) based on published *in vitro* release profile data of Nicorette® chewing gum [14]. Although bucal absorption was neglected, predictions of plasma concentration-time profiles showed very promising results (see Figures S3.3.1j to S3.3.1t and Figures S3.3.2j to S3.3.2t).

2.3 Transdermal patch PBPK model building

The modeling and simulation of the administration of nicotine via transdermal therapeutic systems (TTS) was implemented via a two-compartment skin model. Here, the skin is divided into the lipophilic *stratum corneum* (SC) and hydrophilic deeper skin layers (DSL) which are composed of the *viable Epidermis* and *Dermis*. As shown before, a two-compartment skin model is typically a sufficiently accurate description for the transport of various compounds if the storage capacity and/or the permeability of the SC and DSL compartments should be taken into account [15–17].

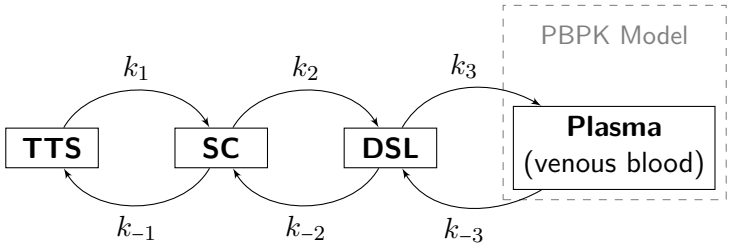

Figure S2.3.1: Schematic depiction of the nicotine transdermal absorption model.

Since detailed information about TTS composition is typically scarce it was assumed that the transdermal patch could be described as a homogenous matrix system. A schematic representation of the transdermal absorption model is depicted in Figure S2.3.1. Diffusion is considered the main driving force of substance transport through the skin. Thus, the mass flux between the compartments was modeled via first-order kinetics (Equations S1 to S3). The transdermal model was implemented in MoBi® and subsequently connected to the PBPK model.

$$\frac{\mathrm{d}m_{TTS}}{\mathrm{d}t} = k_{-1} \cdot m_{SC} - k_1 \cdot m_{TTS} \tag{S1}$$

$$\frac{\mathrm{d}m_{SC}}{\mathrm{d}t} = k_1 \cdot m_{TTS} - k_{-1} \cdot m_{SC} + k_{-2} \cdot m_{DSL} - k_2 \cdot m_{SC} \tag{S2}$$

$$\frac{\mathrm{d}m_{DSL}}{\mathrm{d}t} = k_2 \cdot m_{SC} - k_{-2} \cdot m_{DSL} + k_{-3} \cdot m_{Plasma} - k_3 \cdot m_{DSL} \tag{S3}$$

Simulations for plasma concentration-time profiles after TTS application of nicotine are shown in Figure S3.4.1 and Figure S3.4.2. Estimated transfer parameters are summarized in Table S2.8.3.

2.4 Pulmonary PBPK model building

Inhalation of combustible cigarettes and electronical cigarettes (e-cigarettes) was modeled as zero-order pulmonary administration kinetics since overall specific activity in mainstream smoke was shown to be constant from puff to puff in a radioisotopically labelled tobacco constituents study [18]. The rate of nicotine delivery equals the nicotine dose administered divided by the number of puffs and the puff duration. If the number of puffs and the puff duration were not provided, the delivery rate was set equal to the nicotine dose administered divided by the smoking period. The intracellular subcompartment of the lung was selected as target compartment in PK-Sim®.

Studies on inhalation of combustible cigarettes typically state nicotine doses derived from machine smoked yields of the investigated brand or type of cigarette. However, machine smoked yields of combustible cigarettes are typically not equivalent to human nicotine uptake for the products under investigation since they do not adequately represent human smoking behavior leading to a false

representation of the actual amount of nicotine reaching systemic circulation [19]. To overcome this issue two sets of simulations were performed:

- The application of combustible cigarettes was simulated with the stated cigarette nicotine yield provided by the study protocol (Figure S3.6.1 and Figure S3.6.2).
- The actual pulmonary nicotine exposure with combustible cigarettes was estimated (Table S2.8.2) while fixing all other model parameters (Figure S3.5.1 and Figure S3.5.2). This was executed for all studies with combustible cigarettes where venous blood plasma concentrations were reported.

The mean deviation of estimated pulmonary nicotine exposure to machine smoked nicotine yields was 31 % (see Table S2.8.2). For simulation of plasma concentration-time profiles for e-cigarettes, nicotine doses as stated in the respective study were used. For combustible cigarettes and e-cigarettes, 100 % of the administered dose was assumed to reach the lung compartment since bioavailability of nicotine after smoking is reported to be very high [2].

2.5 PBPK/PD model building

A PD model was added to the PBPK model to be able to describe the positive chronotropic effect of nicotine [20, 21] based on its PK. Direct-effect E_{max} models implemented as relative (proportional to heart rate baseline) and absolute effect with and without tolerance development were used to describe the effect. The model, which best described heart rate including drug effect, was the direct-effect E_{max} model with absolute effect including a tolerance development based on a recently published heart rate tolerance model [22]. This model had been developed to characterize the decrease in heart rate by the selective $S1P_1$ receptor modulator ponesimod.

Here, placebo data had been utilized to characterize heart rate changes during the course of the day due to circadian rhythm in the absence of a drug before the direct-effect I_{max} model with tolerance development was added. However, in contrast to the drug ponesimod, nicotine does not decrease but increases heart rate via activation of nicotine receptors. Therefore, the I_{max} effect was changed to an E_{max} effect and the PD model for heart rate (HR) was defined as

$$circ = amp \cdot \cos\left(\frac{2\pi}{24} \cdot (t - shift)\right) \tag{S4}$$

$$E = \frac{E_{max} \cdot c^h}{EC_{50}^h + c^h} \tag{S5}$$

$$tol = 1 + \frac{A_{tol}^\gamma}{tol_{50}^\gamma} \tag{S6}$$

$$\frac{\mathrm{d}A_{tol}}{\mathrm{d}t} = tol_{in} \cdot c - tol_{out} \cdot A_{tol} \tag{S7}$$

$$\alpha_{total} = \frac{E}{tol} \tag{S8}$$

$$HR = HR_{baseline}(1 + circ) + \alpha_{total} \tag{S9}$$

where $circ$ is a circadian function with a 24-h period, t is the time, amp denotes the daily heart rate variation as percentage of the estimated baseline heart rate ($HR_{baseline}$) and $shift$ represents the time from dosing until time of the maximum daily heart rate. tol_{in} and tol_{out} are first-order rate constants describing appearance and disappearance of tolerance in a tolerance compartment (A_{tol}), c is the concentration of nicotine in the peripheral venous blood plasma, E_{max} the maximum positive

chronotropic effect of nicotine without tolerance, h the hill coefficient and EC_{50} the concentration required to achieve half of the maximum drug effect. tol_{50} and γ represent scaling parameters describing the relationship between the tolerance compartment and the overall tolerance (tol) influencing the drug effect and leading to a total effect α_{total}.

The tolerance compartment was implemented to describe the extent of acute tolerance development of the system and its subsequent reduction of the drug effect on heart rate following the administration of nicotine. The appearance of tolerance was set to depend on the concentration of nicotine which has been shown in the literature [23]. To obtain values for the PD model input parameters, optimization was performed by fitting the PD model to heart rate data of the training dataset using the *parameter identification* function with the Monte Carlo algorithm in MoBi® while fixing the parameters of the PK model. The circadian amplitude (amp) was provided by the published tolerance model [22]. Circadian shift time for each study was fitted if no dosing information with regards to daytime was available. Otherwise, the circadian shift was calculated using the time of dosing and the time for maximum heart rate. Time of peak heart rate was gathered from the published tolerance model and set to 5:42 PM – a value that is in good agreement with data published before [24, 25]. For studies which lack data on absolute heart rate values, published mean heart rate data was added to heart rate changes from baseline [26]. Figure 1 in the main manuscript shows a structural overview of the developed PBPK/PD model. The parameter set for the PD model is summarized in Table S2.9.1 and simulated heart rate profiles after the administration of nicotine in comparison to observed data is depicted in Figure S3.11.1.

2.6 Clinical study data

2.6.1 Clinical study data of nicotine used for PBPK model building and evaluation

Table S2.6.1: Clinical study data of nicotine used for PBPK model building and evaluation.

			Dose		Subjects					
Study	**Route**	**Dataset**	**[mg]**	**[µg/kg]**	**N**	**Smokers [%]**	**Females [%]**	**Age [y]**	**Weight [kg]**	**Cotinine metabolite**
Andersson and Arner 2001 [27]	iv (30 min, s.d.)	e		15.0	11	0.0	0.0	(20–32)	-	no
Benowitz and Jacob 1993 (1) [12]	iv (30 min, s.d.)	i		15.0	11	0.0	18.2	34.0 (22–58)	-	yes
Benowitz and Jacob 1993 (2) [12]	iv (30 min, s.d.)	i		15.0	11	100.0	18.2	33.0 (22–51)	-	yes
Benowitz and Jacob 1993 (3) [12]	iv (30 min, s.d.)	e		60.0	11	100.0	18.2	33.0 (22–51)	-	yes
Benowitz and Jacob 1994a (1)[a] [1]	iv (30 min, s.d.)	e	4.2	60.0	20	100.0	50.0	36.0 (23–51)	70.5 (53.0–100.4)	yes
Benowitz et al. 1991a (1) [28]	iv (24 h, s.d.)	i	19.8		14	100.0	0.0	39.0 (27–64)	72.8 (56.2–103.9)	yes
Benowitz et al. 1994b [29]	iv (24 h, s.d.)	i		288.0	12	100.0	0.0	34.0 (20–55)	76.4 (60.0–96.9)	yes
Feyerabend et al. 1985 (1) [30]	iv (1 min, s.d.)	i	1.8	25.0	5	100.0	0.0	(24–41)	69.3	no
Gourlay and Benowitz 1997 (1) [31]	iv (30 min, s.d.)	e	5.1	60.0	12	100.0	0.0	38.0	-	yes
Molander et al. 2001 (young) [32]	iv (10 min, s.d.)	e		28.0	20	100.0	50.0	(22–43)	-	yes
Molander et al. 2001 (elderly) [32]	iv (10 min, s.d.)	e		28.0	20	100.0	60.0	(65–76)	-	yes
Porchet et al. 1988 (1)[b] [23]	iv (30 min, m.d.)	e		75.0	8	100.0	0.0	36.0 (22–43)	-	no
Porchet et al. 1988 (2)[c] [23]	iv (30 min, m.d.)	e		75.0	8	100.0	0.0	36.0 (22–43)	-	no
Porchet et al. 1988 (3)[d] [23]	iv (30 min, m.d.)	e		75.0	8	100.0	0.0	36.0 (22–43)	-	no
Zevin et al. 1997 (1)[e] [33]	iv (30 min, s.d.)	i		15.0	12	0.0	50.0	33.0 (18–47)	73.0	no
Zevin et al. 1997 (2)[f] [33]	iv (30 min, s.d.)	e		15.0	12	0.0	50.0	33.0 (18–47)	73.0	no
Benowitz et al. 1991b (1) [34]	po (cap, s.d.)	i	3.0		7	100.0	0.0	(24–48)	77.1 (68.1–89.9)	no
Benowitz et al. 1991b (2) [34]	po (cap, s.d.)	e	4.0		2	100.0	0.0	(24–48)	-	no
Benowitz et al. 1991b (3) [34]	po (cap, s.d.)	e	6.0		1	100.0	0.0	(24–48)	-	no
Benowitz et al. 2010 [35]	po (-, q.i.d., 5 days)	e	0.05		12	0.0	50.0	32.6 (20–61)	-	yes
Green et al. 1999 (1) [36]	po (cap, s.d.)	i	6.0		12	0.0	41.7	28.0 (21–33)	73.0 (57.0–96.0)	yes
Green et al. 1999 (2) [36]	po (cap, s.d.)	e	15.0		12	0.0	41.7	28.0 (21–33)	73.0 (57.0–96.0)	yes
Jarvis et al. 1988 [37]	po (cap, 7 times/day, 5 days)	e	4.0		1	0.0	-	(27–54)	-	yes
Xu et al. 2002 (NM) [5]	po (cap, s.d.)	i	4.0		6	7.1	64.3	-	-	yes
Xu et al. 2002 (PM) [5]	po (cap, s.d.)	i	4.0		3	7.1	64.3	-	-	yes
Benowitz et al. 1988 (1) [21]	gum (s.d.)	e	4.0		10	100.0	0.0	(24–61)	-	no
Choi et al. 2003 (1) [38]	gum (s.d.)	e	2.0		25	100.0	52.0	33.7	-	no
Choi et al. 2003 (2) [38]	gum (13 gums, m.d.)	e	2.0		24	100.0	53.8	29.0	-	no
Choi et al. 2003 (3) [38]	gum (s.d.)	e	4.0		20	100.0	50.0	31.0	-	no
Choi et al. 2003 (4) [38]	gum (13 gums, m.d.)	e	4.0		26	100.0	53.8	29.0	-	no
Dautzenberg et al. 2007 [39]	gum (12 gums, m.d.)	e	2.0		24	100.0	0	-	-	no
Du 2018 (1) [40]	gum (s.d.)	e	2.0		62	100.0	47.6	26.8 (19–51)	-	no
Du 2018 (2) [40]	gum (s.d.)	e	4.0		73	100.0	47.6	26.8 (19–51)	-	no
Hansson et al. 2017 (1) [41]	gum (s.d.)	e	2.0		42	100.0	43.2	28.4 (19–49)	-	no
Hansson et al. 2017 (2) [41]	gum (s.d.)	e	4.0		40	100.0	43.2	28.4 (19–49)	-	no

values for age and weight are given as mean (range)

-, not given; **cap**, capsule; **cigs.**, cigarettes; **combust.**, combustible; **e**, external test dataset; **e-cigs**, e-cigarettes; **i**, internal training dataset; **iv**, intravenous; **m.d.**, multiple dose; **N**, number of individuals studied; **NM**, normal metabolizer; **PM**, poor metabolizer; **po**, oral; **q.i.d.**, four times daily; **q.d.**, once daily; **s.d.**, single dose

[a] fraction of nicotine dose metabolized to cotinine depicted [b] two nicotine iv infusions 90 minutes separated [c] two nicotine iv infusions 150 minutes separated [d] two nicotine iv infusions 240 minutes separated [e] nicotine iv and placebo po administered concurrently [f] nicotine iv and cotinine po administered concurrently [g] loading dose of the nicotine patch [h] six patches over seven days with no patch on day two

Table S2.6.1: Clinical study data of nicotine used for PBPK model building and evaluation. *(continued)*

Study	Route	Dataset	Dose		Subjects					Cotinine metabolite
			[mg]	[µg/kg]	N	Smokers [%]	Females [%]	Age [y]	Weight [kg]	
Hansson et al. 2017 (3) [41]	gum (12 gums, m.d.)	e	4.0		33	100.0	50.0	30.0 (19–50)	-	no
Bannon et al. 1989 (1) [42]	transdermal (24 h, s.d.)	e	15.0[g]		9	100.0	-	24.6	-	no
Bannon et al. 1989 (2) [42]	transdermal (24 h, s.d.)	i	30.0[g]		9	100.0	-	24.6	-	no
Bannon et al. 1989 (3) [42]	transdermal (24 h, q.d., 7 days)	e	30.0[g]		9	100.0	-	28.3	-	no
Bannon et al. 1989 (4) [42]	transdermal (24 h, s.d.)	e	60.0[g]		9	100.0	-	24.6	-	no
Benowitz et al. 1991a (2) [28]	transdermal (24 h, s.d.)	i	52.5[g]		11	100.0	0.0	39.0 (27–64)	72.8 (56.2–103.9)	no
Fant et al. 2000 (Alza) [43]	transdermal (24 h, q.d., 3 days)	i	114.0[g]		25	100.0	36.0	25.8	73.3	no
Fant et al. 2000 (Novartis) [43]	transdermal (24 h, q.d., 3 days)	i	52.5[g]		25	100.0	36.0	25.8	73.3	no
Fant et al. 2000 (Upjohn) [43]	transdermal (16 h, q.d., 3 days)	i	24.9[g]		25	100.0	36.0	25.8	73.3	no
Gupta et al. 1993 (1) [44]	transdermal (24 h, s.d.)	i	105.0[g]		12	100.0	0.0	34.0 (20–55)	76.4 (60.0–96.9)	yes
Gupta et al. 1993 (2) [44]	transdermal (24 h, q.d., 7 days)[h]	e	105.0[g]		12	100.0	0.0	34.0 (20–55)	76.4 (60.0–96.9)	yes
Armitage et al. 1975 [45]	inhalation (combust. cigs., s.d.)	e	2.1		8	100.0	0.0	(29–51)	-	no
Benowitz et al. 1988 (2) [21]	inhalation (combust. cigs., s.d.)	e	1.5		10	100.0	0.0	(24–61)	-	no
Benowitz et al. 1982 (1) [46]	inhalation (30 combust. cigs., m.d.)	e	0.4		12	100.0	42.0	38.8 (21–63)	-	no
Benowitz et al. 1982 (2) [46]	inhalation (30 combust. cigs., m.d.)	e	1.2		12	100.0	42.0	38.8 (21–63)	-	no
Benowitz et al. 1982 (3) [46]	inhalation (30 combust. cigs., m.d.)	e	2.5		12	100.0	42.0	38.8 (21–63)	-	no
Fearon et al. 2017 (Study 1) [47]	inhalation (combust. cigs., s.d.)	e	1.0		24	100.0	29.2	34.0 (24–51)	76.4 (46.2–107.5)	no
Fearon et al. 2017 (Study 2) [47]	inhalation (combust. cigs., s.d.)	e	0.5		18	100.0	33.3	33.5 (24–54)	76.3 (49.0–95.5)	no
Feyerabend et al. 1985 (2) [30]	iv and inhalation (1 min, m.d. plus 6 combust. cigs.)	e	1.8; 1.3		5	100.0	0.0	(24–41)	69.3 (62.0–80.2)	no
Feyerabend et al. 1985 (3) [30]	inhalation (13 combust. cigs., m.d.)	e	0.8		1	100.0	0.0	(24–41)	71.2	no
Feyerabend et al. 1985 (4) [30]	inhalation (21 combust. cigs., m.d.)	e	1.3		1	100.0	0.0	(24–41)	71.0	no
Feyerabend et al. 1985 (5) [30]	inhalation (13 combust. cigs., m.d.)	e	2.4		1	100.0	0.0	(24–41)	71.2	no
Gourlay and Benowitz 1997 (2) [31]	inhalation (combust. cigs., s.d.)	e	1.9		6	100.0	0.0	38.0	85.0	no
Mendelson et al. 2008 [48]	inhalation (3 combust. cigs., m.d.)	e	0.8		12	100.0	0.0	25.7	-	no
Rose et al. 2010 [13]	inhalation (combust. cigs., s.d.)	i	0.1		13	100.0	30.8	41.0	89.0	no
Russell et al. 1983 [49]	inhalation (combust. cigs., s.d.)	e	1.4		3	33.0	0.0	(30–50)	-	no
St. Helen et al. 2016 [50]	inhalation (e-cigs., s.d.)	e	1.2		13	100.0	46.2	38.4 (19–58)	-	no
St. Helen et al. 2019 (1) [51]	inhalation (e-cigs., s.d.)	e	0.9		33	100.0	22.2	35.4 (25–41.5)	-	no
St. Helen et al. 2019 (2) [51]	inhalation (combust. cigs., s.d.)	e	-		33	100.0	22.2	35.4 (25–41.5)	-	no
Brain tissue concentration simulation (gum, 2 mg)	gum (16 gums, m.d.)	-	2.0		100	100.0	0.0	30.0 (20–40)	80.4 (70.4–90.4)	-
Brain tissue concentration simulation (gum, 4 mg)	gum (16 gums, m.d.)	-	4.0		100	100.0	0.0	30.0 (20–40)	80.4 (70.4–90.4)	-
Brain tissue concentration simulation (pulmonary)	inhalation (16 cigs., m.d.)	-	1.4		100	100.0	0.0	30.0 (20–40)	80.4 (70.4–90.4)	-
Brain tissue concentration simulation (transdermal)	transdermal (24 h, s.d.)	-	52.5[g]		100	100.0	0.0	30.0 (20–40)	80.4 (70.4–90.4)	-

values for age and weight are given as mean (range)

-, not given; **cap**, capsule; **cigs.**, cigarettes; **combust.**, combustible; **e**, external test dataset; **e-cigs**, e-cigarettes; **i**, internal training dataset; **iv**, intravenous; **m.d.**, multiple dose; **N**, number of individuals studied; **NM**, normal metabolizer; **PM**, poor metabolizer; **po**, oral; **q.i.d.**, four times daily; **q.d.**, once daily; **s.d.**, single dose

[a] fraction of nicotine dose metabolized to cotinine depicted [b] two nicotine iv infusions 90 minutes separated [c] two nicotine iv infusions 150 minutes separated [d] two nicotine iv infusions 240 minutes separated [e] nicotine iv and placebo po administered concurrently [f] nicotine iv and cotinine po administered concurrently [g] loading dose of the nicotine patch [h] six patches over seven days with no patch on day two

2.6.2 Clinical study data of cotinine used for PBPK model building and evaluation

Table S2.6.2: Clinical study data of cotinine used for PBPK model building and evaluation.

			Dose		Subjects				
Study	**Route**	**Dataset**	**[mg]**	**[µg/kg]**	**N**	**Smokers [%]**	**Females [%]**	**Age [y]**	**Weight [kg]**
Benowitz and Jacob 1994a (2) [1]	iv (30 min, s.d.)	e	4.4	60.0	6	0.0	50.0	37.0 (27–39)	73.2 (58–94)
De Schepper et al. 1987 (1) [4]	iv (30 min, s.d.)	i	5.0		4	0.0	0.0	(22–24)	(64–73)
De Schepper et al. 1987 (2) [4]	iv (30 min, s.d.)	i	10.0		4	0.0	0.0	(22–24)	(64–73)
De Schepper et al. 1987 (3) [4]	iv (30 min, s.d.)	i	20.0		3	0.0	0.0	(22–24)	(64–73)
Curvall et al. 1990 (1) [52]	iv (1.5-3 min, s.d.)	e	5.0		7	0.0	22.2	31.6 (23–56)	72.2 (55–85)
Curvall et al. 1990 (2) [52]	iv (1.5-3 min, s.d.)	e	10.0		9	0.0	22.2	31.6 (23–56)	72.2 (55–85)
Curvall et al. 1990 (3) [52]	iv (1.5-3 min, s.d.)	e	20.0		9	0.0	22.2	31.6 (23–56)	72.2 (55–85)
Zevin et al. 1997 (3) [33]	iv (30 min, s.d.)	e		15.0	12	0.0	50.0	33.0 (18–47)	73.0
Zevin et al. 1997 (4) [33]	iv (30 min, s.d.)	e		15.0	12	0.0	50.0	33.0 (18–47)	73.0

values for age and weight are given as mean (range)

e, external test dataset; **i**, internal training dataset; **iv**, intravenous; **N**, number of individuals studied; **s.d.**, single dose

2.6.3 Clinical study data used for PD model building and evaluation

Table S2.6.3: Clinical study data of nicotine used for PD model building and evaluation.

			Dose		Subjects				
Study	**Route**	**Dataset**	**[mg]**	**[µg/kg]**	**N**	**Smokers [%]**	**Females [%]**	**Age [y]**	**Weight [kg]**
Andersson and Arner 2001 [27]	iv (30 min, s.d.)	e		15.0	11	0.0	0.0	(20–32)	-
Porchet et al. 1988 (1)[a] [23]	iv (30 min, m.d.)	i		75.0	8	100.0	0.0	36.0 (22–43)	-
Porchet et al. 1988 (2)[b] [23]	iv (30 min, m.d.)	i		75.0	8	100.0	0.0	36.0 (22–43)	-
Porchet et al. 1988 (3)[c] [23]	iv (30 min, m.d.)	i		75.0	8	100.0	0.0	36.0 (22–43)	-
Benowitz et al. 1988 (1) [21]	gum (s.d.)	e	4.0		10	100.0	0.0	(24–61)	-
Benowitz et al. 1988 (2) [21]	inhalation (combust. cigs., s.d.)	e	1.5		10	100.0	0.0	(24–61)	-
Gilbert et al. 1989 (1) [53]	inhalation (combust. cigs., s.d.)	e	0.1		40	50.0	50.0	28.8 (25–35)	-
Gilbert et al. 1989 (2) [53]	inhalation (combust. cigs., s.d.)	e	0.8		40	50.0	50.0	28.8 (25–35)	-
Gourlay and Benowitz 1997 (2) [31]	inhalation (combust. cigs., s.d.)	e	1.9		6	100.0	0.0	38.0	85.0
Mendelson et al. 2008 [48]	inhalation (3 combust. cigs., m.d.)	e	0.8		12	100.0	0.0	25.7	-
St. Helen et al. 2016 [50]	inhalation (e-cigs., s.d.)	e	1.2		13	100.0	46.1	38.4 (19–58)	-
Heart rate simulation (4 cigs.)	inhalation (4 cigs., m.d.)	-	1.4		100	100.0	0.0	30.0 (20–40)	80.4 (70.4 - 90.4)
Heart rate simulation (16 cigs.)	inhalation (16 cigs., m.d.)	-	1.4		100	100.0	0.0	30.0 (20–40)	80.4 (70.4 - 90.4)
Heart rate simulation (16 gums)	gum (16 gums, m.d.)	-	2.0		100	100.0	0.0	30.0 (20–40)	80.4 (70.4 - 90.4)
Heart rate simulation (transdermal)	transdermal (24 h, s.d.)	-	52.5[d]		100	100.0	0.0	30.0 (20–40)	80.4 (70.4 - 90.4)

values for age and weight are given as mean (range)

-, not given; **cigs.**, cigarettes; **combust.**, combustible; **e**, external test dataset; **i**, internal training dataset; **iv**, intravenous; **m.d.**, multiple dose; **N**, number of individuals studied; **s.d.**, single dose

[a] two nicotine iv infusions 90 minutes separated

[b] two nicotine iv infusions 150 minutes separated

[c] two nicotine iv infusions 240 minutes separated

[d] loading dose of the nicotine patch

2.7 Drug-dependent parameters of the final parent-metabolite nicotine-cotinine PBPK model

Table S2.7.1: Drug-dependent parameters of the final nicotine-cotinine PBPK model.

		Nicotine Model		Cotinine Model		
Parameter	**Unit**	**Value**	**Reference**	**Value**	**Reference**	**Description**
MW	g/mol	162.2	[54][a]	176.2	[54][b]	Molecular weight
pK_{a1}		8.1 (basic)	[55]	4.5 (basic)	[56]	Acid dissociation constant 1
pK_{a2}		3.3 (basic)	[55]			Acid dissociation constant 2
logP		1.6*	1.2, 1.4 [55, 57]	-0.1*	0.21 [54][b]	Lipophilicity
Solubility (pH)	mg/mL	93.3 (7.0)	[54][a]	117.0 (7.0)	[54][b]	Solubility
f_u	%	95.1	80.0-95.1 [58]	97.4	[59]	Fraction unbound (plasma)
CYP2A6 K_M	µmol/L	29.4*	11.0, 32.0, 33.0, 144.0 [8–11]			CYP2A6 Michaelis-Menten constant
CYP2A6-NM k_{cat} (nonsmokers)	1/min	12.0*	n.a.			CYP2A6-NM catalytic rate constant for nonsmokers
CYP2A6-NM k_{cat} (smokers)	1/min	10.5*	n.a.			CYP2A6-NM catalytic rate constant for smokers
CYP2A6-PM k_{cat}	1/min	0.0	[5]			CYP2A6-PM catalytic rate constant
CYP2B6 K_M	µmol/L	820.0	[60]			CYP2B6 Michaelis-Menten constant
CYP2B6 k_{cat}	1/min	16.0*	n.a.			CYP2B6 catalytic rate constant
BBB-transporter$_{in}$ K_M	µmol/L	92.4	[3]			BBB-transporter$_{in}$ Michaelis-Menten constant
BBB-transporter$_{in}$ k_{cat}	1/s	5.3E+03*	n.a.			BBB-transporter$_{in}$ catalytic rate constant
BBB-transporter$_{out}$ K_M	µmol/L	7.0E-05*	n.a.			BBB-transporter$_{out}$ Michaelis-Menten constant
BBB-transporter$_{out}$ k_{cat}	1/s	0.4*	n.a.			BBB-transporter$_{out}$ catalytic rate constant
Cell permeabilities		calculated	PK-Sim® Standard [61]	calculated	PK-Sim® Standard [61]	Permeation across cell membranes
Partition coefficients		calculated[c]	Rodgers and Rowland [62–64]	calculated[c]	PK-Sim® Standard [61]	Organ-plasma partition coefficients
GFR fraction		1.0		6.0E-02*		Fraction of GFR used for passive elimination by the kidney
Unspecific hepatic clearance	1/min	0.3*	n.a.	2.0E-02*	n.a.	Elimination from plasma (first order process in the liver)

BBB, blood-brain-barrier; **CYP**, cytochrome P450; **GFR**, glomerular filtration rate; **n.a.**, not available; **NM**, normal metabolizer; **PM**, poor metabolizer

* model input parameter estimated

[a] DrugBank entry for nicotine. https://www.drugbank.ca/drugs/DB00184. Accessed 21 Oct 2019

[b] DrugBank entry for cotinine. https://www.drugbank.ca/metabolites/DBMET00519. Accessed 21 Oct 2019

[c] for details see Table S2.7.2

Table S2.7.2: Tissue-plasma partition coefficients of the final nicotine-cotinine PBPK model.

Tissue	**Nicotine**[a]	**Cotinine**[b]
Bone	1.27	0.70
Brain	1.89	0.88
Fat	0.74	0.74
Gonads	3.27	0.82
Heart	2.24	0.81
Kidney	4.15	0.82
Stomach	2.90	0.84
Small intestine	2.90	0.84
Large intestine	2.90	0.84
Liver periportal	3.96	0.81
Liver pericentral	3.96	0.81
Lung	3.25	0.83
Muscle	3.05	0.83
Pancreas	2.46	0.77
Skin	2.10	0.72
Spleen	2.86	0.80

Partition coefficients between intracellular space and plasma

[a] Estimated via Rodgers and Rowland [62–64]

[b] Estimated via PK-Sim® Standard [61]

2.8 Formulation-dependent parameters of the final nicotine-cotinine PBPK model

Table S2.8.1: Formulation-dependent parameters of the final nicotine-cotinine PBPK model for oral application of nicotine.

	Dissolution				
Study	**t_{lag} [min]**	**50 % dissolved [min]**	**Shape**	**Tablet time delay factor**	**Description**
Benowitz et al. 1991b (1) [34]	10.5	22.0	1.9	0.2	capsule
Benowitz et al. 1991b (2) [34]	10.5	22.0	1.9	0.2	capsule
Benowitz et al. 1991b (3) [34]	10.5	22.0	1.9	0.2	capsule
Benowitz et al. 2010 [35]	-	-	-	-	oral solution
Green et al. 1999 (1) [36]	167.4	346.9	0.5	0.7	capsule
Green et al. 1999 (2) [36]	167.4	346.9	0.5	0.7	capsule
Jarvis et al. 1988 [37]	-	-	-	-	oral solution
Xu et al. 2002 (NM) [5]	5	59.6	1.8	0.2	capsule
Xu et al. 2002 (PM) [5]	5	59.6	1.8	0.2	capsule
Benowitz et al. 1988 (1) [21]	-	-	-	-	gum[a]
Choi et al. 2003 (1) [38]	-	-	-	-	gum[a]
Choi et al. 2003 (2) [38]	-	-	-	-	gum[a]
Choi et al. 2003 (3) [38]	-	-	-	-	gum[a]
Choi et al. 2003 (4) [38]	-	-	-	-	gum[a]
Du 2018 (1) [40]	-	-	-	-	gum[a]
Du 2018 (2) [40]	-	-	-	-	gum[a]
Dautzenberg et al. 2007 [39]	-	-	-	-	gum[a]
Hansson et al. 2017 (1) [41]	-	-	-	-	gum[a]
Hansson et al. 2017 (2) [41]	-	-	-	-	gum[a]
Hansson et al. 2017 (3) [41]	-	-	-	-	gum[a]
Brain tissue concentration simulation (gum, 2 mg)	-	-	-	-	gum[a]
Brain tissue concentration simulation (gum, 4 mg)	-	-	-	-	gum[a]
Heart rate simulation (gum, 2 mg)	-	-	-	-	gum[a]

NM, normal metabolizer; **PM**, poor metabolizer

[a] Release kinetics profile used from Morjaria et al. (PK-Sim® table release) [14]

Table S2.8.2: Reported machine smoked nicotine yield and estimated human pulmonary nicotine exposure of combustible cigarettes for studies under investigation.

Study	Exposure [mg]	
	Machine smoked nicotine yield	Estimated yield
Benowitz et al. 1982 (1) [46]	0.4	0.4
Fearon et al. 2017 (Study 2) [47]	0.5	0.7
Feyerabend et al. 1985 (3) [30]	0.8	1.1
Mendelson et al. 2008 [48]	0.8	1.2
Fearon et al. 2017 (Study 1) [47]	1.0	1.3
Benowitz et al. 1982 (2) [46]	1.2	1.4
Feyerabend et al. 1985 (4) [30]	1.3	1.5
Feyerabend et al. 1985 (2) [30]	1.3	2.0
Russell et al. 1983 [49]	1.4	2.2
Benowitz et al. 1988 (2) [21]	1.5	1.6
Gourlay and Benowitz 1997 (2) [31]	1.9	2.2
Feyerabend et al. 1985 (5) [30]	2.4	1.5
Benowitz et al. 1982 (3) [46]	2.5	1.8
St. Helen et al. 2019 (2)	-	2.4

-, not given

Table S2.8.3: Drug product-dependent and system-dependent parameters of the transdermal nicotine PBPK model.

Study	Loading dose [mg]	TTS/SC		SC/DSL		DSL/Plasma	
		k_1 [$\frac{1}{min}$]	k_{-1} [$\frac{1}{min}$]	k_2 [$\frac{1}{min}$]	k_{-2} [$\frac{1}{min}$]	k_3 [$\frac{1}{min}$]	k_{-3} [$\frac{1}{min}$]
Bannon et al. 1989 (1) [42]	15.00	8.63E-04	2.79E-03	1.93E+01	3.39E+00	9.63E-03	4.72E-03
Bannon et al. 1989 (2) [42]	30.00	8.63E-04	2.79E-03	1.93E+01	3.39E+00	9.63E-03	4.72E-03
Bannon et al. 1989 (3) (m.d.) [42]	30.00	8.63E-04	2.79E-03	1.93E+01	3.39E+00	9.63E-03	4.72E-03
Bannon et al. 1989 (4) [42]	60.00	8.63E-04	2.79E-03	1.93E+01	3.39E+00	9.63E-03	4.72E-03
Benowitz et al. 1991a (2) [28]	52.50	2.24E-04	8.35E-02	8.27E-01	1.18E-04	8.10E-03	1.64E-05
Fant et al. 2000 [43] (Upjohn, m.d.)	24.90	3.69E-01	4.60E+00	2.98E-02	8.57E-01	5.42E-01	1.85E+00
Fant et al. 2000 [43] (Novartis, m.d.)	52.50	1.11E-03	8.29E-03	5.00E-03	1.68E-02	3.46E+01	7.61E-01
Fant et al. 2000 [43] (Alza, m.d.)	114.00	1.57E-01	1.35E+01	2.24E+00	1.63E-01	3.60E-02	6.26E+01
Gupta et al. 1993 (1) [44]	105.05	9.83E-01	2.40E+01	1.17E-01	9.93E-01	8.24E-01	4.00E+01
Gupta et al. 1993 (2) (m.d.) [44]	105.05	9.83E-01	2.40E+01	1.17E-01	9.93E-01	8.24E-01	4.00E+01
Brain tissue concentration simulation (transdermal)	52.50	1.11E-03	8.29E-03	5.00E-03	1.68E-02	3.46E+01	7.61E-01
Heart rate simulation (transdermal)	52.50	1.11E-03	8.29E-03	5.00E-03	1.68E-02	3.46E+01	7.61E-01

k_1, first order rate constant for nicotine transport from nicotine patch into *stratum corneum*

k_{-1}, first order rate constant for nicotine transport from *stratum corneum* back into nicotine patch

k_2, first order rate constant for nicotine transport from *stratum corneum* into deeper skin layers

k_{-2}, first order rate constant for nicotine transport from deeper skin layers back into *stratum corneum*

k_3, first order rate constant for nicotine transport from deeper skin layers into plasma

k_{-3}, first order rate constant for nicotine transport from plasma back into deeper skin layers

DSL, deeper skin layers; **m.d.**, multiple dose; **SC**, stratum corneum; **TTS**, transdermal therapeutic system

2.9 Parameters of the final PD heart rate model

Table S2.9.1: Drug-dependent and system-dependent parameters of the final PD model.

Parameter	Unit	Value	Reference	Standard deviation	Description[a]
E_{max}	bpm	111.6	n.a.		Maximum possible heart rate elevation without tolerance
EC_{50}	ng/mL	33.7	n.a.		Concentration at half-maximum elevation
h		1.3	n.a.		Hill coefficient
tol_{in}	1/h	15.3	n.a.		Tolerance appearance rate
tol_{out}	1/h	0.2	n.a.		Tolerance disappearance rate
tol_{50}	ng/mL	11.7	n.a.		Scaling parameter for tolerance
γ		0.4	n.a.		Nonlinearity parameter
amp	%	6.3[c]	[22]		Circadian amplitude
$HR_{BL[27]}$	bpm	111.5	n.a.	10.0 [26]	Baseline heart rate for [27]
$HR_{BL[21](1)}$	bpm	65.2	n.a.	7.0 [26]	Baseline heart rate for [21] (1)
$HR_{BL[21](2)}$	bpm	64.7	n.a.	7.0 [26]	Baseline heart rate for [21] (2)
$HR_{BL[53](1)}$	bpm	73.6	n.a.	10.0 [26]	Baseline heart rate for [53] (1)
$HR_{BL[53](2)}$	bpm	78.5	n.a.	10.0 [26]	Baseline heart rate for [53] (2)
$HR_{BL[31]}$	bpm	81.6	n.a.	7.0 [26]	Baseline heart rate for [31]
$HR_{BL[48]}$	bpm	68.8	n.a.	10.0 [26]	Baseline heart rate for [48]
$HR_{BL[50]}$	bpm	72.2	n.a.	7.0 [26]	Baseline heart rate for [50]
$HR_{BL[23](1)}$	bpm	60.1	n.a.	7.0 [26]	Baseline heart rate for [23](1)
$HR_{BL[23](2)}$	bpm	60.1	n.a.	7.0 [26]	Baseline heart rate for [23](2)
$HR_{BL[23](3)}$	bpm	60.1	n.a.	7.0 [26]	Baseline heart rate for [23](3)
$HR_{BL,\ HR\ simulations}$	bpm	78.0	[26]	7.0 [26]	Baseline heart rate for HR simulations
$shift_{BL[27]}$	h	9.7	[22, 27][b]		Circadian time shift for [27]
$shift_{BL[21](1)}$	h	10.7	n.a.		Circadian time shift for [21] (1)
$shift_{BL[21](2)}$	h	10.7	n.a.		Circadian time shift for [21] (2)
$shift_{BL[53](1)}$	h	8.2	[22, 53][b]		Circadian time shift for [53] (1)
$shift_{BL[53](2)}$	h	8.2	[22, 53][b]		Circadian time shift for [53] (2)
$shift_{BL[31]}$	h	2.7	n.a.		Circadian time shift for [31]
$shift_{BL[48]}$	h	7.7	[22, 48][b]		Circadian time shift for [48]
$shift_{BL[50]}$	h	8.2	[22, 50][b]		Circadian time shift for [50]
$shift_{BL[23](1)}$	h	6.7	n.a.		Circadian time shift for [23] (1)
$shift_{BL[23](2)}$	h	6.7	n.a.		Circadian time shift for [23] (2)
$shift_{BL[23](3)}$	h	6.7	n.a.		Circadian time shift for [23] (3)

n.a., not available

[a] Descriptions carried over from [22]

[b] Computed

[c] amp was set to 0 for HR simulations in Section 3.12 for better comparability

2.10 System-dependent parameters and virtual populations

System-dependent parameters for the PBPK/PD model, including reference concentrations with geometric standard deviation, tissue expression as well as protein half-lives of all enzymes and transporters implemented in the model are summarized in Table S2.10.1.

Table S2.10.1: System-dependent parameters and expression of relevant enzymes, transporters and other ADME processes.

	Reference concentration			Half-live [h]	
	Mean [µmol/L][a]	GSD[b]	Relative expression	Liver	Intestine
Enzymes					
CYP2A6-NM	2.72 [65]	1.40	RT-PCR[c] [66]	26.0	23.0
CYP2A6-PM	2.72 [65]	1.40	RT-PCR[c] [66]	26.0	23.0
CYP2B6	1.56 [65]	1.40	ProteomicsDB[d] [7]	32.0	23.0
Transporters					
BBB-transporter$_{in}$	1.00[e] [6]	1.40		36.0	23.0
BBB-transporter$_{out}$	1.00[e] [6]	1.40		36.0	23.0
Processes					
Unspecific hepatic clearance of nicotine	-	1.40			
Unspecific hepatic clearance of cotinine	-	1.40			

ADME, absorption, distribution, metabolism and elimination; **CYP**, cytochrome P450; **GSD**, Geometric standard deviation; **NM**, normal metabolizer; **PM**, poor metabolizer; **RT-PCR**, reverse transcription polymerase chain reaction

[a] In the tissue of the highest expression

[b] Geometric standard deviation with coefficient of variation (CV) of 35 % assumed

[c] PK-Sim® expression database profile

[d] ProteomicsDB entry for CYP2B6. https://www.proteomicsdb.org/proteomicsdb/#human/proteinDetails/P20813/expression. Accessed 21 Oct 2019

[e] If no information available it was set to 1.0 µmol/L and k_{cat} optimized according to [6]

Virtual populations of 100 individuals for each study were set up according to the population demographics of each respective simulated study. If no age range was specified, virtual populations were created with individuals 20 to 50 years of age and without specific body weight or height restrictions as implemented in PK-Sim®.

In the generated virtual populations demographics such as age, height, weight and corresponding organ volumes, tissue compositions, blood flow rates, etc. were varied by an implemented algorithm in PK-Sim® within the limits of the ICRP (International Commission on Radiological Protection) or Japanese databases [61, 67]. Furthermore, the reference concentrations of both the metabolizing enzymes CYP2A6 and CYP2B6 and the nicotine transporters in the BBB as well as unspecific hepatic clearance rates of nicotine and cotinine were set to be log-normally distributed with a relative standard deviation of 35 %. Heart rate was set to be normally distributed with variabilities according to Umetani et al. [26]. For details on study populations see Tables S2.6.1 to S2.6.3. Simulations were generated with the virtual populations with geometric mean ± geometric standard deviation and plotted with the corresponding observed data (see Section 3).

3 PBPK/PD model evaluation

The descriptive (internal training dataset) and predictive (external test dataset) performance of the PBPK/PD model is comprehensively demonstrated: Linear and semilogarithmic plots of population predictions are compared to observed plasma concentration-time profiles, fractions excreted to urine, brain tissue concentrations (Sections 3.1 to 3.6) and heart rate profiles (Section 3.11). Moreover, goodness-of-fit plots comparing predicted to observed plasma concentrations are shown in Figures S3.1.3, S3.2.3, S3.3.3, S3.4.3, S3.5.3, S3.6.3 and S3.11.2.

Predicted compared to observed area under the concentration–time curves from the first to the last data point (AUC_{last}) and maximum concentrations (C_{max}) values of all studies are shown in Figure S3.9.1 and of each route of administration seperately in Figures S3.1.4, S3.2.4, S3.3.4, S3.4.4, S3.5.4 and S3.6.4. The predicted and observed AUC_{last} and C_{max} values of all studies including the geometric mean fold error (GMFE) and the mean relative deviation (MRD) values of all studies are listed in Tables S3.8.1 and S3.8.2.

A local sensitivity analysis was performed with a simulation of the highest studied pulmonary dose in steady-state (30 times 2.5 mg over 15 hours). A detailed description and the results of the sensitivity analysis can be found in Section 3.10.

3.1 Intravenous administration of nicotine

In this section, linear and semilogarithmic plots of plasma concentration-time profiles, linear plots of fractions of nicotine dose excreted unchanged to urine (Figs. S3.1.1 and S3.1.2), goodness-of-fit plots of predicted compared to observed plasma concentrations (Fig. S3.1.3) and goodness-of-fit plots of predicted compared to observed AUC_{last} and C_{max} values (Fig. S3.1.4) after intravenous administration of nicotine are shown.

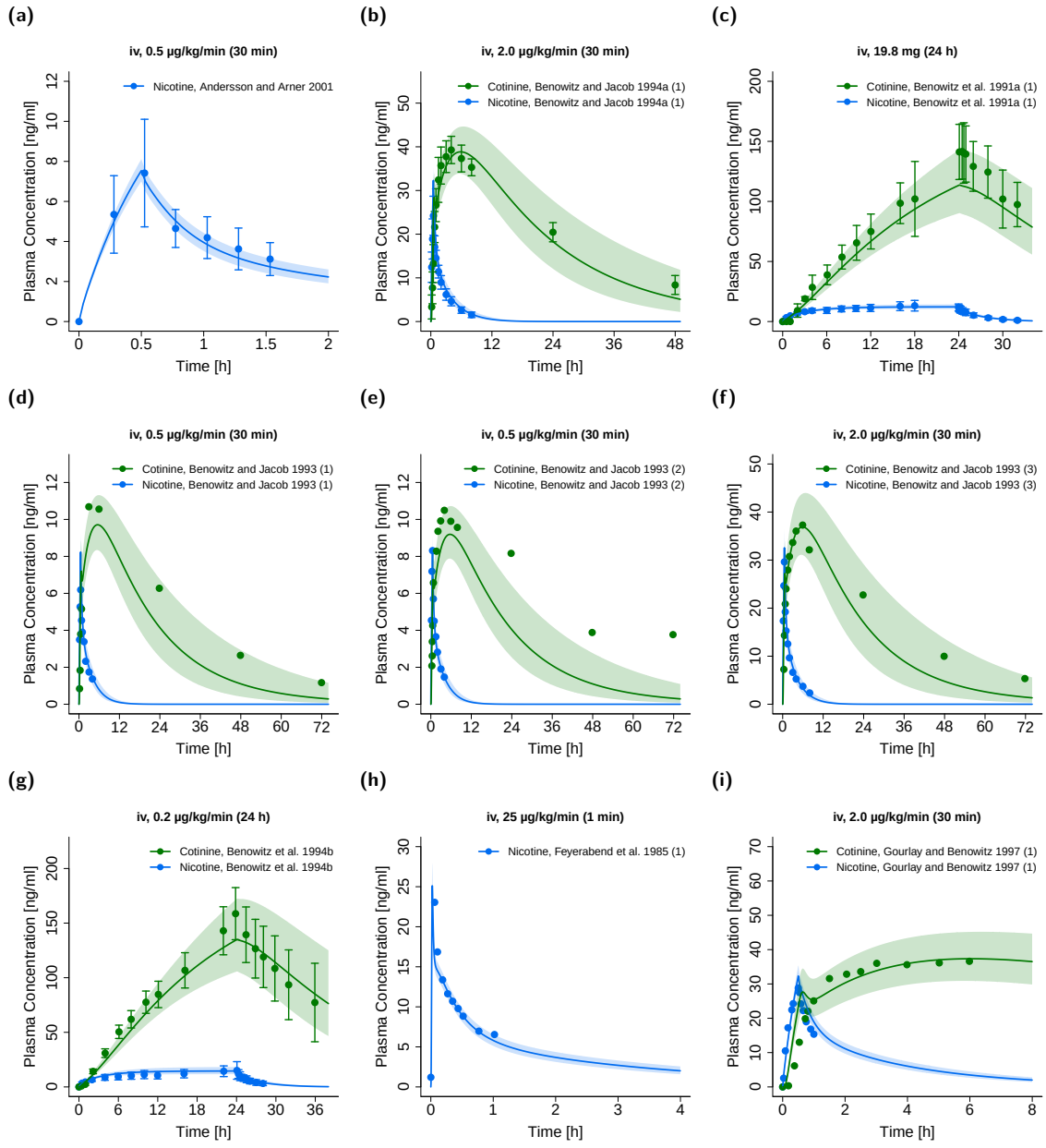

Figure S3.1.1: Nicotine (•, •) and cotinine metabolite (•, •) plasma concentration-time profiles (linear) and nicotine fraction excreted unchanged to urine (•) after intravenous administration of nicotine. Observed data are shown as circles, if available ± standard deviation (SD). Population simulation (n=100) geometric means are shown as lines; the shaded areas represent the predicted population geometric SD. References with numbers in parentheses link to a specific observed dataset described in the study table with detailed information about dosing regimens (Table S2.6.1). Predicted and observed AUC_{last} and C_{max} values are compared in Table S3.8.2. **iv**, intravenous; **m.d.**, multiple dose.

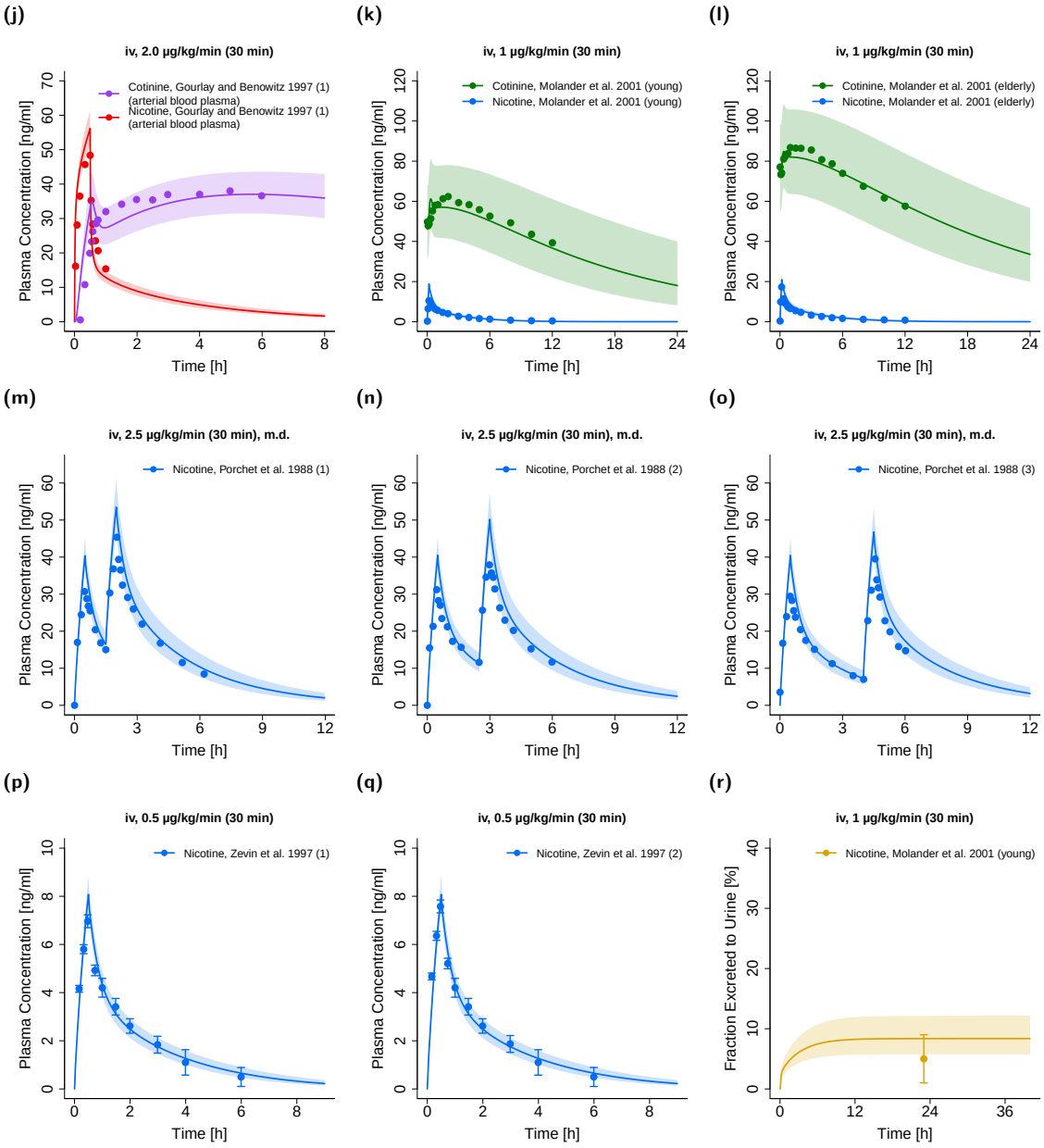

Figure S3.1.1: Nicotine (•, •) and cotinine metabolite (•, •) plasma concentration-time profiles (linear) and nicotine fraction excreted unchanged to urine (•) after intravenous administration of nicotine. Observed data are shown as circles, if available ± standard deviation (SD). Population simulation (n=100) geometric means are shown as lines; the shaded areas represent the predicted population geometric SD. References with numbers in parentheses link to a specific observed dataset described in the study table with detailed information about dosing regimens (Table S2.6.1). Predicted and observed AUC_{last} and C_{max} values are compared in Table S3.8.2. **iv**, intravenous; **m.d.**, multiple dose. (continued)

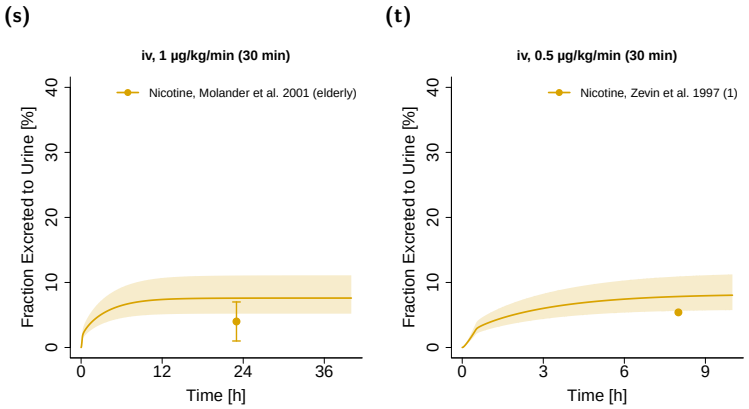

Figure S3.1.1: Nicotine (•, •) and cotinine metabolite (•, •) plasma concentration-time profiles (linear) and nicotine fraction excreted unchanged to urine (•) after intravenous administration of nicotine. Observed data are shown as circles, if available ± standard deviation (SD). Population simulation (n=100) geometric means are shown as lines; the shaded areas represent the predicted population geometric SD. References with numbers in parentheses link to a specific observed dataset described in the study table with detailed information about dosing regimens (Table S2.6.1). Predicted and observed AUC_{last} and C_{max} values are compared in Table S3.8.2. **iv**, intravenous; **m.d.**, multiple dose. (continued)

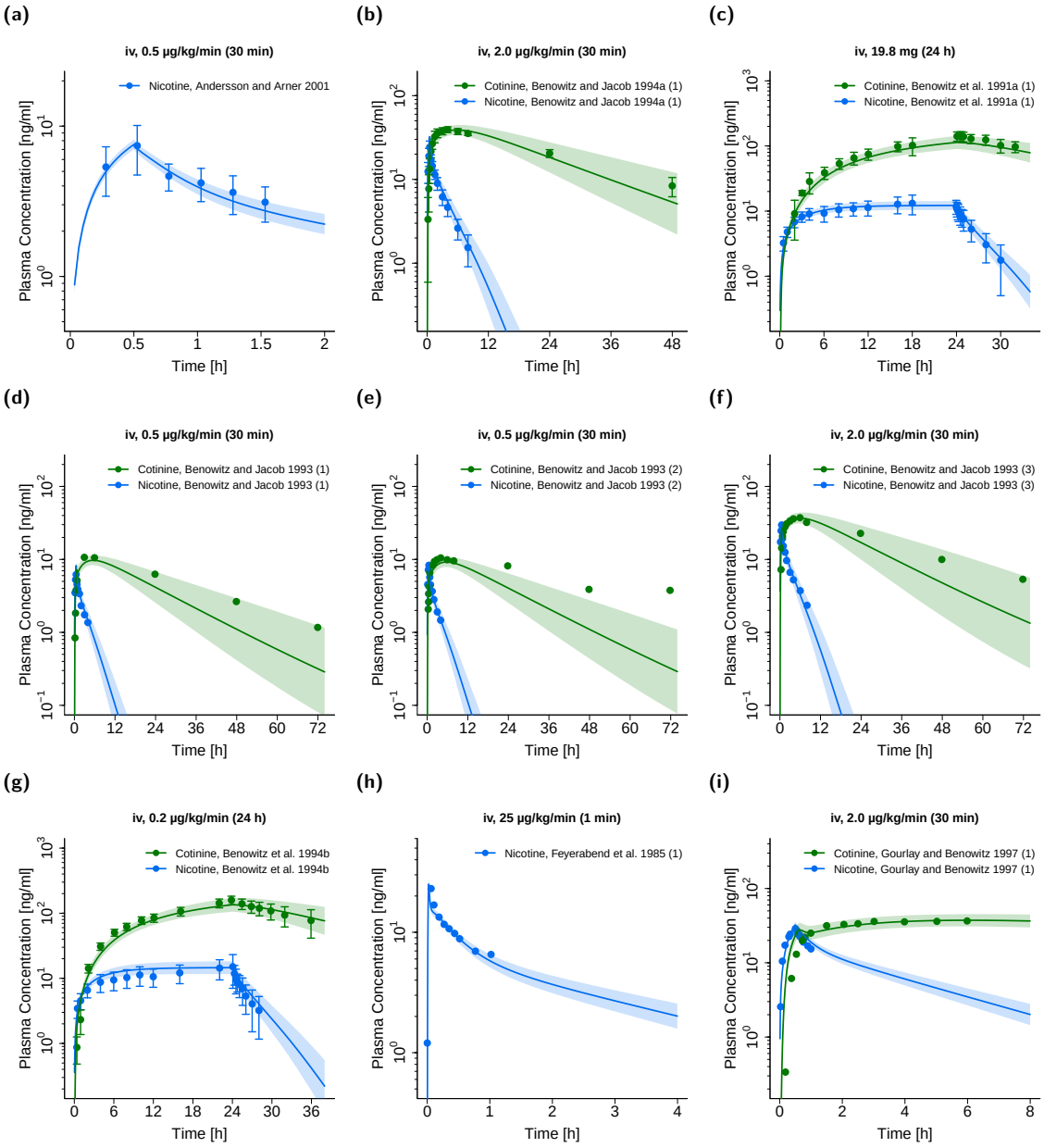

Figure S3.1.2: Nicotine (●, ●) and cotinine metabolite (●, ●) plasma concentration-time profiles (semilogarithmic) after intravenous administration of nicotine. Observed data are shown as circles, if available ± standard deviation (SD). Population simulation (n=100) geometric means are shown as lines; the shaded areas represent the predicted population geometric SD. References with numbers in parentheses link to a specific observed dataset described in the study table with detailed information about dosing regimens (Table S2.6.1). Predicted and observed AUC_{last} and C_{max} values are compared in Table S3.8.2. **iv**, intravenous; **m.d.**, multiple dose.

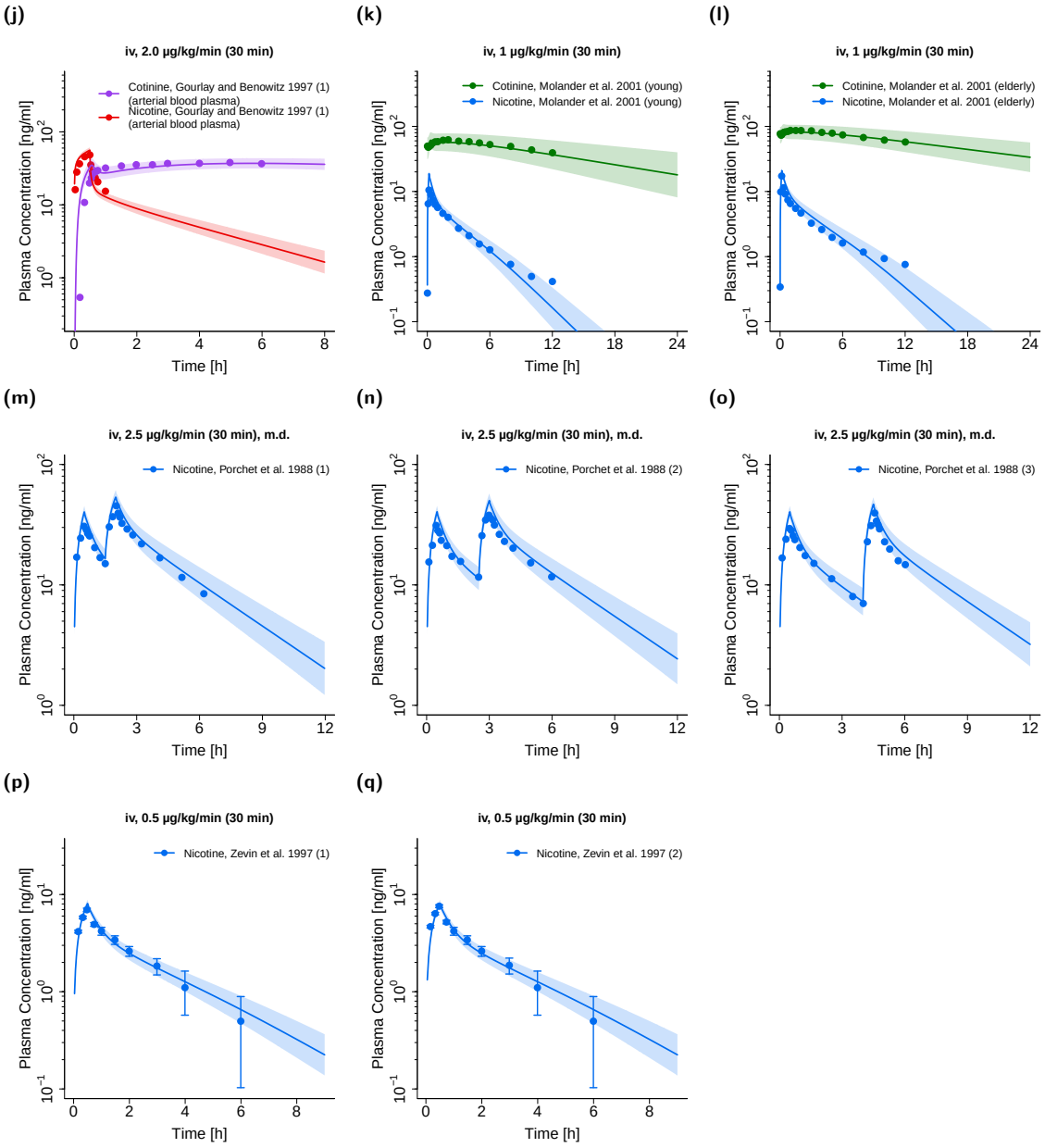

Figure S3.1.2: Nicotine (•, •) and cotinine metabolite (•, •) plasma concentration-time profiles (semilogarithmic) after intravenous administration of nicotine. Observed data are shown as circles, if available ± standard deviation (SD). Population simulation (n=100) geometric means are shown as lines; the shaded areas represent the predicted population geometric SD. References with numbers in parentheses link to a specific observed dataset described in the study table with detailed information about dosing regimens (Table S2.6.1). Predicted and observed AUC_{last} and C_{max} values are compared in Table S3.8.2. **iv**, intravenous; **m.d.**, multiple dose. (continued)

(a) Nicotine

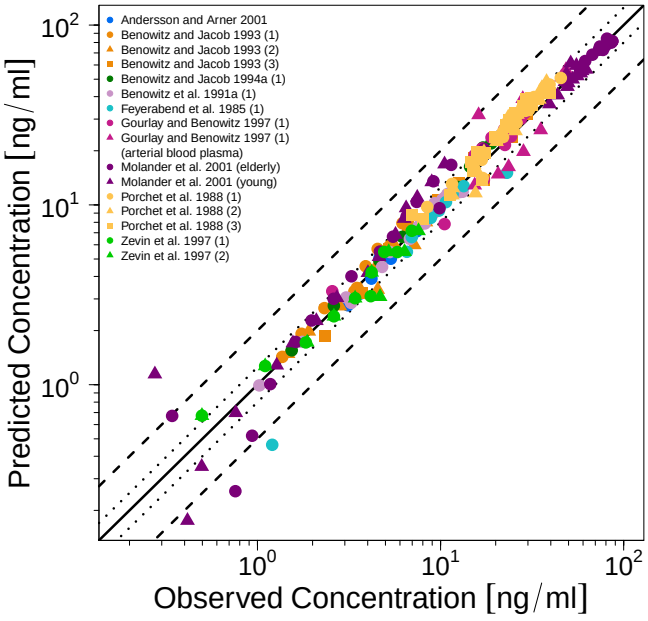

(b) Cotinine metabolite

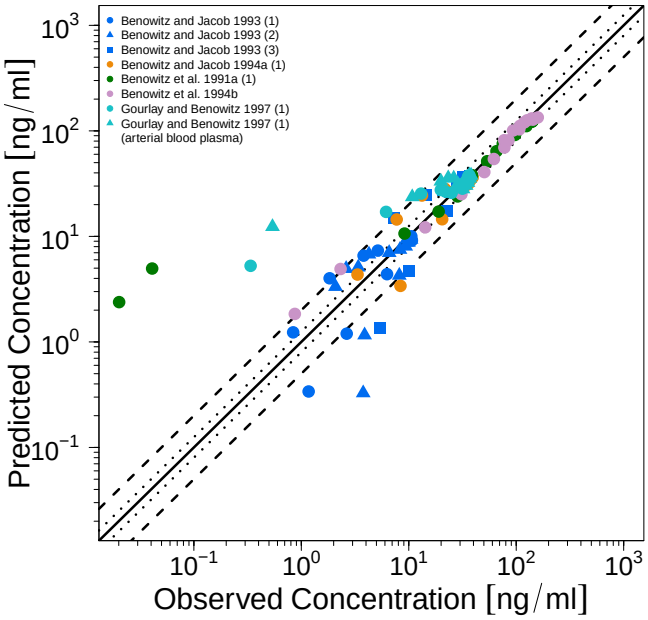

Figure S3.1.3: Predicted versus observed plasma concentrations ((a) nicotine, (b) cotinine metabolite) after intravenous administration of nicotine. The black solid (——) lines mark the lines of identity. Black dotted lines (·····) indicate 1.25-fold, black dashed lines (- -) indicate 2-fold deviation.

(a) AUC

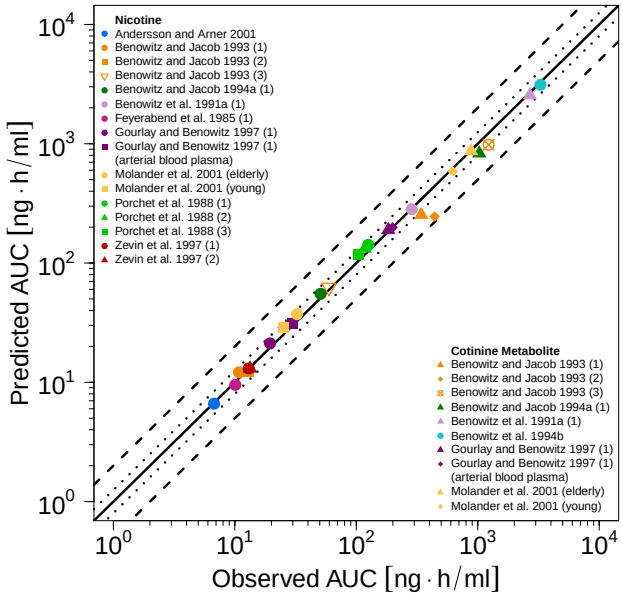

(b) C_{max}

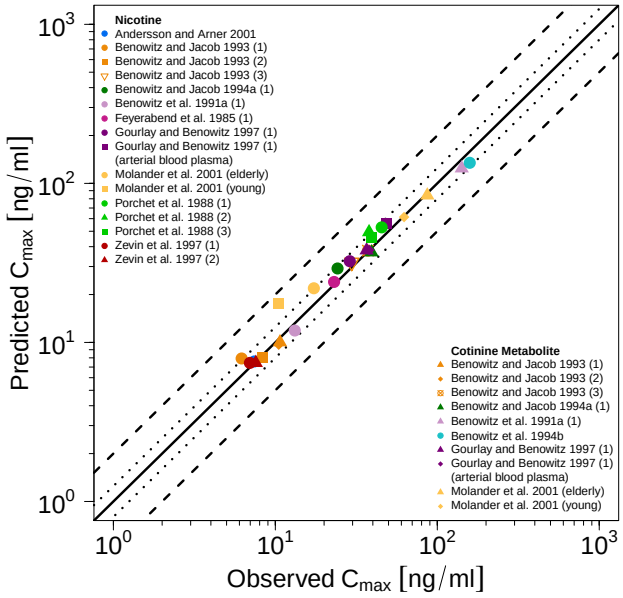

Figure S3.1.4: Predicted versus observed nicotine and cotinine metabolite AUC (a) and C_{max} (b) values after intravenous administration of nicotine. Each symbol represents the AUC_{last} or C_{max} of a different plasma profile. The black solid (——) lines mark the lines of identity. Black dotted lines (·····) indicate 1.25-fold, black dashed lines (- -) indicate 2-fold deviation. **AUC**, area under the plasma concentration–time curve from the first to the last data point; **C_{max}**, maximum plasma concentration.

3.2 Intravenous administration of cotinine

In this section, linear and semilogarithmic plots of plasma concentration-time profiles, linear plots of fractions of cotinine dose excreted unchanged to urine (Figs. S3.2.1 and S3.2.2), a goodness-of-fit plot of predicted compared to observed plasma concentrations (Fig. S3.2.3) and goodness-of-fit plots of predicted compared to observed AUC_{last} and C_{max} values (Fig. S3.2.4) after intravenous administration of cotinine are shown.

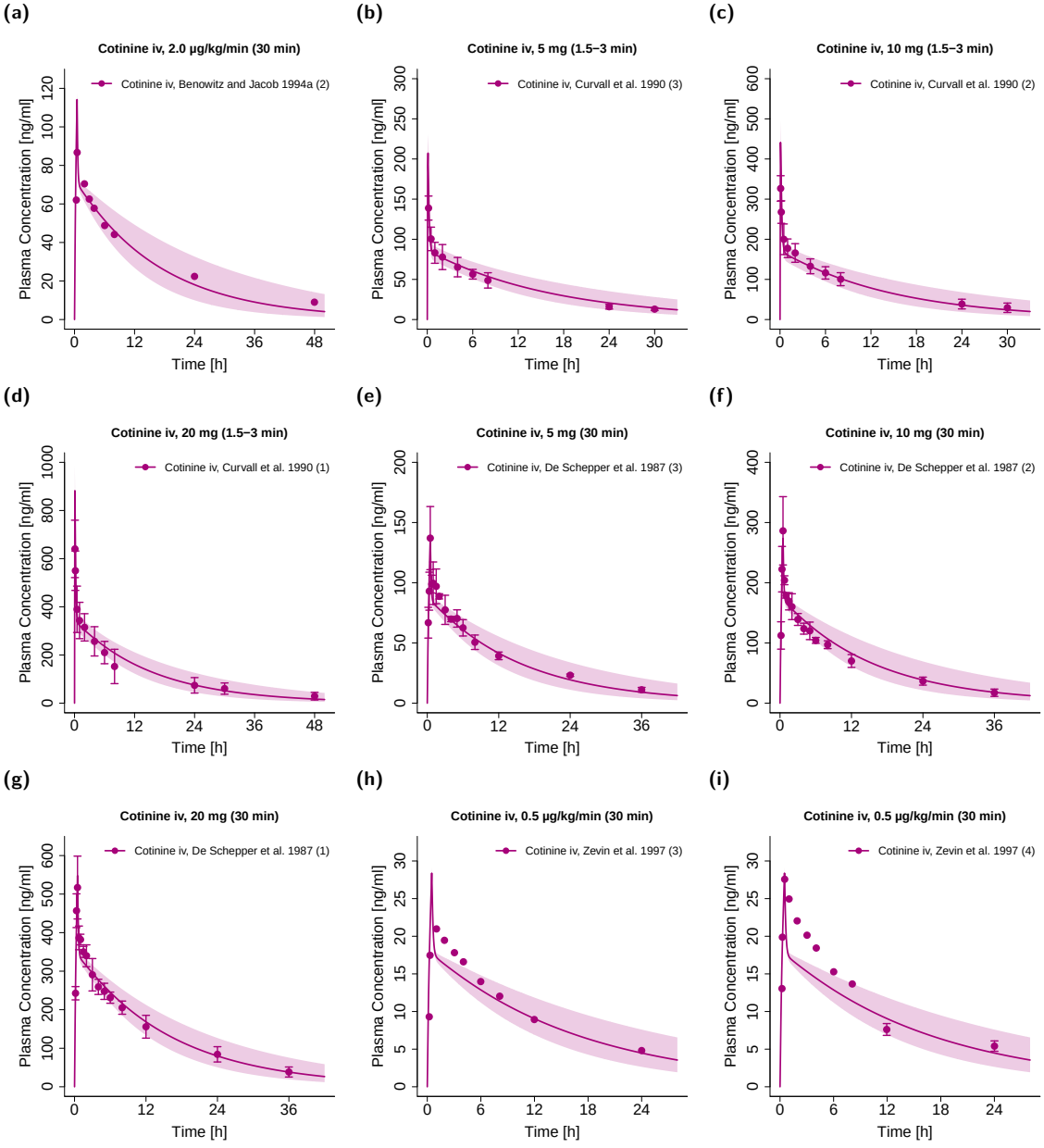

Figure S3.2.1: Cotinine plasma concentration-time profiles (linear) and cotinine fraction excreted unchanged to urine after intravenous administration of cotinine. Observed data are shown as circles (•, •), if available ± standard deviation (SD). Population simulation (n=100) geometric means are shown as lines (–, –); the shaded areas represent the predicted population geometric SD. References with numbers in parentheses link to a specific observed dataset described in the study table (Table S2.6.2). Predicted and observed AUC_{last} and C_{max} values are compared in Table S3.8.2. **iv**, intravenous.

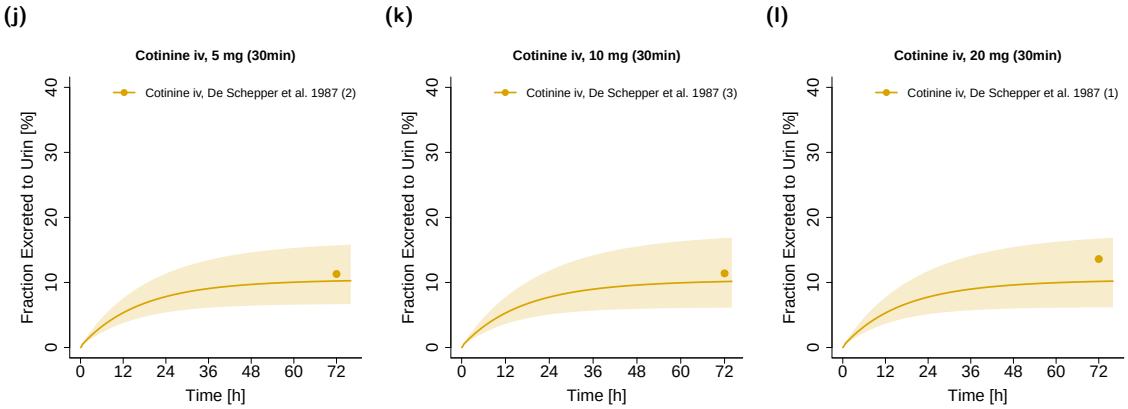

Figure S3.2.1: Cotinine plasma concentration-time profiles (linear) and cotinine fraction excreted unchanged to urine after intravenous administration of cotinine. Observed data are shown as circles (●, ●), if available ± standard deviation (SD). Population simulation (n=100) geometric means are shown as lines (–, –); the shaded areas represent the predicted population geometric SD. References with numbers in parentheses link to a specific observed dataset described in the study table (Table S2.6.2). Predicted and observed AUC_{last} and C_{max} values are compared in Table S3.8.2. **iv**, intravenous. (continued)

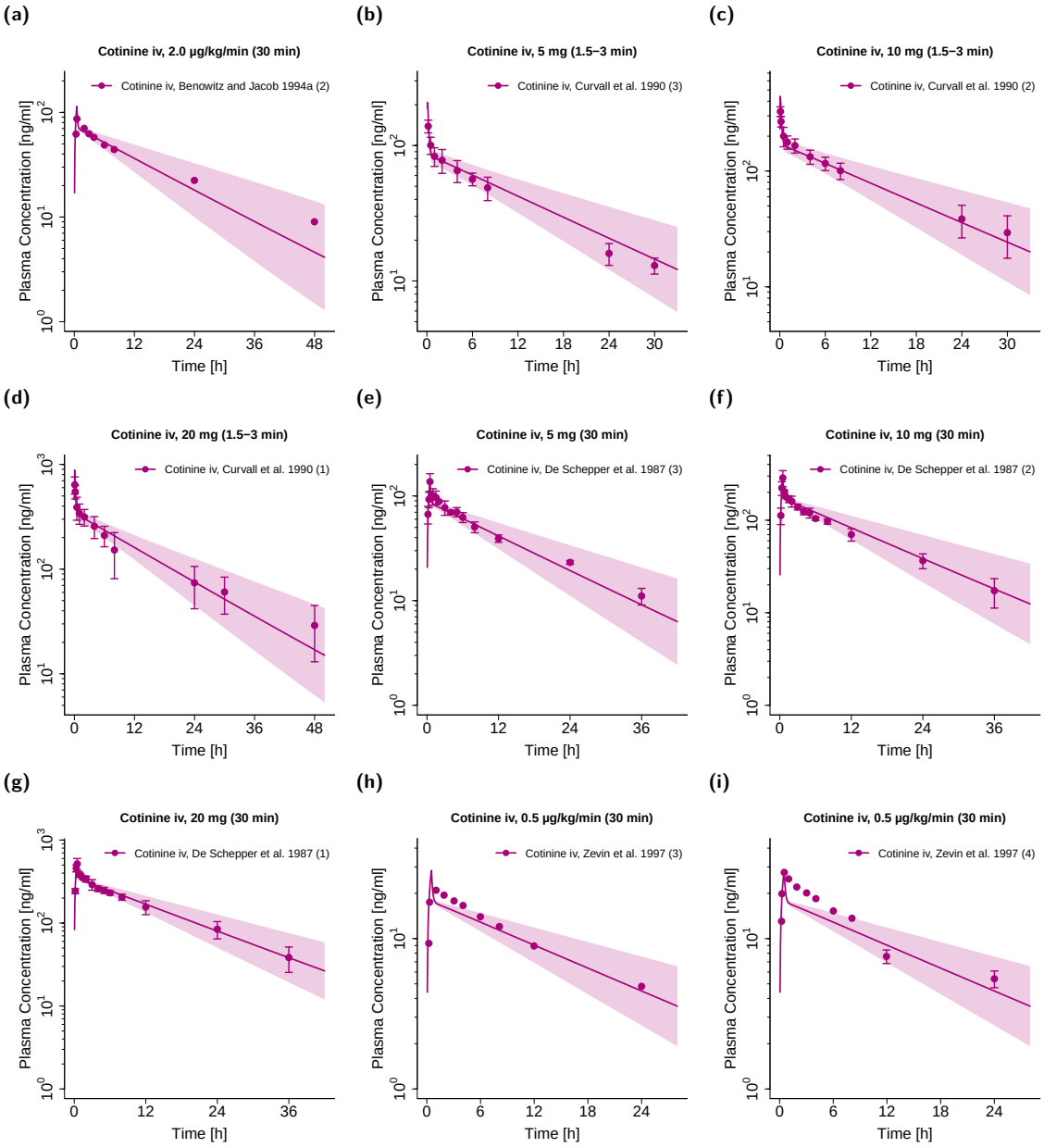

Figure S3.2.2: Cotinine plasma concentration-time profiles (semilogarithmic) after intravenous administration of cotinine. Observed data are shown as circles (•), if available ± standard deviation (SD). Population simulation (n=100) geometric means are shown as lines (–); the shaded areas represent the predicted population geometric SD. References with numbers in parentheses link to a specific observed dataset described in the study table (Table S2.6.2). Predicted and observed AUC_{last} and C_{max} values are compared in Table S3.8.2. **iv**, intravenous.

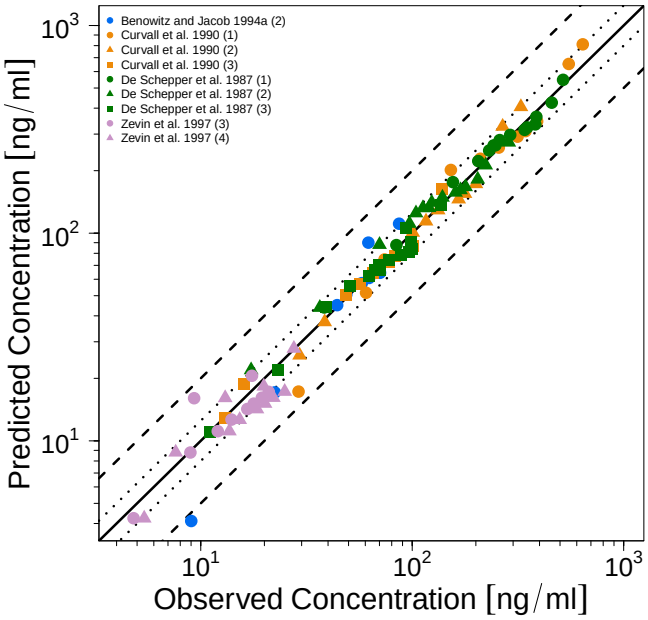

Figure S3.2.3: Predicted versus observed plasma concentrations after intravenous administration of cotinine. The black solid (——) line marks the line of identity. Black dotted lines (·····) indicate 1.25-fold, black dashed lines (- -) indicate 2-fold deviation.

(a) AUC

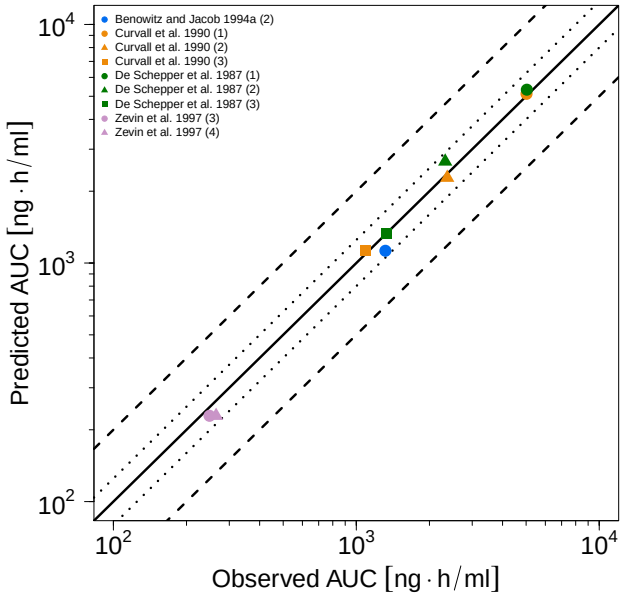

(b) C_{max}

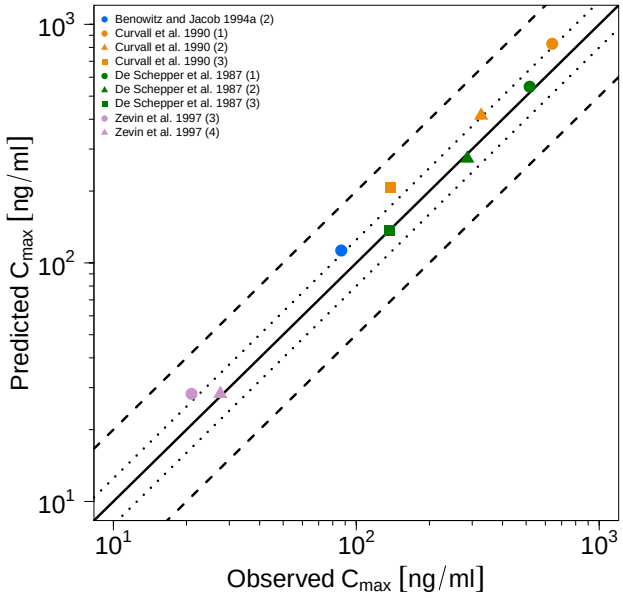

Figure S3.2.4: Predicted versus observed cotinine AUC (a) and C_{max} (b) values after intraveneous administration of cotinine. Each symbol represents the AUC_{last} or C_{max} of a different plasma profile. The black solid (——) lines mark the lines of identity. Black dotted lines (·····) indicate 1.25-fold, black dashed lines (- -) indicate 2-fold deviation. **AUC**, area under the plasma concentration–time curve from the first to the last data point; **C_{max}**, maximum plasma concentration.

3.3 Oral administration of nicotine (including nicotine gums)

In this section, linear and semilogarithmic plots of plasma concentration-time profiles (Figs. S3.3.1 and S3.3.2), goodness-of-fit plots of predicted compared to observed plasma concentrations (Fig. S3.3.3) and goodness-of-fit plots of predicted compared to observed AUC_{last} and C_{max} values (Fig. S3.3.4) after oral administration of nicotine including nicotine gums are shown.

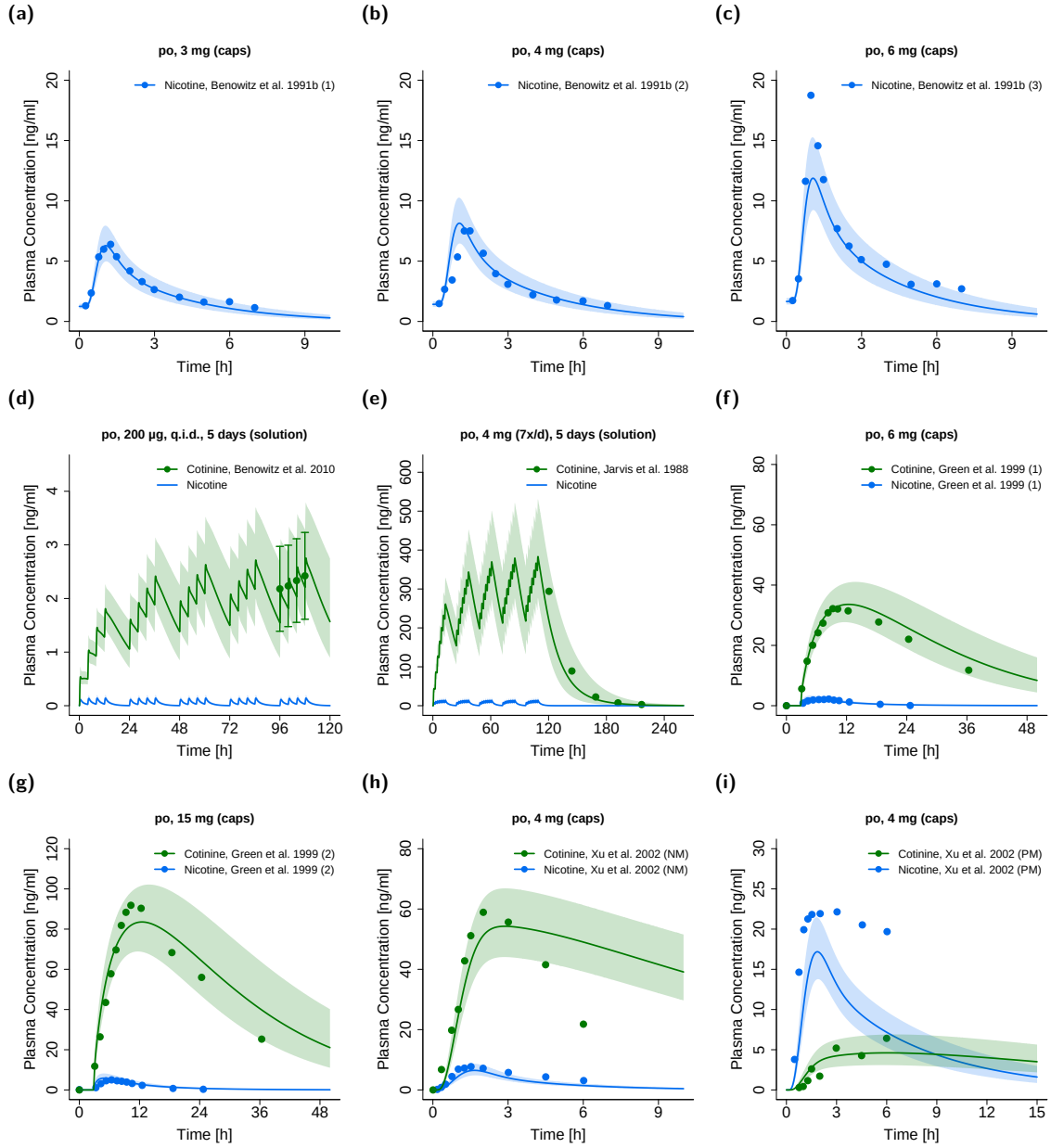

Figure S3.3.1: Nicotine and cotinine metabolite plasma concentration-time profiles (linear) after oral administration of nicotine. Observed data are shown as circles (•, •), if available ± standard deviation (SD). Population simulation (n=100) geometric means are shown as lines (–, –); the shaded areas represent the predicted population geometric SD. References with numbers in parentheses link to a specific observed dataset described in the study table with detailed information about dosing regimens (Table S2.6.1). Predicted and observed AUC_{last} and C_{max} values are compared in Table S3.8.2. **m.d.**, multiple dose; **NM**, Normal Metabolizer; **PM**, Poor Metabolizer; **po**, oral; **q.i.d.**, four times daily.

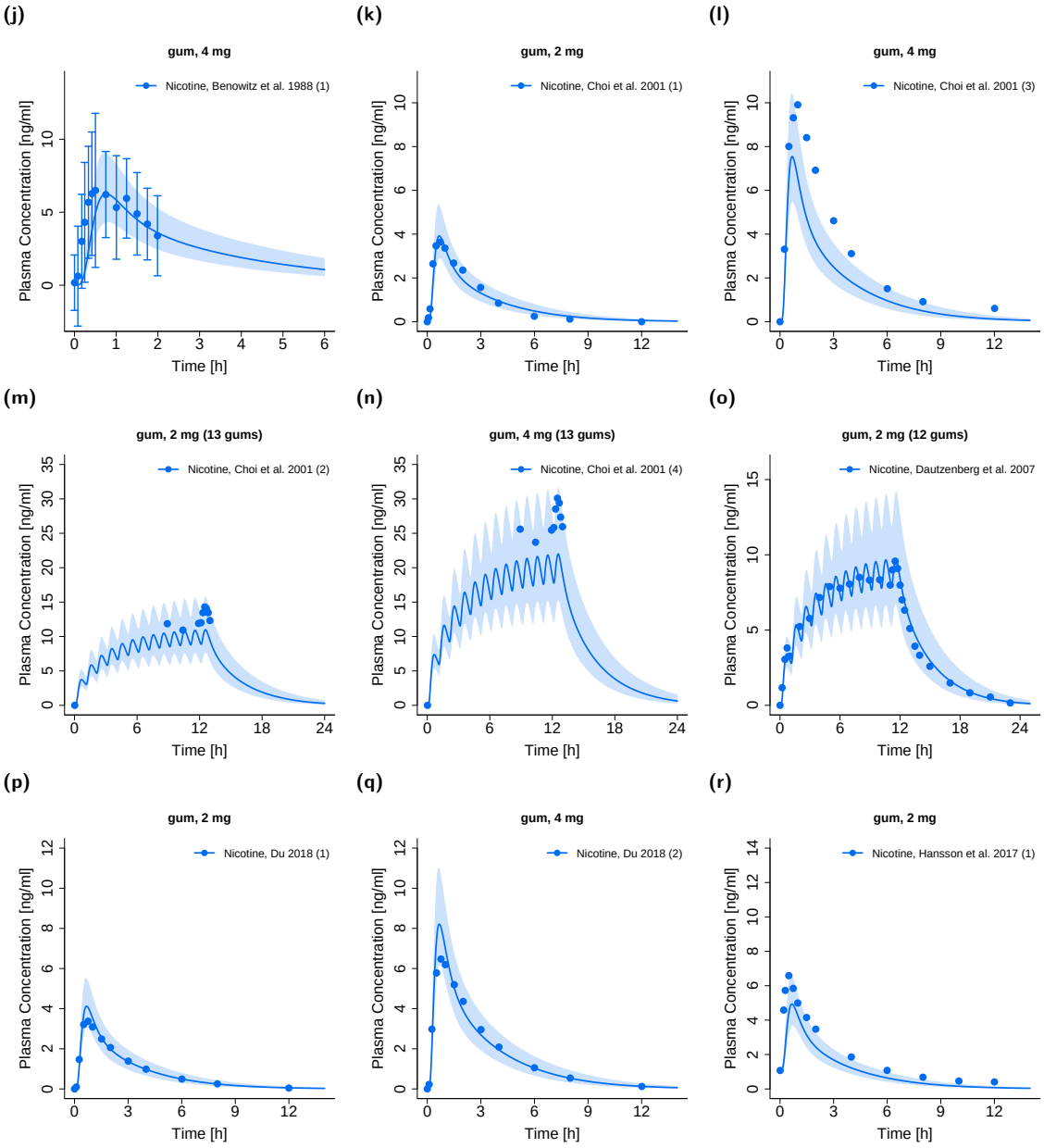

Figure S3.3.1: Nicotine and cotinine metabolite plasma concentration-time profiles (linear) after oral administration of nicotine. Observed data are shown as circles (●, ●), if available ± standard deviation (SD). Population simulation (n=100) geometric means are shown as lines (–, –); the shaded areas represent the predicted population geometric SD. References with numbers in parentheses link to a specific observed dataset described in the study table with detailed information about dosing regimens (Table S2.6.1). Predicted and observed AUC_{last} and C_{max} values are compared in Table S3.8.2. **m.d.**, multiple dose; **NM**, Normal Metabolizer; **PM**, Poor Metabolizer; **po**, oral; **q.i.d.**, four times daily. (continued)

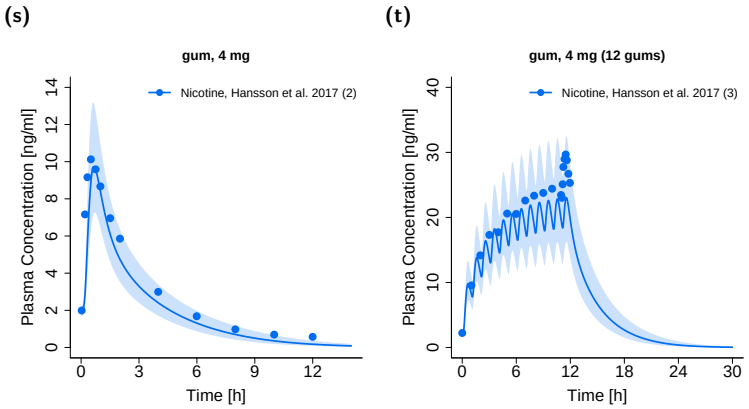

Figure S3.3.1: Nicotine and cotinine metabolite plasma concentration-time profiles (linear) after oral administration of nicotine. Observed data are shown as circles (●, ●), if available ± standard deviation (SD). Population simulation (n=100) geometric means are shown as lines (–, –); the shaded areas represent the predicted population geometric SD. References with numbers in parentheses link to a specific observed dataset described in the study table with detailed information about dosing regimens (Table S2.6.1). Predicted and observed AUC_{last} and C_{max} values are compared in Table S3.8.2. **m.d.**, multiple dose; **NM**, Normal Metabolizer; **PM**, Poor Metabolizer; **po**, oral; **q.i.d.**, four times daily. (continued)

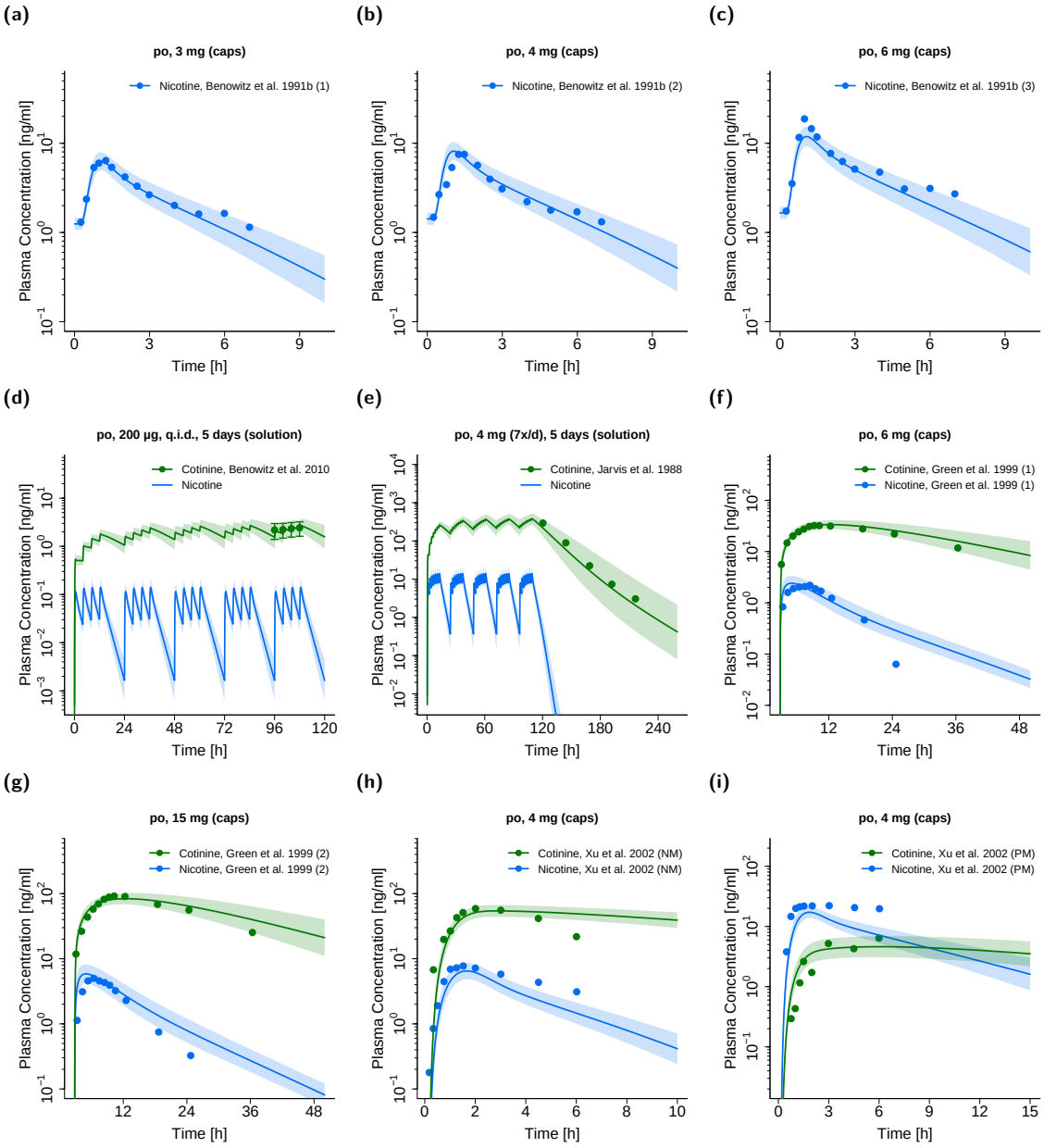

Figure S3.3.2: Nicotine and cotinine metabolite plasma concentration-time profiles (semilogarithmic) after oral administration of nicotine. Observed data are shown as circles (●, ●), if available ± standard deviation (SD). Population simulation (n=100) geometric means are shown as lines (–, –); the shaded areas represent the predicted population geometric SD. References with numbers in parentheses link to a specific observed dataset described in the study table with detailed information about dosing regimens (Table S2.6.1). Predicted and observed AUC_{last} and C_{max} values are compared in Table S3.8.2. **m.d.**, multiple dose; **NM**, Normal Metabolizer; **PM**, Poor Metabolizer; **po**, oral; **q.i.d.**, four times daily.

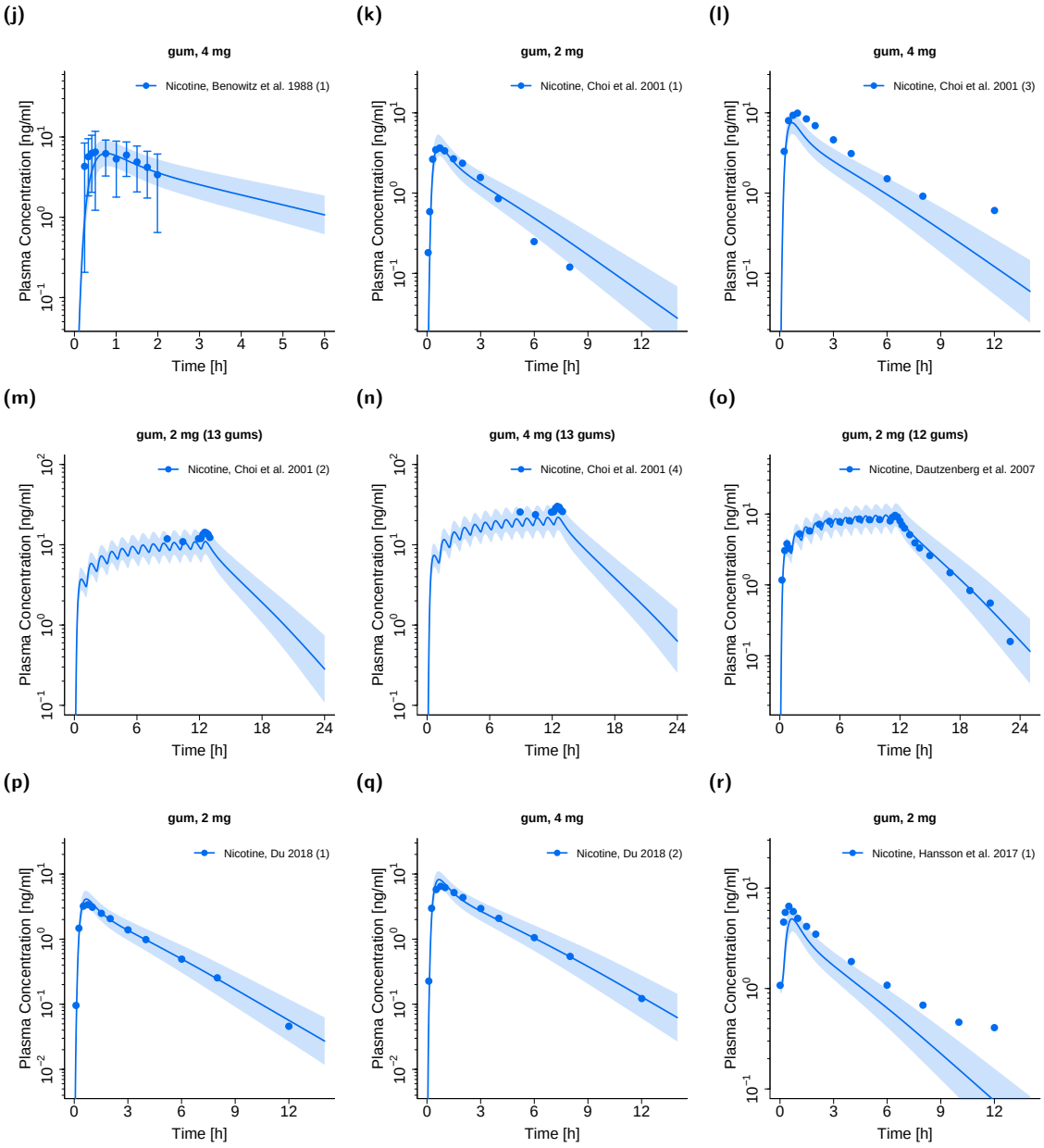

Figure S3.3.2: Nicotine and cotinine metabolite plasma concentration-time profiles (semilogarithmic) after oral administration of nicotine. Observed data are shown as circles (●, ●), if available ± standard deviation (SD). Population simulation (n=100) geometric means are shown as lines (–, –); the shaded areas represent the predicted population geometric SD. References with numbers in parentheses link to a specific observed dataset described in the study table with detailed information about dosing regimens (Table S2.6.1). Predicted and observed AUC_{last} and C_{max} values are compared in Table S3.8.2. **m.d.**, multiple dose; **NM**, Normal Metabolizer; **PM**, Poor Metabolizer; **po**, oral; **q.i.d.**, four times daily. (continued)

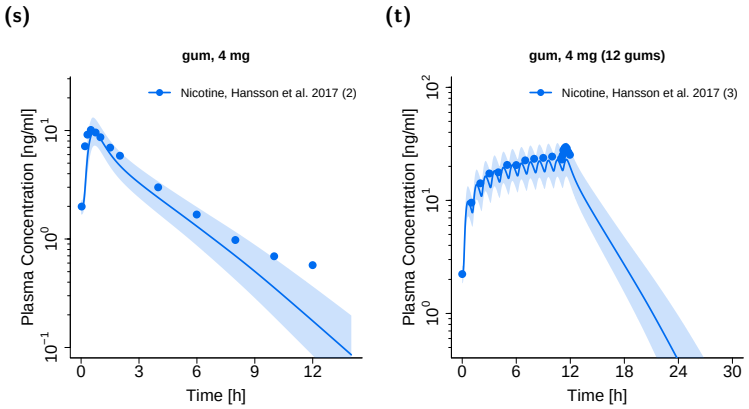

Figure S3.3.2: Nicotine and cotinine metabolite plasma concentration-time profiles (semilogarithmic) after oral administration of nicotine. Observed data are shown as circles (●, ●), if available ± standard deviation (SD). Population simulation (n=100) geometric means are shown as lines (–, –); the shaded areas represent the predicted population geometric SD. References with numbers in parentheses link to a specific observed dataset described in the study table with detailed information about dosing regimens (Table S2.6.1). Predicted and observed AUC_{last} and C_{max} values are compared in Table S3.8.2. **m.d.**, multiple dose; **NM**, Normal Metabolizer; **PM**, Poor Metabolizer; **po**, oral; **q.i.d.**, four times daily. (continued)

(a) Nicotine

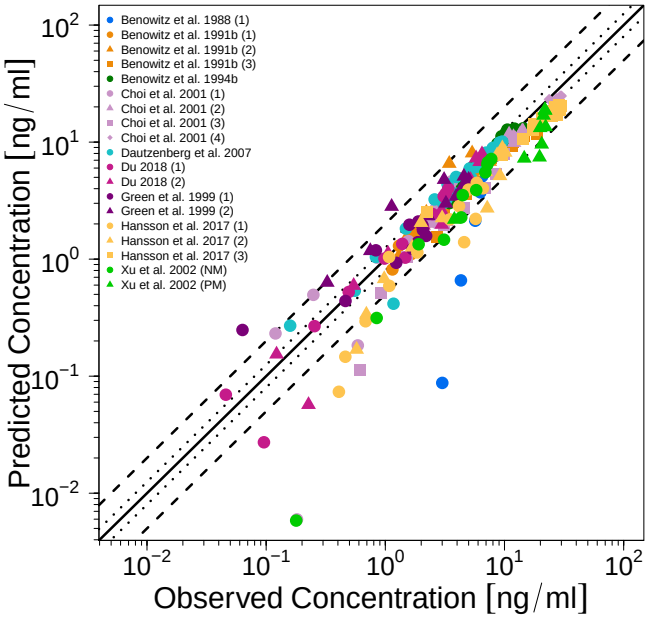

(b) Cotinine metabolite

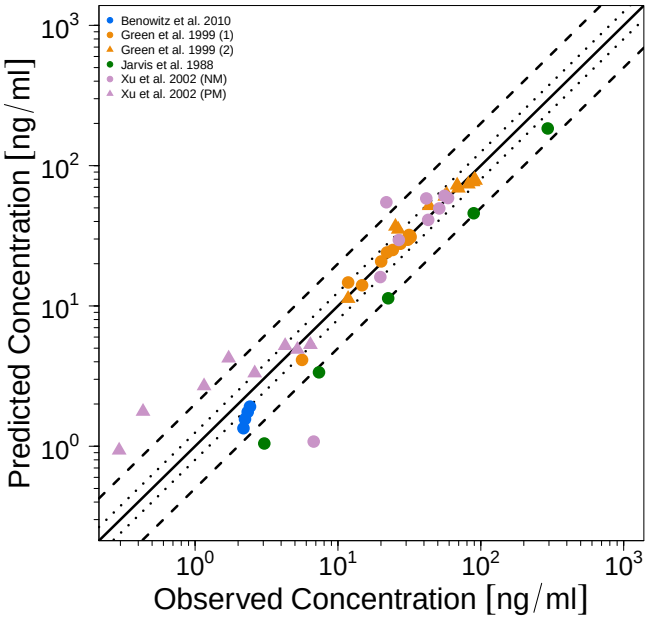

Figure S3.3.3: Predicted versus observed plasma concentrations ((a) nicotine, (b) cotinine metabolite) after oral administration of nicotine (including nicotine gums). The black solid (——) lines mark the lines of identity. Black dotted lines (·····) indicate 1.25-fold, black dashed lines (– –) indicate 2-fold deviation.

(a) AUC

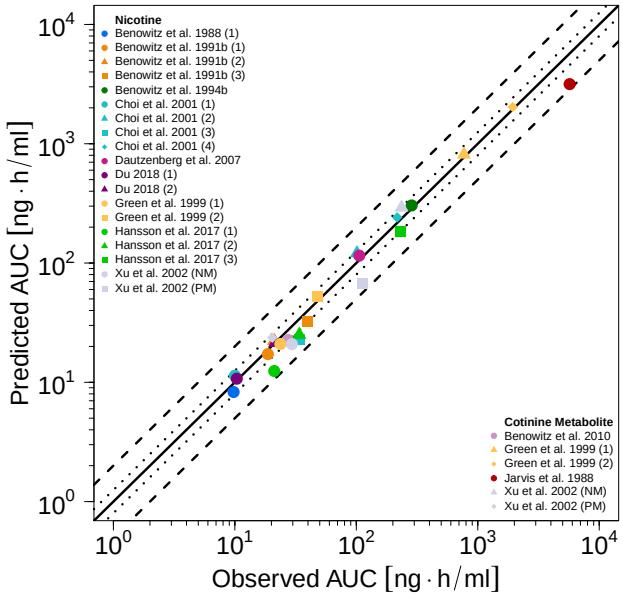

(b) C_{max}

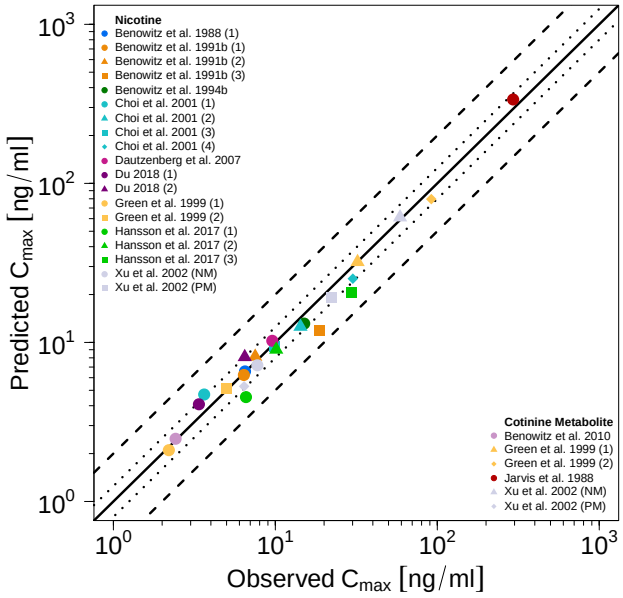

Figure S3.3.4: Predicted versus observed nicotine and cotinine metabolite AUC (a) and C_{max} (b) values after oral administration of nicotine. Each symbol represents the AUC_{last} or C_{max} of a different plasma profile. The black solid (——) lines mark the lines of identity. Black dotted lines (·····) indicate 1.25-fold, black dashed lines (- -) indicate 2-fold deviation. **AUC**, area under the plasma concentration–time curve from the first to the last data point; **C_{max}**, maximum plasma concentration.

3.4 Transdermal administration of nicotine (nicotine patches)

In this section, linear and semilogarithmic plots of plasma concentration-time profiles (Figs. S3.4.1 and S3.4.2), goodness-of-fit plots of predicted compared to observed plasma concentrations (Fig. S3.4.3) and goodness-of-fit plots of predicted compared to observed AUC_{last} and C_{max} values (Fig. S3.4.4) after transdermal administration of nicotine with nicotine patches are shown.

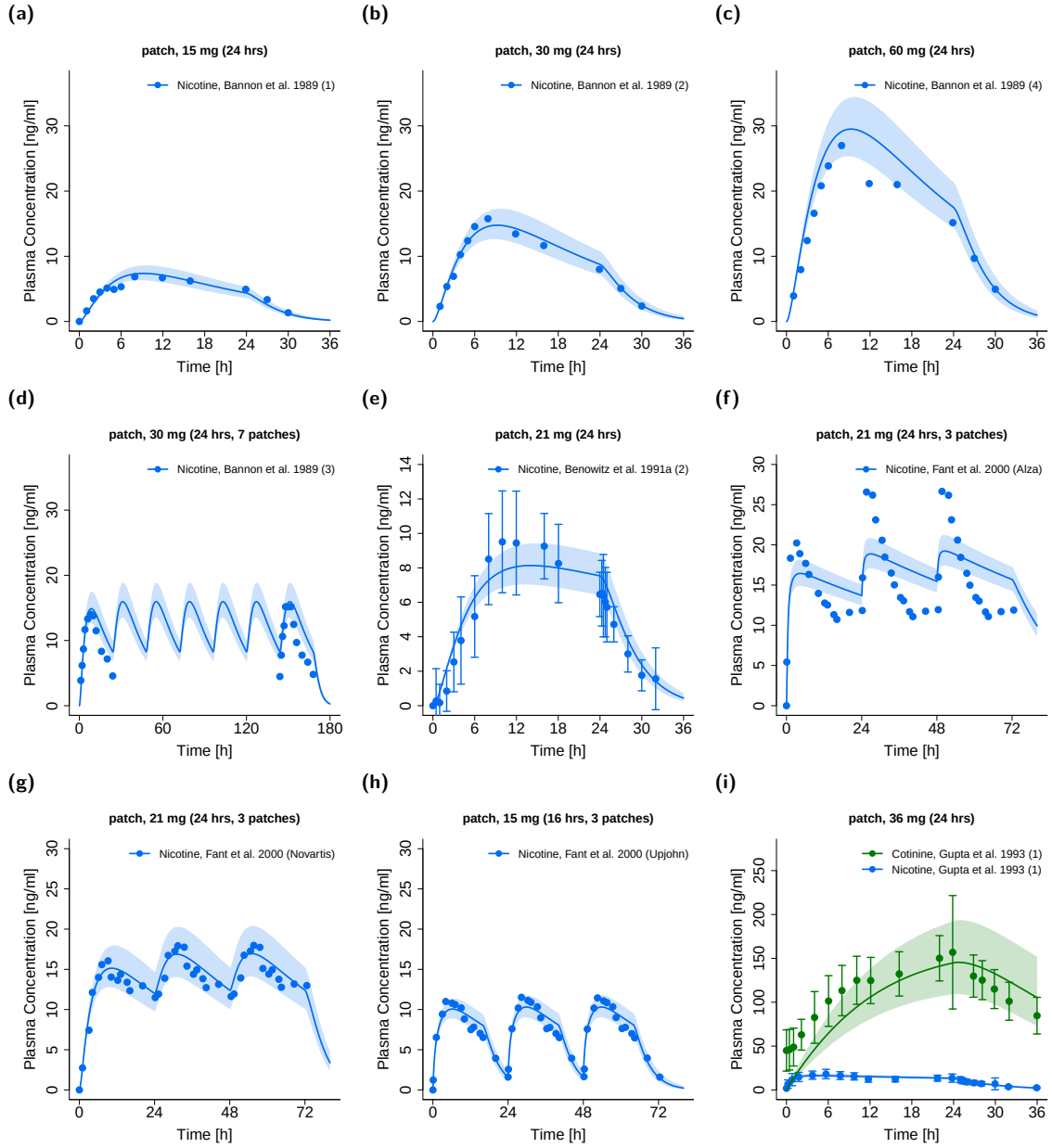

Figure S3.4.1: Nicotine and cotinine metabolite plasma concentration-time profiles (linear) after transdermal administration of nicotine (nicotine patch). Observed data are shown as circles (●, ●), if available ± standard deviation (SD). Population simulation (n=100) geometric means are shown as lines (–, –); the shaded areas represent the predicted population geometric SD. References with numbers in parentheses link to a specific observed dataset described in the study table with detailed information about dosing regimens (Table S2.6.1). Predicted and observed AUC_{last} and C_{max} values are compared in Table S3.8.2. **patch**, transdermal therapeutic system (nicotine patch).

(j)

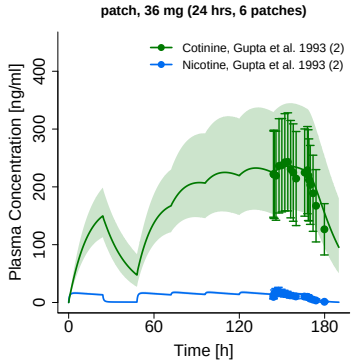

Figure S3.4.1: Nicotine and cotinine metabolite plasma concentration-time profiles (linear) after transdermal administration of nicotine (nicotine patch). Observed data are shown as circles (•, •), if available ± standard deviation (SD). Population simulation (n=100) geometric means are shown as lines (–, –); the shaded areas represent the predicted population geometric SD. References with numbers in parentheses link to a specific observed dataset described in the study table with detailed information about dosing regimens (Table S2.6.1). Predicted and observed AUC_{last} and C_{max} values are compared in Table S3.8.2. **patch**, transdermal therapeutic system (nicotine patch). (continued)

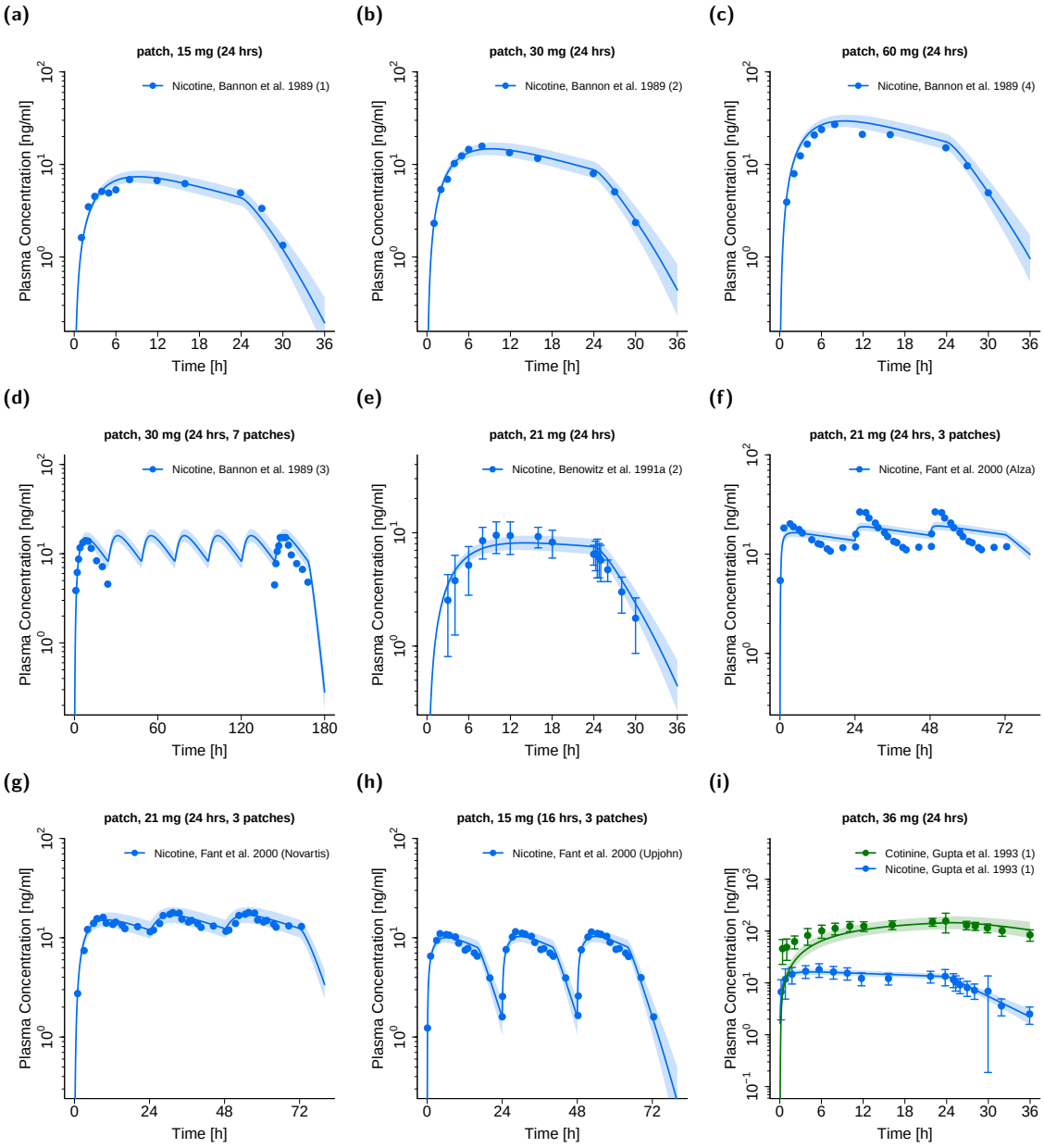

Figure S3.4.2: Nicotine and cotinine metabolite plasma concentration-time profiles (semilogarithmic) after transdermal administration of nicotine (nicotine patch). Observed data are shown as circles (●, ●), if available ± standard deviation (SD). Population simulation (n=100) geometric means are shown as lines (–, –); the shaded areas represent the predicted population geometric SD. References with numbers in parentheses link to a specific observed dataset described in the study table with detailed information about dosing regimens (Table S2.6.1). Predicted and observed AUC_{last} and C_{max} values are compared in Table S3.8.2. **patch**, transdermal therapeutic system (nicotine patch).

(j)

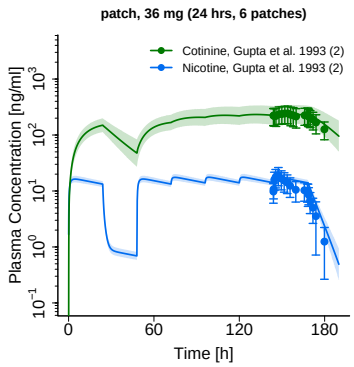

Figure S3.4.2: Nicotine and cotinine metabolite plasma concentration-time profiles (semilogarithmic) after transdermal administration of nicotine (nicotine patch). Observed data are shown as circles (•, •), if available ± standard deviation (SD). Population simulation (n=100) geometric means are shown as lines (–, –); the shaded areas represent the predicted population geometric SD. References with numbers in parentheses link to a specific observed dataset described in the study table with detailed information about dosing regimens (Table S2.6.1). Predicted and observed AUC_{last} and C_{max} values are compared in Table S3.8.2. **patch**, transdermal therapeutic system (nicotine patch). (continued)

(a) Nicotine

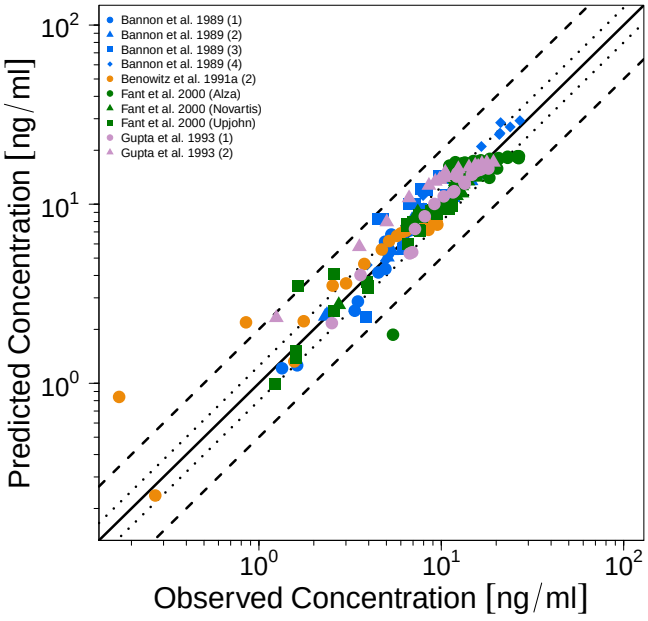

(b) Cotinine metabolite

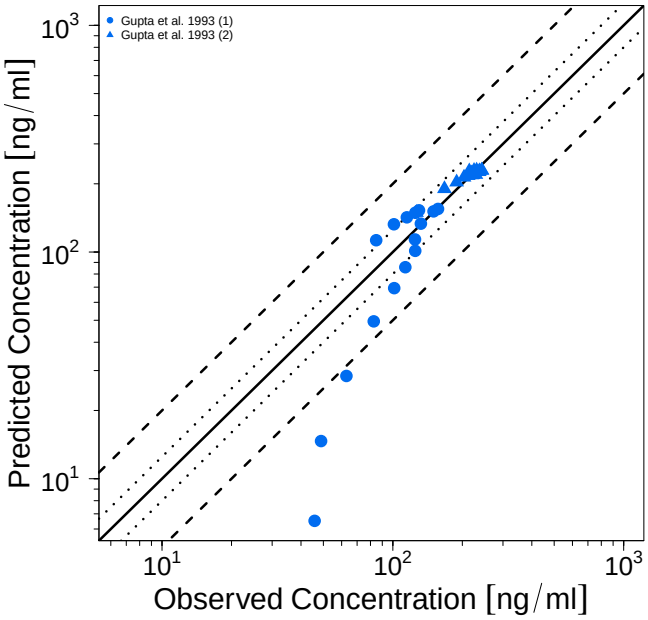

Figure S3.4.3: Predicted versus observed plasma concentrations ((a) nicotine, (b) cotinine metabolite) after transdermal administration of nicotine (nicotine patches). The black solid (——) lines mark the lines of identity. Black dotted lines (·····) indicate 1.25-fold, black dashed lines (– –) indicate 2-fold deviation.

(a) AUC

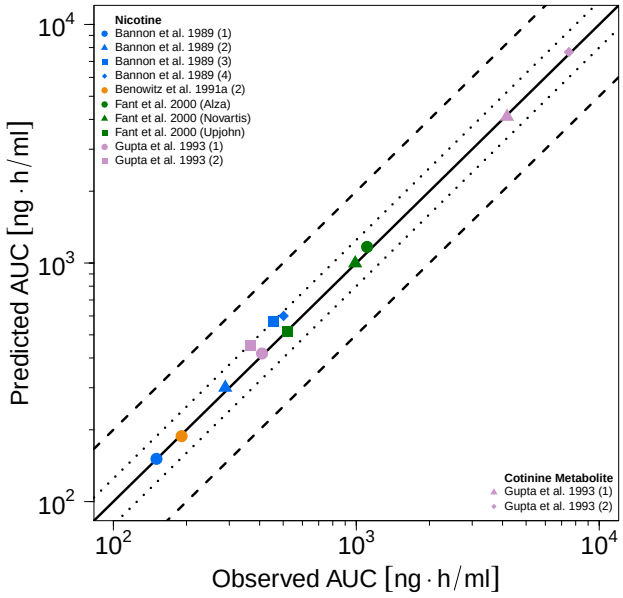

(b) C_{max}

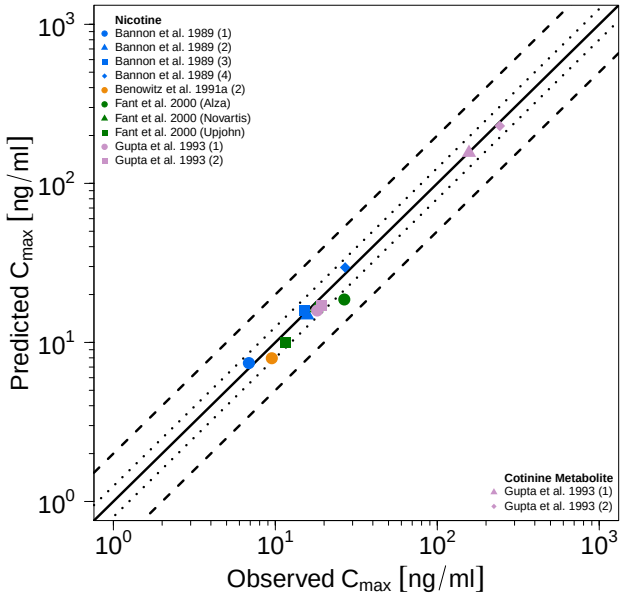

Figure S3.4.4: Predicted versus observed nicotine and cotinine metabolite AUC (a) and C_{max} (b) values after transdermal administration of nicotine (nicotine patches). Each symbol represents the AUC_{last} or C_{max} of a different plasma profile. The black solid (——) lines mark the lines of identity. Black dotted lines (·····) indicate 1.25-fold, black dashed lines (– –) indicate 2-fold deviation. **AUC**, area under the plasma concentration–time curve from the first to the last data point; **C_{max}**, maximum plasma concentration.

3.5 Pulmonary administration of nicotine (combustible cigarettes with estimated pulmonary nicotine exposure and e-cigarettes)

In this section, linear and semilogarithmic plots of plasma and brain tissue concentration-time profiles (Figs. S3.5.1 and S3.5.2), goodness-of-fit plots of predicted compared to observed plasma concentrations (Fig. S3.5.3) and predicted versus observed AUC_{last} and C_{max} values (Fig. S3.5.4) after administration of combustible cigarettes (with estimated pulmonary nicotine exposure) and e-cigarettes are shown.

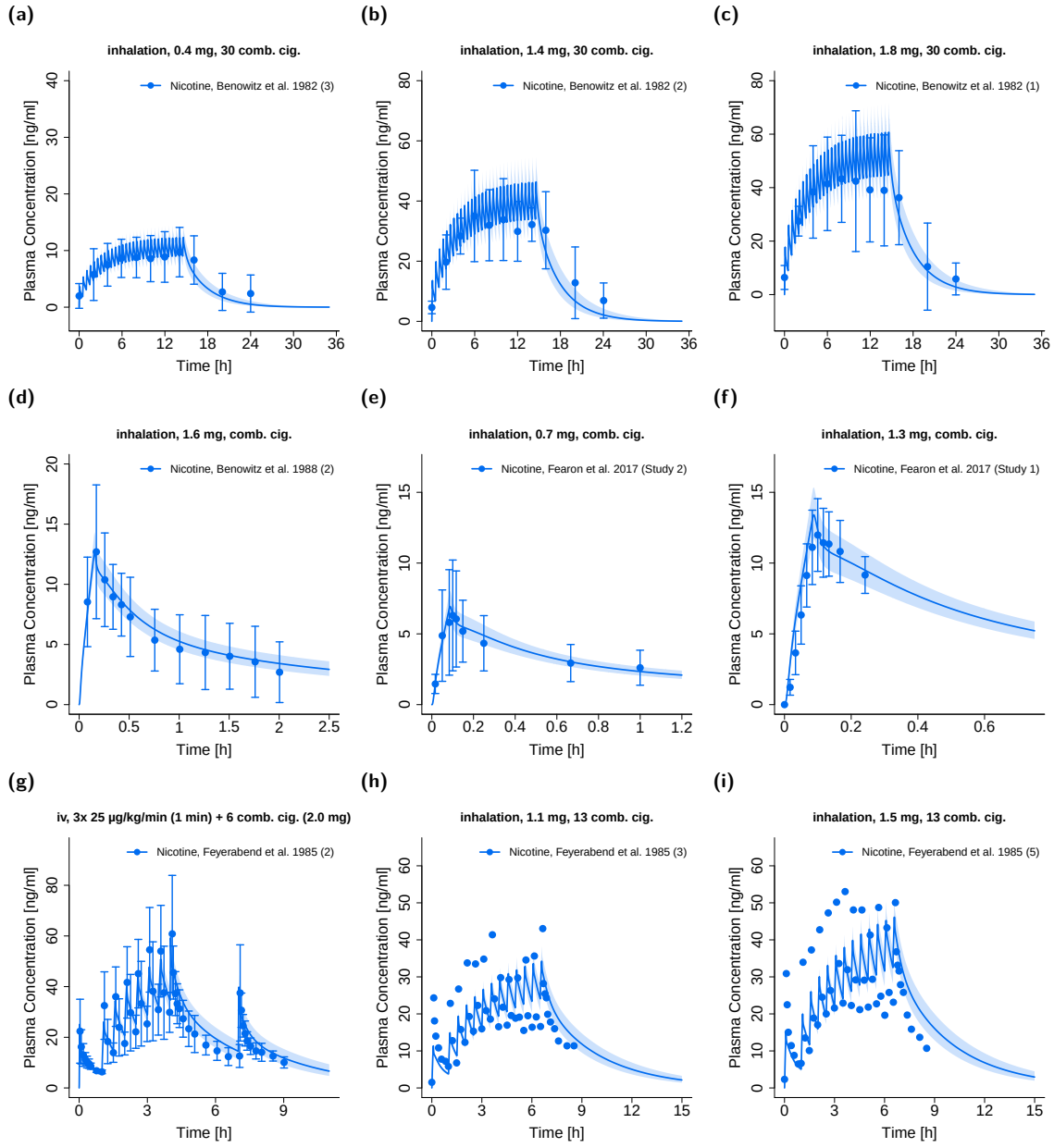

Figure S3.5.1: Nicotine plasma (•, •) and brain tissue (•) concentration-time profiles (linear) after inhalation (combustible cigarettes and e-cigarettes). Observed data are shown as circles, if available ± standard deviation (SD). Population simulation (n=100) geometric means are shown as lines; the shaded areas represent the predicted population geometric SD. For venous blood plasma simulations (–) estimated pulmonary nicotine exposures for combustible cigarettes were used (see Table S2.8.2). References with numbers in parentheses link to a specific observed dataset described in the study table (Table S2.6.1). Predicted and observed AUC_{last} and C_{max} values are compared in Table S3.8.2. **comb. cig.**, combustible cigarette; **e-cig.**, e-cigarette; **iv**, intravenous.

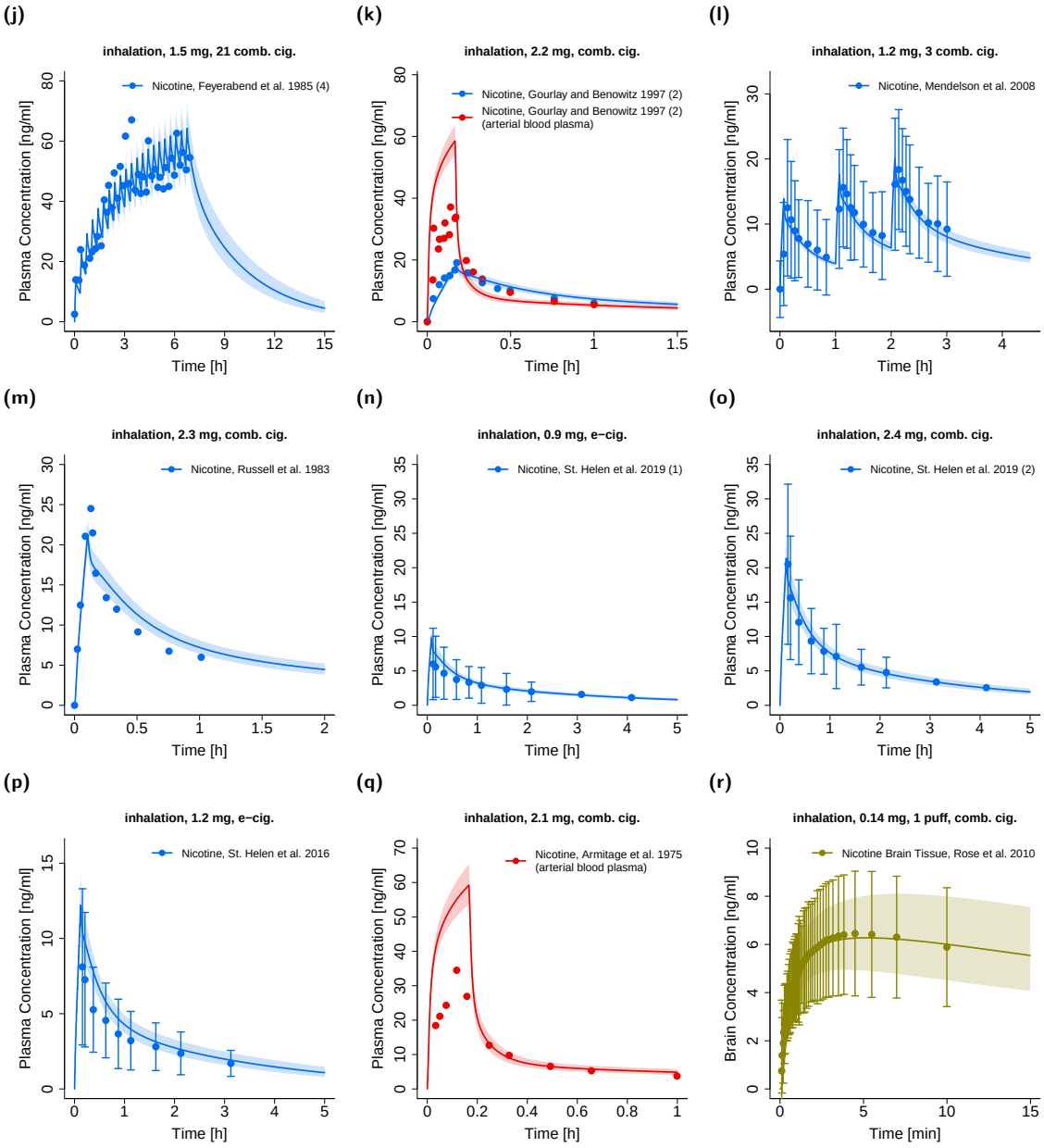

Figure S3.5.1: Nicotine plasma (•, •) and brain tissue (•) concentration-time profiles (linear) after inhalation (combustible cigarettes and e-cigarettes). Observed data are shown as circles, if available ± standard deviation (SD). Population simulation (n=100) geometric means are shown as lines; the shaded areas represent the predicted population geometric SD. For venous blood plasma simulations (–) estimated pulmonary nicotine exposures for combustible cigarettes were used (see Table S2.8.2). References with numbers in parentheses link to a specific observed dataset described in the study table (Table S2.6.1). Predicted and observed AUC_{last} and C_{max} values are compared in Table S3.8.2. **comb. cig.**, combustible cigarette; **e-cig.**, e-cigarette; **iv**, intravenous. (continued)

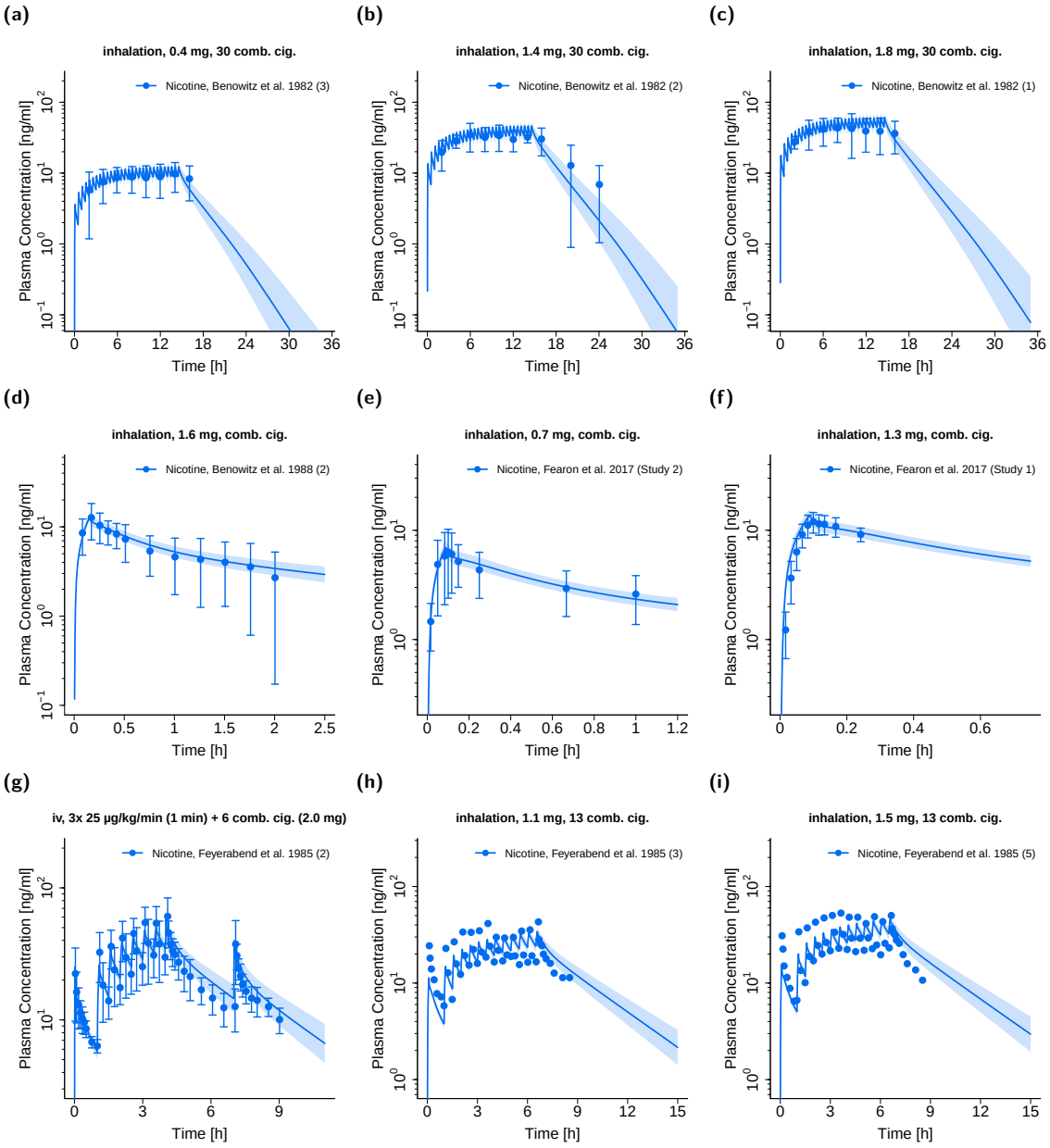

Figure S3.5.2: Nicotine plasma (●, ●) and brain tissue (●) concentration-time profiles (semilogarithmic) after inhalation (combustible cigarettes and e-cigarettes). Observed data are shown as circles, if available ± standard deviation (SD). Population simulation (n=100) geometric means are shown as lines; the shaded areas represent the predicted population geometric SD. For venous blood plasma simulations (–) estimated pulmonary nicotine exposures for combustible cigarettes were used (see Table S2.8.2). References with numbers in parentheses link to a specific observed dataset described in the study table (Table S2.6.1). Predicted and observed AUC_{last} and C_{max} values are compared in Table S3.8.2. **comb. cig.**, combustible cigarette; **e-cig.**, e-cigarette; **iv**, intravenous.

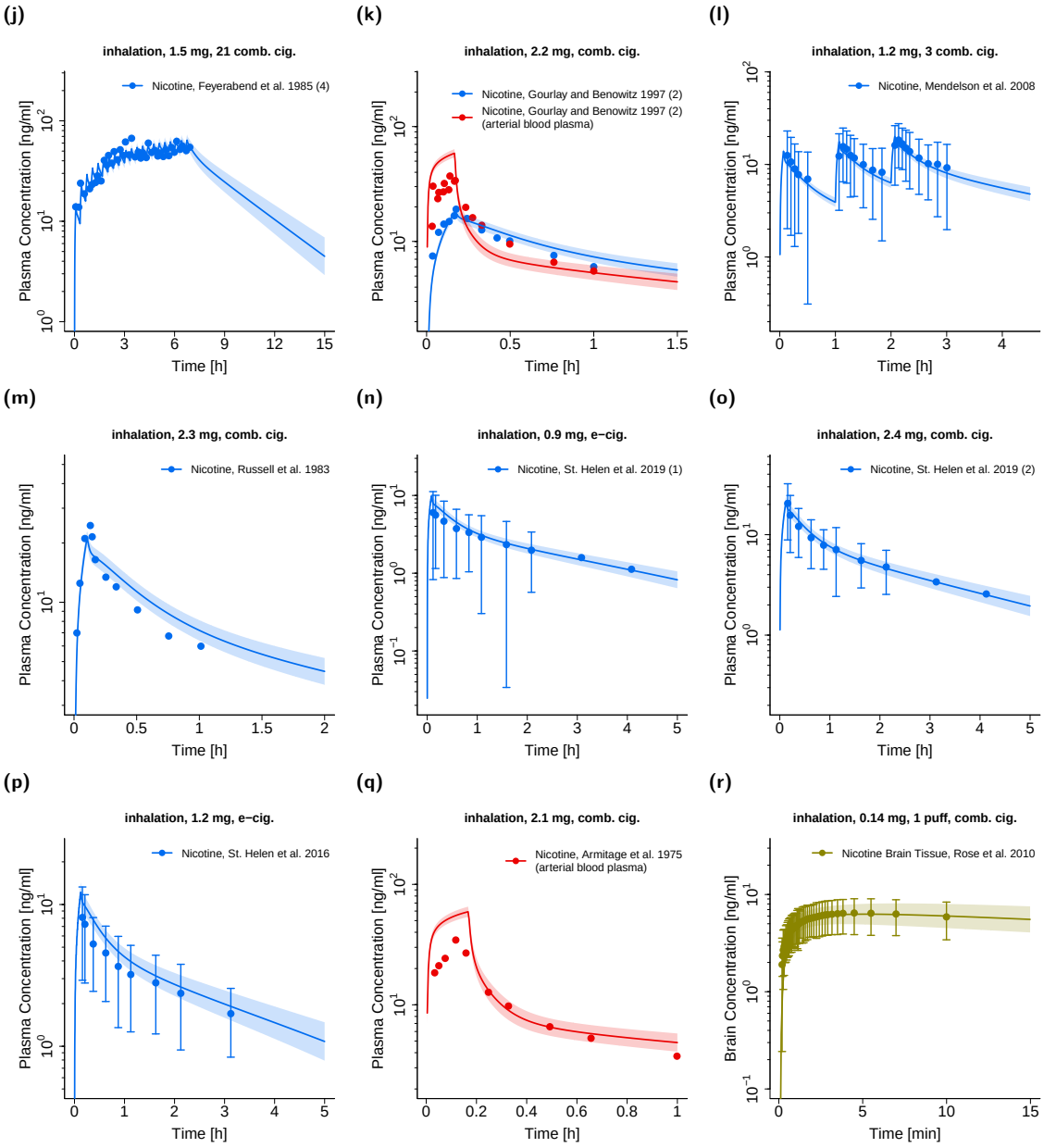

Figure S3.5.2: Nicotine plasma (●, ●) and brain tissue (●) concentration-time profiles (semilogarithmic) after inhalation (combustible cigarettes and e-cigarettes). Observed data are shown as circles, if available ± standard deviation (SD). Population simulation (n=100) geometric means are shown as lines; the shaded areas represent the predicted population geometric SD. For venous blood plasma simulations (–) estimated pulmonary nicotine exposures for combustible cigarettes were used (see Table S2.8.2). References with numbers in parentheses link to a specific observed dataset described in the study table (Table S2.6.1). Predicted and observed AUC_{last} and C_{max} values are compared in Table S3.8.2. **comb. cig.**, combustible cigarette; **e-cig.**, e-cigarette; **iv**, intravenous. (continued)

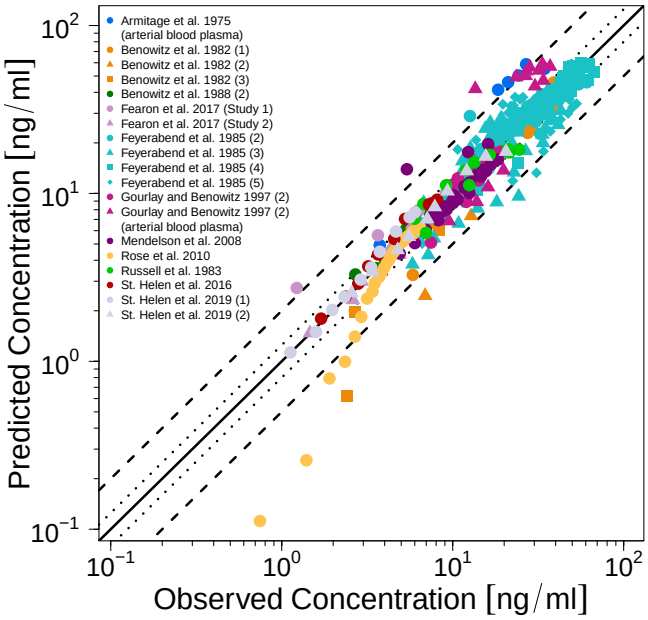

Figure S3.5.3: Predicted versus observed nicotine concentrations after pulmonary administration of combustible cigarettes (with estimated pulmonary nicotine exposure) and e-cigarettes. The black solid (——) line marks the line of identity. Black dotted lines (·····) indicate 1.25-fold, black dashed lines (- -) indicate 2-fold deviation.

(a) AUC

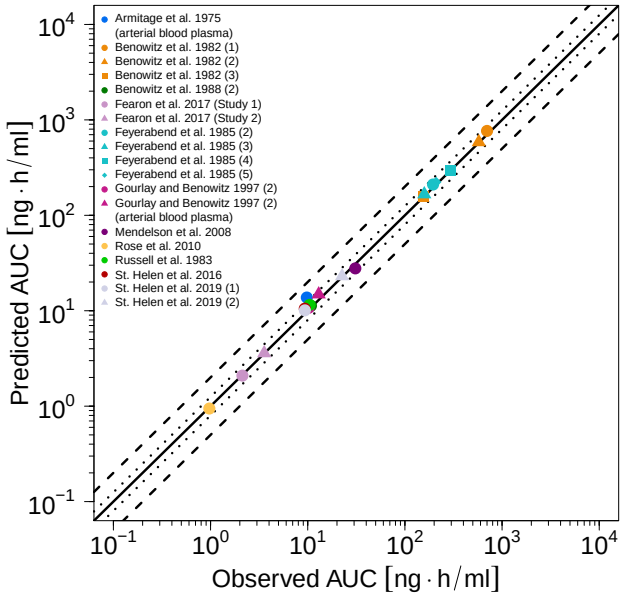

(b) C_{max}

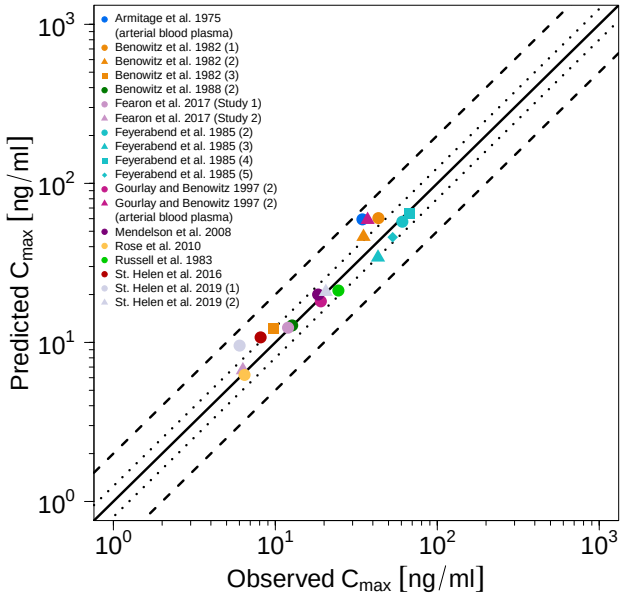

Figure S3.5.4: Predicted versus observed nicotine AUC (a) and C_{max} (b) values after pulmonary administration of combustible cigarettes (with estimated pulmonary nicotine exposure) and e-cigarettes. Each symbol represents the AUC_{last} or C_{max} of a different profile. The black solid (——) lines mark the lines of identity. Black dotted lines (·····) indicate 1.25-fold, black dashed lines (- -) indicate 2-fold deviation. **AUC**, area under the concentration–time curve from the first to the last data point; **C_{max}**, maximum concentration.

3.6 Pulmonary administration of nicotine (combustible cigarettes with machine smoked nicotine yields)

In this section, linear and semilogarithmic plots of plasma concentration-time profiles (Figs. S3.6.1 and S3.6.2), goodness-of-fit plots of predicted compared to observed plasma concentrations (Fig. S3.6.3) and goodness-of-fit plots of predicted compared to observed AUC_{last} and C_{max} values (Fig. S3.6.4) after administration of combustible cigarettes (with machine smoked nicotine yields) are shown.

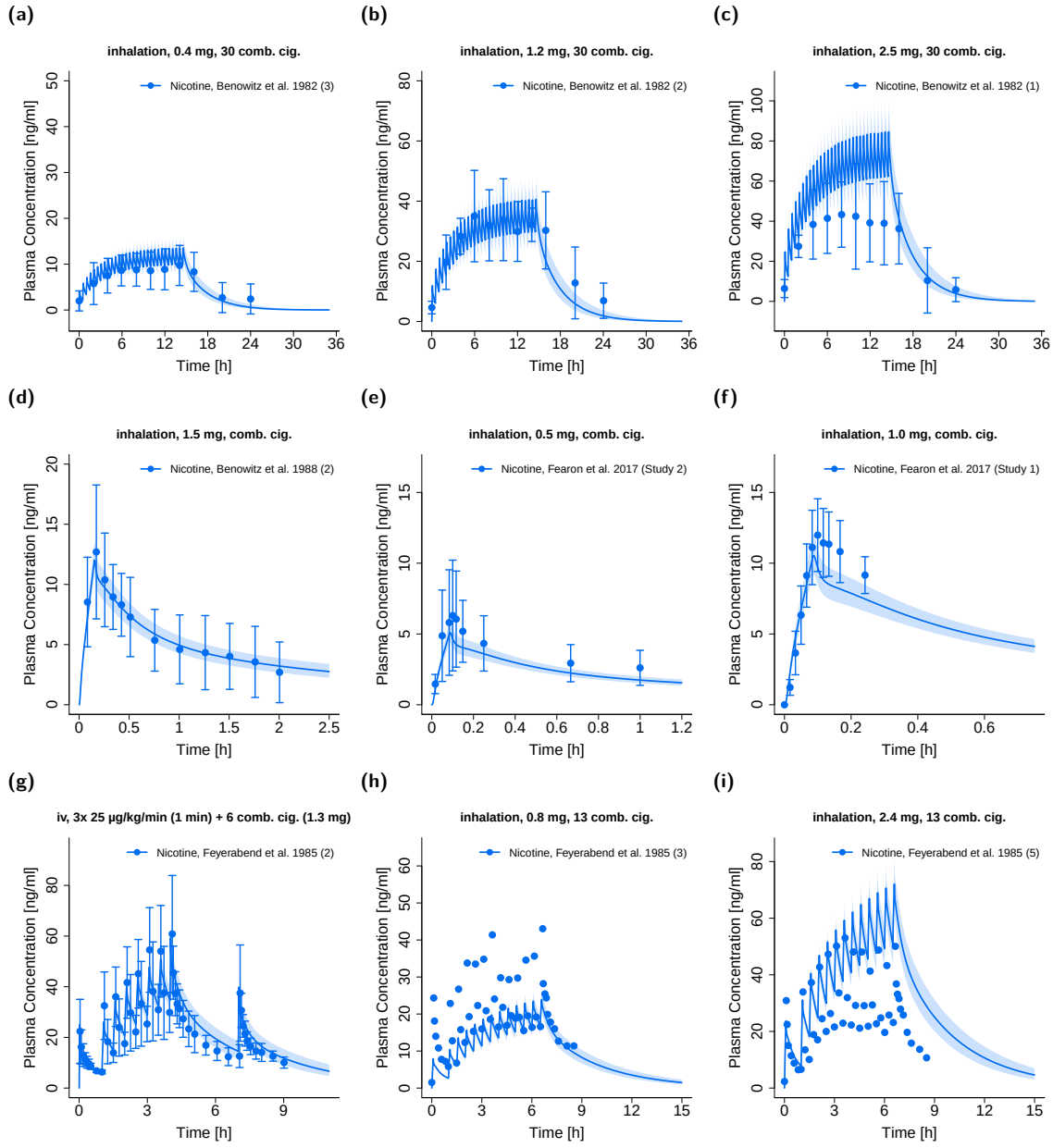

Figure S3.6.1: Nicotine plasma (•, •) concentration-time profiles (linear) after inhalation (combustible cigarettes with machine smoked nicotine yields). Observed data are shown as circles, if available ± standard deviation (SD). Population simulation (n=100) geometric means are shown as lines; the shaded areas represent the predicted population geometric SD. Machine smoked nicotine yields from the respective studies were used for nicotine doses (see Table S2.8.2). References with numbers in parentheses link to a specific observed dataset described in the study table (Table S2.6.1). **comb. cig.**, combustible cigarette; **iv**, intravenous.

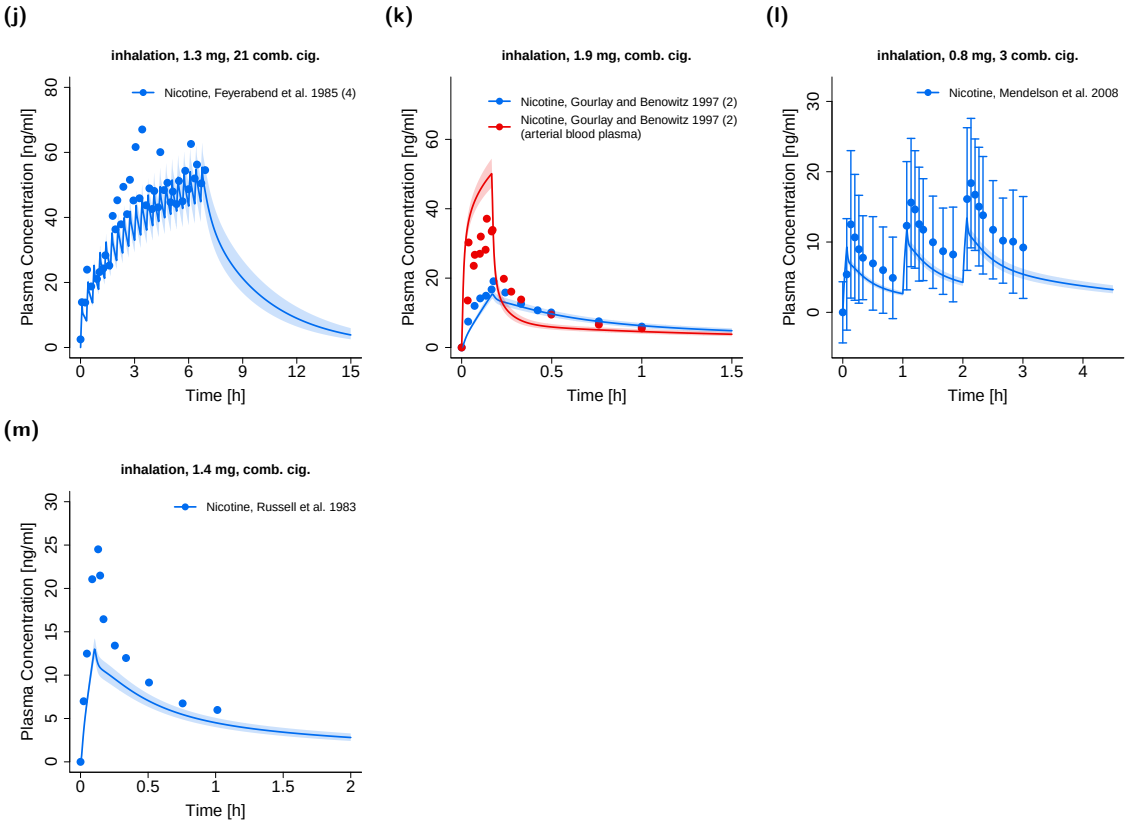

Figure S3.6.1: Nicotine plasma (•, •) concentration-time profiles (linear) after inhalation (combustible cigarettes with machine smoked nicotine yields). Observed data are shown as circles, if available ± standard deviation (SD). Population simulation (n=100) geometric means are shown as lines; the shaded areas represent the predicted population geometric SD. Machine smoked nicotine yields from the respective studies were used for nicotine doses (see Table S2.8.2). References with numbers in parentheses link to a specific observed dataset described in the study table (Table S2.6.1). **comb. cig.**, combustible cigarette; **iv**, intravenous. (continued)

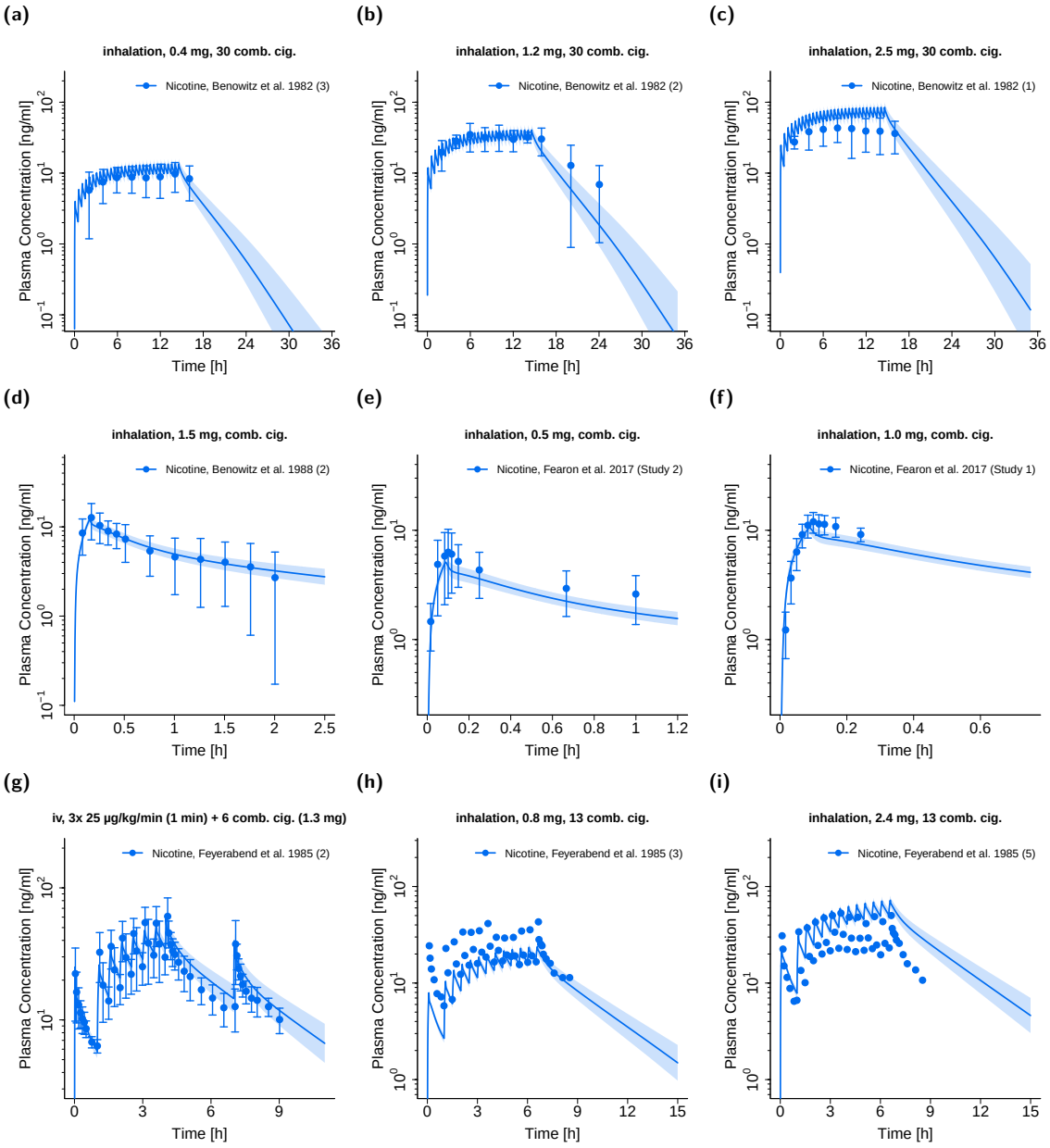

Figure S3.6.2: Nicotine plasma (●, ●) concentration-time profiles (semilogarithmic) after inhalation (combustible cigarettes with machine smoked nicotine yields). Observed data are shown as circles, if available ± standard deviation (SD). Population simulation (n=100) geometric means are shown as lines; the shaded areas represent the predicted population geometric SD. Machine smoked nicotine yields from the respective studies were used for nicotine doses (see Table S2.8.2). References with numbers in parentheses link to a specific observed dataset described in the study table (Table S2.6.1). **comb. cig.**, combustible cigarette; **iv**, intravenous.

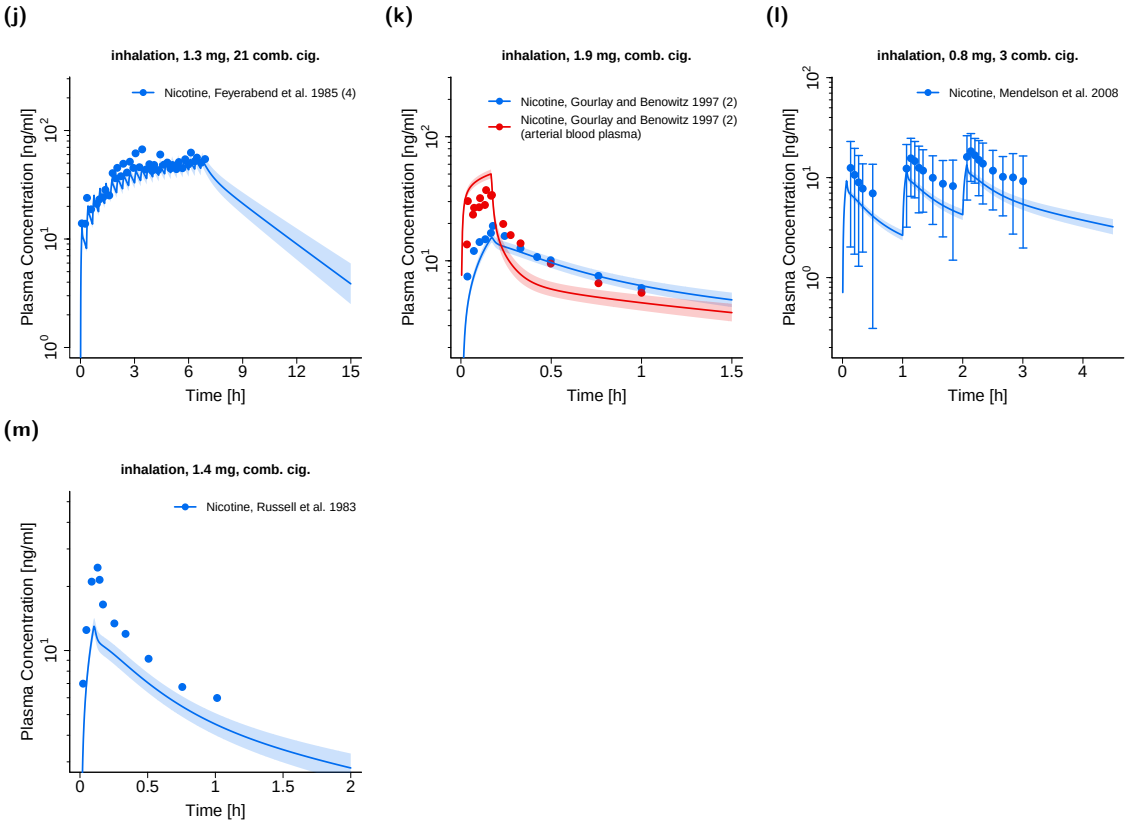

Figure S3.6.2: Nicotine plasma (●, ●) concentration-time profiles (semilogarithmic) after inhalation (combustible cigarettes with machine smoked nicotine yields). Observed data are shown as circles, if available ± standard deviation (SD). Population simulation (n=100) geometric means are shown as lines; the shaded areas represent the predicted population geometric SD. Machine smoked nicotine yields from the respective studies were used for nicotine doses (see Table S2.8.2). References with numbers in parentheses link to a specific observed dataset described in the study table (Table S2.6.1). **comb. cig.**, combustible cigarette; **iv**, intravenous. (continued)

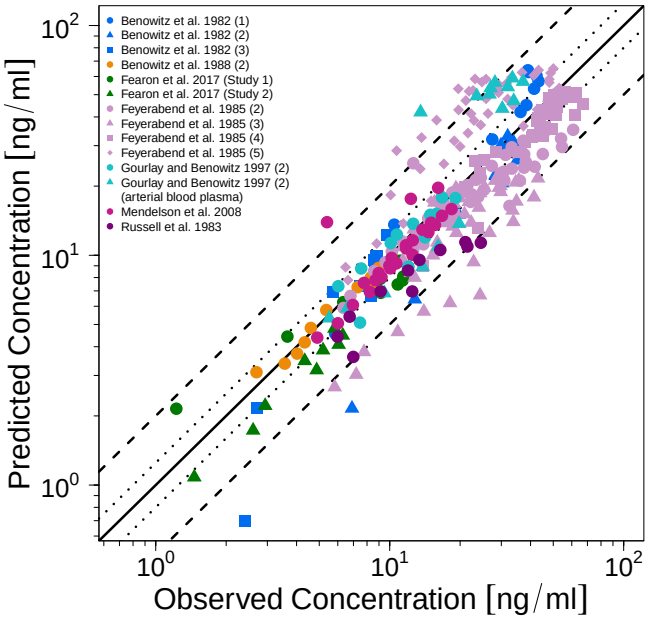

Figure S3.6.3: Predicted versus observed nicotine plasma concentrations after pulmonary administration of combustible cigarettes with machine smoked nicotine yields. The black solid (——) line marks the line of identity. Black dotted lines (·····) indicate 1.25-fold, black dashed lines (– –) indicate 2-fold deviation.

(a) AUC

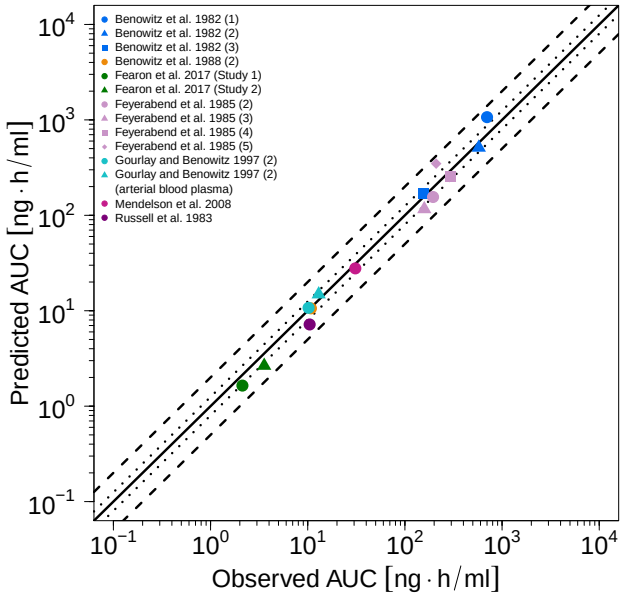

(b) C_{max}

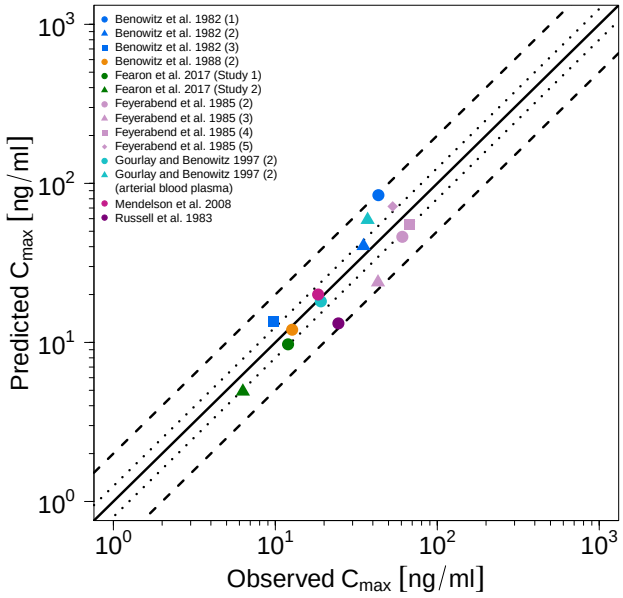

Figure S3.6.4: Predicted versus observed nicotine AUC_{last} (a) and C_{max} (b) values after pulmonary administration of combustible cigarettes with machine smoked nicotine yields. Each symbol represents the AUC_{last} or C_{max} of a different plasma profile. The black solid (——) lines mark the lines of identity. Black dotted lines (·····) indicate 1.25-fold, black dashed lines (– –) indicate 2-fold deviation. **AUC**, area under the plasma concentration–time curve from the first to the last data point; **C_{max}**, maximum plasma concentration.

3.7 Brain tissue concentration simulations

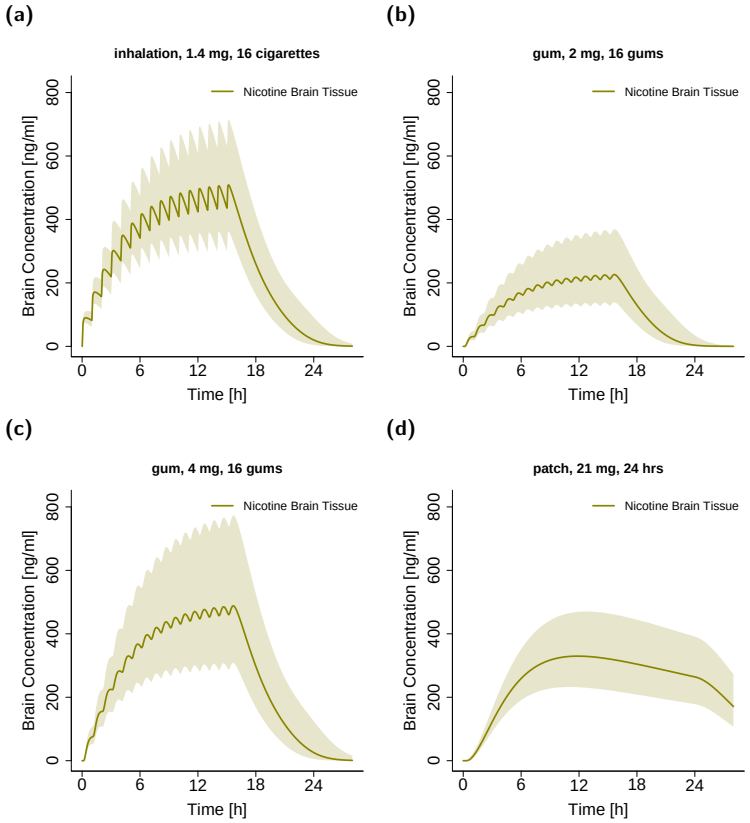

Figure S3.7.1: Simulations of nicotine brain tissue concentration-time profiles after pulmonary (16 hours), oral (2 mg and 4 mg gums, 16 hours) and transdermal (patch, 24 hours) nicotine administration. Population simulation (n=100) geometric means are shown as lines (–); the shaded areas represent the predicted population geometric SD. Detailed information about dosing regimens, study populations and model input parameters is given in Tables S2.6.1, S2.8.1 and S2.8.3. **patch**, transdermal therapeutic system (nicotine patch).

3.8 Quantitative PBPK model evaluation

As quantitative performance measures, mean relative deviations (MRD) of the predicted plasma concentrations for all observed and the corresponding predicted plasma concentrations and the geometric mean fold errors (GMFE) of the AUC_{last} and C_{max} were calculated according to Equation S10 and Equation S11, respectively.

$$MRD = 10^x \text{ with } x = \sqrt{\frac{1}{n}\sum_{i=1}^{n}(\log_{10}\hat{c}_i - \log_{10} c_i)^2} \tag{S10}$$

Here, c_i is the ith observed plasma concentration, $\hat{c}_i$ is the respective predicted plasma concentration and n equals the number of observed values. Overall MRD values of ≤ 2 were considered as reasonable predictions [68]. MRD values for all studies are given in Table S3.8.1.

The GMFE was calculated for all observed AUC_{last} and C_{max} values according to Equation S11.

$$GMFE = 10^x \text{ with } x = \frac{1}{n}\sum_{i=1}^{n}|\log_{10}(\frac{\hat{a}_i}{a_i})| \tag{S11}$$

Here, a_i is the ith observed AUC_{last} or C_{max} value, respectively, $\hat{a}_i$ is the predicted AUC_{last} or C_{max} value, respectively, and n equals the number of studies. The calculated GMFE values are shown in Table S3.8.2.

3.8.1 Mean relative deviation (MRD) values of nicotine and cotinine concentration predictions

Table S3.8.1: Mean relative deviation (MRD) values of nicotine and cotinine plasma concentration predictions.

Route	Dose	MRD	Reference
Nicotine			
iv (1 min, s.d.)	25.0 µg/kg	1.41	Feyerabend et al. 1985 (1) [30]
iv (10 min, s.d.)	28.0 µg/kg	1.62	Molander et al. 2001 (young) [32]
iv (10 min, s.d.)	28.0 µg/kg	1.50	Molander et al. 2001 (elderly) [32]
iv (24 h, s.d.)	19.8 mg	1.06	Benowitz et al. 1991a (1) [28]
iv (24 h, s.d.)	288.0 µg/kg	1.12	Benowitz et al. 1994b [29]
iv (30 min, m.d.)	75.0 µg/kg	1.16	Porchet et al. 1988 (1) [23]
iv (30 min, m.d.)	75.0 µg/kg	1.19	Porchet et al. 1988 (2) [23]
iv (30 min, m.d.)	75.0 µg/kg	1.19	Porchet et al. 1988 (3) [23]
iv (30 min, s.d.)	15.0 µg/kg	1.09	Andersson and Arner 2001 [27]
iv (30 min, s.d.)	60.0 µg/kg	1.11	Benowitz and Jacob 1994a (1) [1]
iv (30 min, s.d.)	15.0 µg/kg	1.15	Benowitz and Jacob 1993 (1) [12]
iv (30 min, s.d.)	15.0 µg/kg	1.13	Benowitz and Jacob 1993 (2) [12]
iv (30 min, s.d.)	60.0 µg/kg	1.16	Benowitz and Jacob 1993 (3) [12]
iv (30 min, s.d.)	60.0 µg/kg	1.20	Gourlay and Benowitz 1997 (1) [31]
iv (30 min, s.d.)	60.0 µg/kg	1.40	Gourlay and Benowitz 1997 (1) (arterial blood plasma) [31]
iv (30 min, s.d.)	15.0 µg/kg	1.17	Zevin et al. 1997 (1) [33]
iv (30 min, s.d.)	15.0 µg/kg	1.20	Zevin et al. 1997 (2) [33]
iv and inhalation (1 min, m.d. plus 6 combustible cigarettes)	1.8; 2.0 mg	1.21	Feyerabend et al. 1985 (2) [30]
po (cap, s.d.)	4.0 mg	1.17	Benowitz et al. 1991b (2) [34]
po (cap, s.d.)	3.0 mg	1.26	Benowitz et al. 1991b (1) [34]
po (cap, s.d.)	6.0 mg	1.31	Benowitz et al. 1991b (3) [34]
po (cap, s.d.)	6.0 mg	1.60	Green et al. 1999 (1) [36]
po (cap, s.d.)	15.0 mg	1.48	Green et al. 1999 (2) [36]
po (cap, s.d.)	4.0 mg	3.10	Xu et al. 2002 (NM) [5]
po (cap, s.d.)	4.0 mg	1.75	Xu et al. 2002 (PM) [5]

Overall MRD: 1.52 (80/91 with MRD ≤ 2)

-, not given; **cap**, capsule; **iv**, intravenous; **m.d.**, multiple dose; **MRD**, mean relative deviation; **NM**, normal metabolizer; **PM**, poor metabolizer; **po**, oral; **q.d.**, once daily; **q.i.d.**, four times daily; **s.d.**, single dose;

[a] cotinine metabolite

Table S3.8.1: Mean relative deviation (MRD) values of nicotine and cotinine plasma concentration predictions. *(continued)*

Route	Dose	MRD	Reference
gum (m.d., 12 gums)	2.0 mg	1.28	Dautzenberg et al. 2007 [39]
gum (m.d., 12 gums)	4.0 mg	1.37	Hansson et al. 2017 (3) [41]
gum (m.d., 13 gums)	4.0 mg	1.89	Choi et al. 2001 (3) [38]
gum (m.d., 13 gums)	2.0 mg	1.15	Choi et al. 2001 (2) [38]
gum (s.d.)	4.0 mg	3.51	Benowitz et al. 1988 (1) [21]
gum (s.d.)	2.0 mg	2.96	Choi et al. 2001 (1) [38]
gum (s.d.)	4.0 mg	1.21	Choi et al. 2001 (4) [38]
gum (s.d.)	2.0 mg	1.50	Du 2018 (1) [40]
gum (s.d.)	4.0 mg	1.55	Du 2018 (2) [40]
gum (s.d.)	2.0 mg	2.26	Hansson et al. 2017 (1) [41]
gum (s.d.)	4.0 mg	1.72	Hansson et al. 2017 (2) [41]
inhalation (13 combustible cigarettes, m.d.)	1.1 mg	1.40	Feyerabend et al. 1985 (3) [30]
inhalation (13 combustible cigarettes, m.d.)	1.5 mg	1.39	Feyerabend et al. 1985 (5) [30]
inhalation (21 combustible cigarettes, m.d.)	1.5 mg	1.15	Feyerabend et al. 1985 (4) [30]
inhalation (3 combustible cigarettes, m.d.)	1.2 mg	1.27	Mendelson et al. 2008 [48]
inhalation (30 combustible cigarettes, m.d.)	1.8 mg	1.58	Benowitz et al. 1982 (3) [46]
inhalation (30 combustible cigarettes, m.d.)	1.4 mg	1.48	Benowitz et al. 1982 (2) [46]
inhalation (30 combustible cigarettes, m.d.)	0.4 mg	1.25	Benowitz et al. 1982 (1) [46]
inhalation (combustible cigarettes, s.d.)	2.2 mg	1.19	Gourlay and Benowitz 1997 (2) [31]
inhalation (combustible cigarettes, s.d.)	2.2 mg	1.73	Gourlay and Benowitz 1997 (2) (arterial blood plasma) [31]
inhalation (combustible cigarettes, s.d.)	1.6 mg	1.09	Benowitz et al. 1988 (2) [21]
inhalation (combustible cigarettes, s.d.)	0.7 mg	1.08	Fearon et al. 2017 (Study 2) [47]
inhalation (combustible cigarettes, s.d.)	1.3 mg	1.36	Fearon et al. 2017 (Study 1) [47]
inhalation (combustible cigarettes, s.d.)	2.2 mg	1.20	Russell et al. 1983 [49]
inhalation (combustible cigarettes, s.d.)	2.4 mg	1.08	St. Helen et al. 2019 (2) [51]
inhalation (combustible cigarettes, s.d.)	2.1 mg	1.69	Armitage et al. 1975 (arterial blood plasma) [45]
inhalation (combustible cigarettes, s.d.)	0.14 mg	1.57	Rose et al. 2010 [13]
inhalation (e-cigarettes, s.d.)	0.9 mg	1.17	St. Helen et al. 2019 (1) [51]
inhalation (e-cigarettes, s.d.)	1.2 mg	1.16	St. Helen et al. 2016 [50]
transdermal (16 h, m.d.)	15.0 mg	1.08	Fant et al. 2000 (Novartis) [43]
transdermal (24 h, m.d.)	21.0 mg	1.34	Fant et al. 2000 (Alza) [43]
transdermal (24 h, m.d.)	21.0 mg	1.19	Fant et al. 2000 (Upjohn) [43]
transdermal (24 h, m.d., 7 days)	30.0 mg	1.36	Bannon et al. 1989 (3) [42]
transdermal (24 h, q.d., 7 days)	36.0 mg	1.40	Gupta et al. 1993 (2) [44]
transdermal (24 h, s.d.)	52.5 mg	1.56	Benowitz et al. 1991a (2) [28]
transdermal (24 h, s.d.)	15 mg	1.18	Bannon et al. 1989 (1) [42]
transdermal (24 h, s.d.)	30 mg	1.07	Bannon et al. 1989 (2) [42]
transdermal (24 h, s.d.)	60 mg	1.22	Bannon et al. 1989 (4) [42]
transdermal (24 h, s.d.)	36 mg	1.12	Gupta et al. 1993 (1) [44]
Nicotine MRD		**1.44**	**(60/64 with MRD ≤ 2)**
Cotinine			
iv (1.5-3 min, s.d.)	20.0 mg	1.10	Curvall et al. 1990 (3) [52]
iv (1.5-3 min, s.d.)	10.0 mg	1.14	Curvall et al. 1990 (2) [52]
iv (1.5-3 min, s.d.)	5.0 mg	1.24	Curvall et al. 1990 (1) [52]
iv (10 min, s.d.)[a]	28.0 µg/kg	1.08	Molander et al. 2001 (young) [32]
iv (10 min, s.d.)[a]	28.0 µg/kg	1.04	Molander et al. 2001 (elderly) [32]
iv (24 h, s.d.)[a]	19.8 mg	4.74	Benowitz et al. 1991a (1) [28]
iv (24 h, s.d.)[a]	288.0 µg/kg	1.32	Benowitz et al. 1994b [29]
iv (30 min, s.d.)[a]	60.0 µg/kg	1.46	Benowitz and Jacob 1994a (1) [1]
iv (30 min, s.d.)	60.0 µg/kg	1.37	Benowitz and Jacob 1994a (2) [1]
iv (30 min, s.d.)[a]	15.0 µg/kg	1.87	Benowitz and Jacob 1993 (1) [12]
iv (30 min, s.d.)[a]	60.0 µg/kg	2.22	Benowitz and Jacob 1993 (2) [12]
iv (30 min, s.d.)[a]	60.0 µg/kg	1.68	Benowitz and Jacob 1993 (3) [12]
iv (30 min, s.d.)[a]	60.0 µg/kg	2.32	Gourlay and Benowitz 1997 (1) [31]
iv (30 min, s.d.)[a]	60.0 µg/kg	2.36	Gourlay and Benowitz 1997 (1) (arterial blood plasma) [31]
iv (30 min, s.d.)	15.0 µg/kg	1.25	Zevin et al. 1997 (3) [33]
iv (30 min, s.d.)	15.0 µg/kg	1.26	Zevin et al. 1997 (4) [33]
iv (30 min, s.d.)	20.0 mg	1.10	De Schepper et al. 1987 (3) [4]
iv (30 min, s.d.)	10.0 mg	1.14	De Schepper et al. 1987 (2) [4]
Overall MRD: 1.52 (80/91 with MRD ≤ 2)			

-, not given; **cap**, capsule; **iv**, intravenous; **m.d.**, multiple dose; **MRD**, mean relative deviation; **NM**, normal metabolizer; **PM**, poor metabolizer; **po**, oral; **q.d.**, once daily; **q.i.d.**, four times daily; **s.d.**, single dose;
[a] cotinine metabolite

Table S3.8.1: Mean relative deviation (MRD) values of nicotine and cotinine plasma concentration predictions. *(continued)*

Route	Dose	MRD	Reference
iv (30 min, s.d.)	5.0 mg	1.09	De Schepper et al. 1987 (1) [4]
po (-, q.i.d., 5 days)[a]	0.05 mg	1.42	Benowitz et al. 2010 [35]
po (cap, 7 times/day, 5 days)[a]	4.0 mg	2.14	Jarvis et al. 1988 [37]
po (cap, s.d.)[a]	6.0 mg	1.12	Green et al. 1999 (1) [36]
po (cap, s.d.)[a]	15.0 mg	1.18	Green et al. 1999 (2) [36]
po (cap, s.d.)[a]	4.0 mg	2.01	Xu et al. 2002 (NM) [5]
po (cap, s.d.)[a]	4.0 mg	2.20	Xu et al. 2002 (PM) [5]
transdermal (24 h, q.d., 7 days)[a]	36.0 mg	1.06	Gupta et al. 1993 (2) [44]
transdermal (24 h, s.d.)[a]	36.0 mg	1.91	Gupta et al. 1993 (1) [44]
Cotinine MRD		**1.77**	**(20/27 with MRD ≤ 2)**

Overall MRD: 1.52 (80/91 with MRD ≤ 2)

-, not given; **cap**, capsule; **iv**, intravenous; **m.d.**, multiple dose; **MRD**, mean relative deviation; **NM**, normal metabolizer; **PM**, poor metabolizer; **po**, oral; **q.d.**, once daily; **q.i.d.**, four times daily; **s.d.**, single dose;
[a] cotinine metabolite

3.8.2 Geometric mean fold error (GMFE) for nicotine and cotinine concentration-time profiles

Table S3.8.2: Predicted and observed AUC_{last} and C_{max} values of nicotine, cotinine metabolite and cotinine after intravenous administration

		AUC_{last}			C_{max}			
Route	Dose	Pred	Obs	Pred/Obs	Pred	Obs	Pred/Obs	Reference
Nicotine								
iv (1 min, s.d.)	25.0 µg/kg	9.52	10.09	0.94	24.01	23.05	1.04	Feyerabend et al. 1985 (1) [30]
iv (10 min, s.d.)	28.0 µg/kg	28.70	24.92	1.15	17.63	10.51	1.68	Molander et al. 2001 (young) [32]
iv (10 min, s.d.)	28.0 µg/kg	37.25	32.47	1.15	21.91	17.29	1.27	Molander et al. 2001 (elderly) [32]
iv (24 h, s.d.)	19.8 mg	282.59	286.29	0.99	11.88	13.19	0.90	Benowitz et al. 1991a (1) [28]
iv (24 h, s.d.)	288.0 µg/kg	304.03	285.59	1.06	13.14	15.07	0.87	Benowitz et al. 1994b [29]
iv (30 min, m.d.)	75.0 µg/kg	141.94	125.34	1.13	52.92	45.36	1.17	Porchet et al. 1988 (1) [23]
iv (30 min, m.d.)	75.0 µg/kg	132.54	117.64	1.13	49.40	37.91	1.30	Porchet et al. 1988 (2) [23]
iv (30 min, m.d.)	75.0 µg/kg	117.40	103.33	1.14	45.99	39.51	1.16	Porchet et al. 1988 (3) [23]
iv (30 min, s.d.)	15.0 µg/kg	6.62	6.74	0.98	7.59	7.42	1.02	Andersson and Arner 2001 [27]
iv (30 min, s.d.)	60.0 µg/kg	55.19	50.80	1.09	29.18	24.22	1.20	Benowitz and Jacob 1994a (1) [1]
iv (30 min, s.d.)	15.0 µg/kg	12.14	10.80	1.12	7.93	6.19	1.28	Benowitz and Jacob 1993 (1) [12]
iv (30 min, s.d.)	15.0 µg/kg	12.40	12.87	0.96	8.02	8.31	0.97	Benowitz and Jacob 1993 (2) [12]
iv (30 min, s.d.)	60.0 µg/kg	62.36	59.51	1.05	31.87	29.62	1.08	Benowitz and Jacob 1993 (3) [12]
iv (30 min, s.d.)	60.0 µg/kg	21.19	19.50	1.09	32.42	28.81	1.12	Gourlay and Benowitz 1997 (1) [31]
iv (30 min, s.d.)	60.0 µg/kg	30.85	29.86	1.03	56.34	48.36	1.17	Gourlay and Benowitz 1997 (1) (arterial blood plasma) [31]
iv (30 min, s.d.)	15.0 µg/kg	13.06	13.00	1.00	7.44	6.96	1.07	Zevin et al. 1997 (1) [33]
iv (30 min, s.d.)	15.0 µg/kg	13.06	13.35	0.98	7.44	7.58	0.98	Zevin et al. 1997 (2) [33]
iv and inhalation (1 min, m.d. plus 6 combustible cigarettes)	1.8; 2.0 mg	210.37	194.84	1.08	57.41	60.83	0.94	Feyerabend et al. 1985 (2) [30]
po (cap, s.d.)	4.0 mg	17.24	18.70	0.92	6.24	6.39	0.98	Benowitz et al. 1991b (2) [34]
po (cap, s.d.)	3.0 mg	22.28	21.08	1.06	8.14	7.51	1.08	Benowitz et al. 1991b (1) [34]
po (cap, s.d.)	6.0 mg	32.16	39.65	0.81	11.88	18.75	0.63	Benowitz et al. 1991b (3) [34]
po (cap, s.d.)	6.0 mg	20.96	23.69	0.88	2.10	2.20	0.96	Green et al. 1999 (1) [36]
po (cap, s.d.)	15.0 mg	52.25	47.69	1.10	5.10	5.00	1.02	Green et al. 1999 (2) [36]
po (cap, s.d.)	4.0 mg	20.91	29.45	0.71	7.18	7.74	0.93	Xu et al. 2002 (NM) [5]
po (cap, s.d.)	4.0 mg	67.38	112.77	0.60	19.30	22.15	0.87	Xu et al. 2002 (PM) [5]
gum (m.d., 12 gums)	2.0 mg	115.38	105.77	1.09	10.24	9.58	1.07	Dautzenberg et al. 2007 [39]
gum (m.d., 12 gums)	4.0 mg	185.20	232.74	0.80	20.65	29.68	0.70	Hansson et al. 2017 (3) [41]
gum (m.d., 13 gums)	4.0 mg	22.63	34.08	0.66	9.40	9.91	0.95	Choi et al. 2001 (3) [38]
gum (m.d., 13 gums)	2.0 mg	120.80	101.20	1.19	12.56	14.30	0.88	Choi et al. 2001 (2) [38]
gum (s.d.)	4.0 mg	8.30	9.76	0.85	6.57	6.50	1.01	Benowitz et al. 1988 (1) [21]
gum (s.d.)	2.0 mg	11.36	10.01	1.13	4.71	3.64	1.29	Choi et al. 2001 (1) [38]
gum (s.d.)	4.0 mg	241.18	217.14	1.11	25.16	30.10	0.84	Choi et al. 2001 (4) [38]
gum (s.d.)	2.0 mg	10.73	10.37	1.03	4.08	3.37	1.21	Du 2018 (1) [40]
gum (s.d.)	4.0 mg	21.40	21.48	1.00	8.10	6.47	1.25	Du 2018 (2) [40]

Total GMFE (AUC_{last}): 1.12 (1.00–1.80)
Total GMFE (C_{max}) : 1.15 (1.00–1.72)

-, not given; **AUC**, area under the concentration–time curve from the first to the last data point; **cap**, capsule; **C_{max}**, maximum concentration; **GMFE**, geometric mean fold error; **iv**, intravenous; **m.d.**, multiple dose; **NM**, normal metabolizer; **obs**, observed; **PM**, poor metabolizer; **po**, oral; **pred**, predicted; **q.d.**, once daily; **q.i.d.**, four times daily; **s.d.**, single dose;
[a] cotinine metabolite

Table S3.8.2: Predicted and observed AUC_{last} and C_{max} values of nicotine, cotinine after intravenous administration and cotinine metabolite *(continued)*

		AUC_{last}			**C_{max}**			
Route	Dose	Pred	Obs	Pred/Obs	Pred	Obs	Pred/Obs	Reference
gum (s.d.)	2.0 mg	12.43	21.11	0.59	4.53	6.59	0.69	Hansson et al. 2017 (1) [41]
gum (s.d.)	4.0 mg	25.07	33.92	0.74	9.02	10.13	0.89	Hansson et al. 2017 (2) [41]
inhalation (13 combustible cigarettes, m.d.)	1.1 mg	166.34	158.34	1.05	34.22	43.04	0.80	Feyerabend et al. 1985 (3) [30]
inhalation (13 combustible cigarettes, m.d.)	1.5 mg	222.82	209.81	1.06	45.87	53.04	0.86	Feyerabend et al. 1985 (5) [30]
inhalation (21 combustible cigarettes, m.d.)	1.5 mg	292.69	291.80	1.00	64.21	67.05	0.96	Feyerabend et al. 1985 (4) [30]
inhalation (3 combustible cigarettes, m.d.)	1.2 mg	27.80	30.89	0.90	20.01	18.38	1.09	Mendelson et al. 2008 [48]
inhalation (30 combustible cigarettes, m.d.)	1.8 mg	155.80	156.44	1.00	12.26	9.72	1.26	Benowitz et al. 1982 (3) [46]
inhalation (30 combustible cigarettes, m.d.)	1.4 mg	585.29	576.54	1.02	46.16	35.03	1.32	Benowitz et al. 1982 (2) [46]
inhalation (30 combustible cigarettes, m.d.)	0.4 mg	766.59	700.24	1.09	60.49	43.29	1.40	Benowitz et al. 1982 (1) [46]
inhalation (combustible cigarettes, s.d.)	2.2 mg	10.73	10.20	1.05	18.12	19.10	0.95	Gourlay and Benowitz 1997 (2) [31]
inhalation (combustible cigarettes, s.d.)	2.2 mg	14.87	12.97	1.15	58.99	37.13	1.59	Gourlay and Benowitz 1997 (2) (arterial blood plasma) [31]
inhalation (combustible cigarettes, s.d.)	1.6 mg	11.27	10.79	1.04	12.79	12.70	1.01	Benowitz et al. 1988 (2) [21]
inhalation (combustible cigarettes, s.d.)	0.7 mg	3.60	3.57	1.01	6.69	6.30	1.06	Fearon et al. 2017 (Study 2) [47]
inhalation (combustible cigarettes, s.d.)	1.3 mg	2.09	2.13	0.98	12.38	11.98	1.03	Fearon et al. 2017 (Study 1) [47]
inhalation (combustible cigarettes, s.d.)	2.2 mg	11.53	10.46	1.10	21.21	24.51	0.87	Russell et al. 1983 [49]
inhalation (combustible cigarettes, s.d.)	2.4 mg	23.06	22.58	1.02	20.80	20.50	1.01	St. Helen et al. 2019 (2) [51]
inhalation (combustible cigarettes, s.d.)	2.1 mg	13.76	9.79	1.41	59.41	34.50	1.72	Armitage et al. 1975 (arterial blood plasma) [45]
inhalation (combustible cigarettes, s.d.)	0.14 mg	0.94	0.97	0.97	6.25	6.45	0.97	Rose et al. 2010 [13]
inhalation (e-cigarettes, s.d.)	0.9 mg	10.10	9.34	1.08	9.55	6.02	1.59	St. Helen et al. 2019 (1) [51]
inhalation (e-cigarettes, s.d.)	1.2 mg	10.52	9.33	1.13	10.76	8.11	1.33	St. Helen et al. 2016 [50]
transdermal (16 h, m.d.)	15.0 mg	997.83	989.51	1.01	16.41	17.97	0.91	Fant et al. 2000 (Novartis) [43]
transdermal (24 h, m.d.)	21.0 mg	1168.23	1107.57	1.05	18.62	26.65	0.70	Fant et al. 2000 (Alza) [43]
transdermal (24 h, m.d.)	21.0 mg	516.08	521.19	0.99	9.96	11.52	0.86	Fant et al. 2000 (Upjohn) [43]
transdermal (24 h, m.d., 7 days)	30.0 mg	568.18	457.57	1.24	15.98	15.19	1.05	Bannon et al. 1989 (3) [42]
transdermal (24 h, q.d., 7 days)	36.0 mg	451.81	366.48	1.23	17.16	19.33	0.89	Gupta et al. 1993 (2) [44]
transdermal (24 h, s.d.)	52.5 mg	188.12	190.92	0.99	7.96	9.51	0.84	Benowitz et al. 1991a (2) [28]
transdermal (24 h, s.d.)	15.0 mg	151.09	150.41	1.00	7.42	6.86	1.08	Bannon et al. 1989 (1) [42]
transdermal (24 h, s.d.)	30.0 mg	300.41	288.76	1.04	14.81	15.76	0.94	Bannon et al. 1989 (2) [42]
transdermal (24 h, s.d.)	60.0 mg	600.29	501.96	1.20	29.60	26.98	1.10	Bannon et al. 1989 (4) [42]
transdermal (24 h, s.d.)	36.0 mg	417.71	409.07	1.02	15.87	18.12	0.88	Gupta et al. 1993 (1) [44]
Nicotine GMFE			**1.11 (1.00–1.70)**			**1.17 (1.01–1.72)**		
Cotinine								
iv (1.5-3 min, s.d.)	20.0 mg	1123.80	1091.34	1.03	207.30	138.84	1.49	Curvall et al. 1990 (3) [52]
iv (1.5-3 min, s.d.)	10.0 mg	2278.15	2367.41	0.96	414.59	326.58	1.27	Curvall et al. 1990 (2) [52]
iv (1.5-3 min, s.d.)	5.0 mg	5120.26	5019.92	1.02	829.19	640.50	1.29	Curvall et al. 1990 (1) [52]
iv (10 min, s.d.)[a]	28.0 µg/kg	587.72	622.84	0.94	61.40	62.36	0.98	Molander et al. 2001 (young) [32]
iv (10 min, s.d.)[a]	28.0 µg/kg	868.09	882.38	0.98	84.08	86.76	0.97	Molander et al. 2001 (elderly) [32]

Total GMFE (AUC_{last}): 1.12 (1.00–1.80)
Total GMFE (C_{max}) : 1.15 (1.00–1.72)

-, not given; **AUC**, area under the concentration–time curve from the first to the last data point; **cap**, capsule; **C_{max}**, maximum concentration; **GMFE**, geometric mean fold error; **iv**, intravenous; **m.d.**, multiple dose; **NM**, normal metabolizer; **obs**, observed; **PM**, poor metabolizer; **po**, oral; **pred**, predicted; **q.d.**, once daily; **q.i.d.**, four times daily; **s.d.**, single dose;
[a] cotinine metabolite

Table S3.8.2: Predicted and observed AUC_{last} and C_{max} values of nicotine, cotinine after intravenous administration and cotinine metabolite *(continued)*

		AUC_{last}			C_{max}			
Route	Dose	Pred	Obs	Pred/Obs	Pred	Obs	Pred/Obs	Reference
iv (24 h, s.d.)[a]	19.8 mg	2556.29	2683.54	0.95	124.38	141.56	0.88	Benowitz et al. 1991a (1) [28]
iv (24 h, s.d.)[a]	288.0 µg/kg	3121.84	3278.14	0.95	134.73	158.64	0.85	Benowitz et al. 1994b [29]
iv (30 min, s.d.)[a]	60.0 µg/kg	830.69	1028.67	0.81	36.88	39.28	0.94	Benowitz and Jacob 1994a (1) [1]
iv (30 min, s.d.)	60.0 µg/kg	1125.82	1317.41	0.85	112.74	86.71	1.30	Benowitz and Jacob 1994a (2) [1]
iv (30 min, s.d.)[a]	15.0 µg/kg	253.91	342.80	0.74	10.03	10.69	0.94	Benowitz and Jacob 1993 (1) [12]
iv (30 min, s.d.)[a]	60.0 µg/kg	245.43	440.95	0.56	9.68	10.49	0.92	Benowitz and Jacob 1993 (2) [12]
iv (30 min, s.d.)[a]	60.0 µg/kg	981.12	1228.36	0.80	37.76	37.29	1.01	Benowitz and Jacob 1993 (3) [12]
iv (30 min, s.d.)[a]	60.0 µg/kg	189.53	183.33	1.03	37.97	36.61	1.04	Gourlay and Benowitz 1997 (1) [31]
iv (30 min, s.d.)[a]	60.0 µg/kg	198.99	198.82	1.00	38.10	38.01	1.00	Gourlay and Benowitz 1997 (1) (arterial blood plasma) [31]
iv (30 min, s.d.)	15.0 µg/kg	228.90	248.78	0.92	28.26	20.98	1.35	Zevin et al. 1997 (3) [33]
iv (30 min, s.d.)	15.0 µg/kg	228.93	264.75	0.86	28.26	27.57	1.03	Zevin et al. 1997 (4) [33]
iv (30 min, s.d.)	20.0 mg	1332.21	1329.89	1.00	136.93	137.05	1.00	De Schepper et al. 1987 (3) [4]
iv (30 min, s.d.)	10.0 mg	2664.42	2322.18	1.15	273.85	286.25	0.96	De Schepper et al. 1987 (2) [4]
iv (30 min, s.d.)	5.0 mg	5328.83	5034.70	1.06	547.70	517.04	1.06	De Schepper et al. 1987 (1) [4]
po (-, q.i.d., 5 days)[a]	0.05 mg	22.68	27.48	0.83	2.48	2.42	1.02	Benowitz et al. 2010 [35]
po (cap, 7 times/day, 5 days)[a]	4.0 mg	3161.91	5705.77	0.55	336.93	294.00	1.15	Jarvis et al. 1988 [37]
po (cap, s.d.)[a]	6.0 mg	813.08	769.41	1.06	32.07	32.19	1.00	Green et al. 1999 (1) [36]
po (cap, s.d.)[a]	15.0 mg	2030.27	1942.74	1.05	79.60	91.85	0.87	Green et al. 1999 (2) [36]
po (cap, s.d.)[a]	4.0 mg	291.79	235.60	1.24	61.21	58.91	1.04	Xu et al. 2002 (NM) [5]
po (cap, s.d.)[a]	4.0 mg	23.67	20.36	1.16	5.29	6.42	0.83	Xu et al. 2002 (PM) [5]
transdermal (24 h, q.d., 7 days)[a]	36.0 mg	7638.70	7499.03	1.02	228.97	243.25	0.94	Gupta et al. 1993 (2) [44]
transdermal (24 h, s.d.)[a]	36.0 mg	4106.03	4172.18	0.98	155.78	156.90	0.99	Gupta et al. 1993 (1) [44]
Cotinine GMFE			**1.14 (1.00–1.80)**			**1.11 (1.00–1.49)**		

Total GMFE (AUC_{last}): 1.12 (1.00–1.80)
Total GMFE (C_{max}) : 1.15 (1.00–1.72)

-, not given; **AUC**, area under the concentration–time curve from the first to the last data point; **cap**, capsule; **C_{max}**, maximum concentration; **GMFE**, geometric mean fold error; **iv**, intravenous; **m.d.**, multiple dose; **NM**, normal metabolizer; **obs**, observed; **PM**, poor metabolizer; **po**, oral; **pred**, predicted; **q.d.**, once daily; **q.i.d.**, four times daily; **s.d.**, single dose;
[a] cotinine metabolite

3.9 AUC_{last} and C_{max} goodness of fit plots

(a) AUC

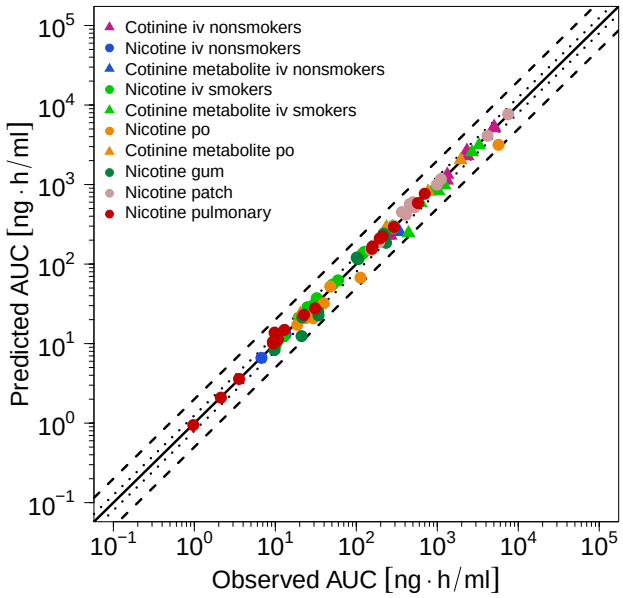

(b) C_{max}

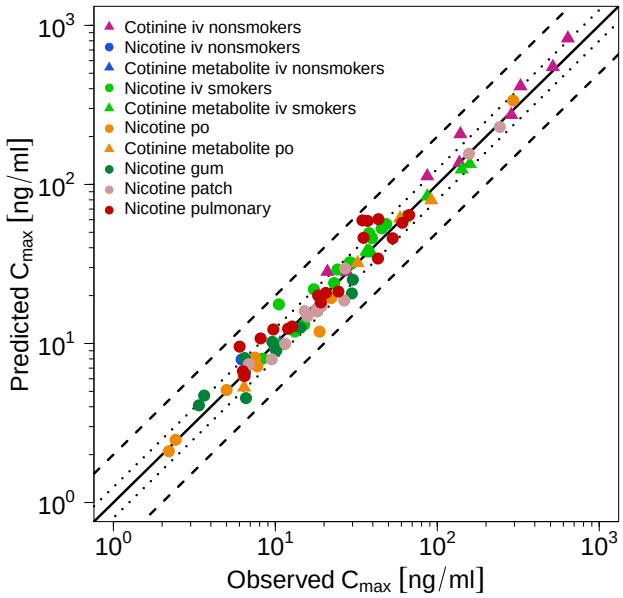

Figure S3.9.1: Predicted versus observed nicotine and cotinine AUC_{last} (a) and C_{max} (b) values. Each symbol represents the AUC_{last} or C_{max} of a different plasma profile (circles: nicotine, triangles: cotinine metabolite and cotinine iv). The black solid (——) lines mark the lines of identity. Black dotted lines (·····) indicate 1.25-fold, black dashed lines (- -) indicate 2-fold deviation. **AUC**, area under the concentration–time curve from the first to the last data point; **C_{max}**, maximum concentration; **iv**, intravenous; **patch**, transdermal therapeutic system (nicotine patch); **po**, oral.

3.10 Nicotine and cotinine PBPK model sensitivity analysis

A sensitivity analysis of the final nicotine and cotinine PBPK model to single parameter changes (local sensitivity analysis) was performed. Sensitivity of the PBPK model was measured as the relative change of the AUC from the last applied dose in a steady-state scenario extrapolated to infinity (AUC_{inf}) of the largest applied pulmonary dose of nicotine in the clinical studies used for the PBPK model development (30 times 2.5 mg during 15 hours). Parameters, optimized as well as parameters fixed to literature values, were included into the analysis if they had significant impact in former models (e.g. glomerular filtration rate fraction) or if they might have a strong influence due to calculation methods used in the model (e.g. fraction unbound) and/or if they have been optimized. Model sensitivity to a model parameter was calculated as the ratio of the relative change of the simulated AUC_{inf} of nicotine and cotinine metabolite, respectively, to the relative variation of the parameter around the value used in the final model according to Equation S12.

$$S = \frac{\Delta AUC_{inf}}{\Delta p} \cdot \frac{p}{AUC_{inf}} \tag{S12}$$

where S is the sensitivity of the AUC_{inf} to the examined model parameter, ΔAUC_{inf} is the change of the AUC_{inf}, AUC_{inf} is the simulated AUC_{inf} with the original parameter value, p is the original model parameter value and Δp is the variation of the model parameter value. A sensitivity value of +1.0 signifies that a 10 % increase of the examined parameter causes a 10 % increase of the simulated AUC_{inf}. The analysis was performed using a relative perturbation of parameters of 10 %.

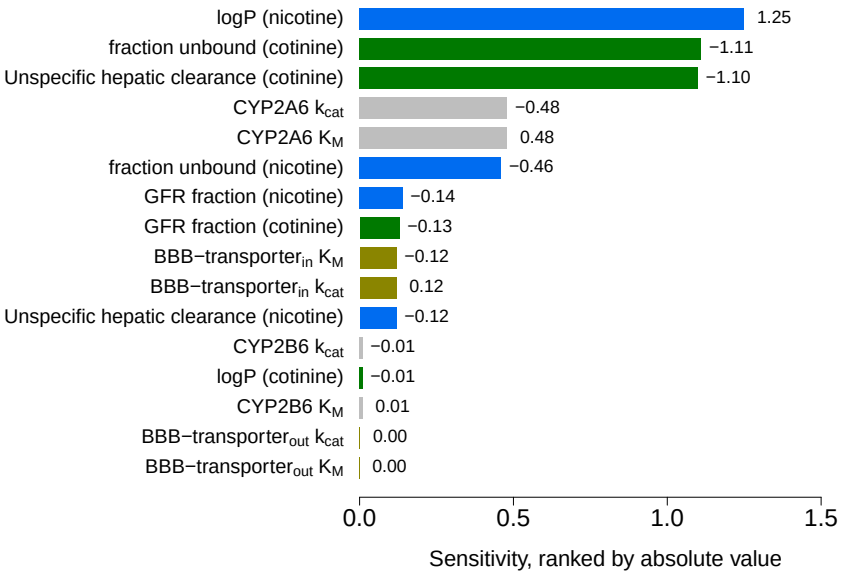

Figure S3.10.1: Nicotine and cotinine PBPK model local sensitivity analysis. Sensitivity of the model to single parameters, measured as change of the simulated area under the plasma concentration-time curve of nicotine and cotinine metabolite, respectively, from the last applied dose in a steady-state scenario (30 times 2.5 mg over 15 hours) extrapolated to infinity (AUC_{inf}). A sensitivity value of +1.0 signifies that a 10 % increase of the examined parameter causes a 10 % increase of the simulated AUC_{inf}.

The results of the local sensitivity analysis (see Figure S3.10.1) reveal that, among the tested parameters, lipophilicity of nicotine and fraction unbound and unspecific hepatic clearance of cotinine have the biggest impact on the tested nicotine and cotinine AUC_{inf}. The analysis underlines the model's

sensitivity to changes in the lipophilicity of nicotine, which plays a key role in many calculation methods (e.g. partition coefficients) in the PBPK model. The fact that the unspecific heaptic clearance of cotinine represents the major route of elimination for cotinine in the model explains the high sensitivity of the model to this parameter. Additionally, the high sensitivity to the fraction unbound of cotinine is to be expected, as the fraction unbound determines the concentrations available for all pharmacokinetic processes. Values for the fractions unbound used in the model have been obtained from literature [58, 59] and were not subject to any fitting endeavours.

3.11 Heart rate population predictions after nicotine intake compared to observed data

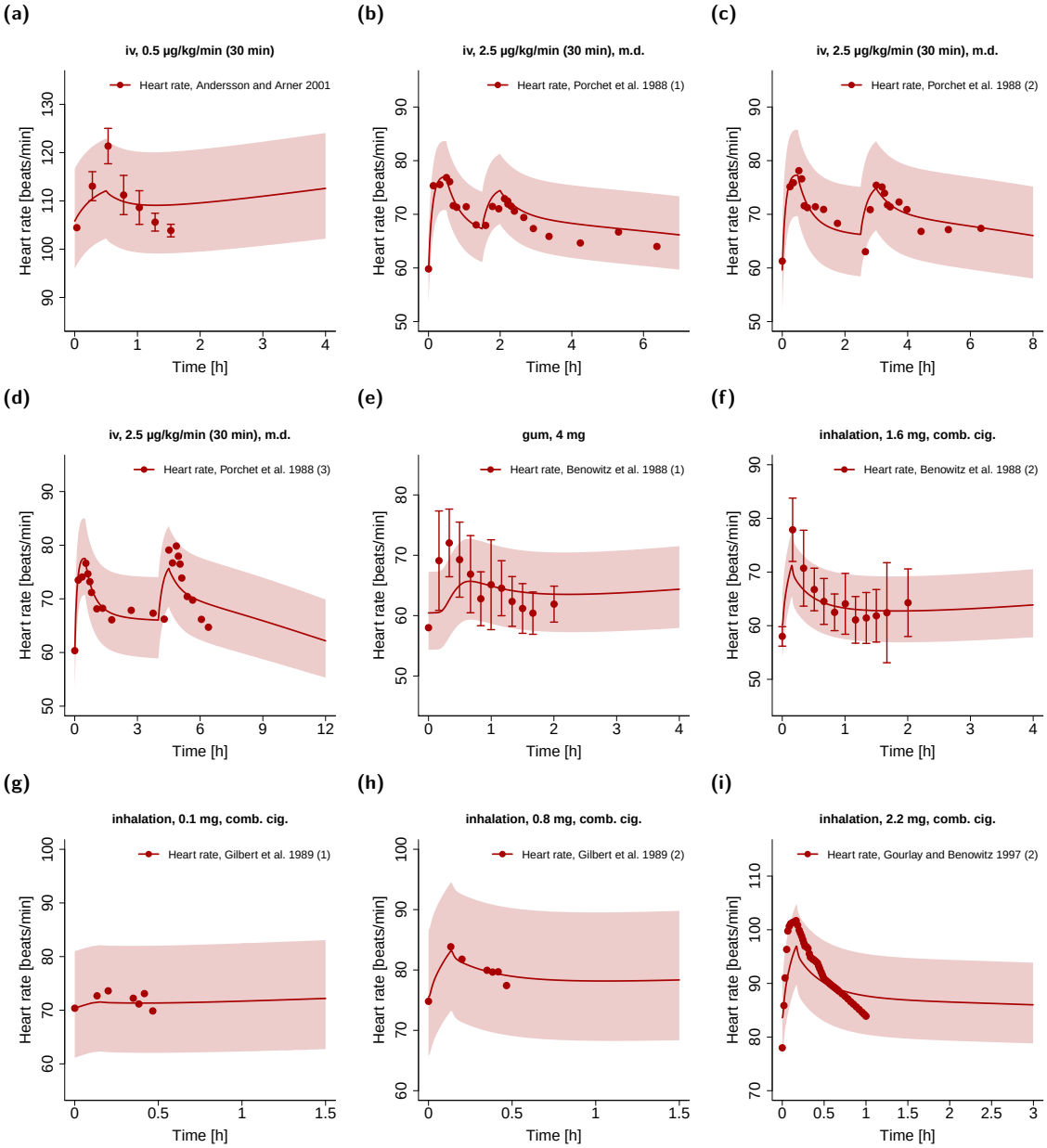

Figure S3.11.1: Heart rate profiles after intravenous, oral and pulmonary administration of nicotine. Observed data are shown as circles (•), if available ± standard deviation (SD). Population simulation (n=100) geometric means are shown as lines (–); the shaded areas represent the predicted population geometric SD. References with numbers in parentheses link to a specific observed dataset described in the study table with detailed information about dosing regimens (Tables S2.6.3 and S2.8.2). **comb. cig.**, combustible cigarette; **e-cig.**, e-cigarette; **iv**, intravenous; **m.d.**, multiple dose.

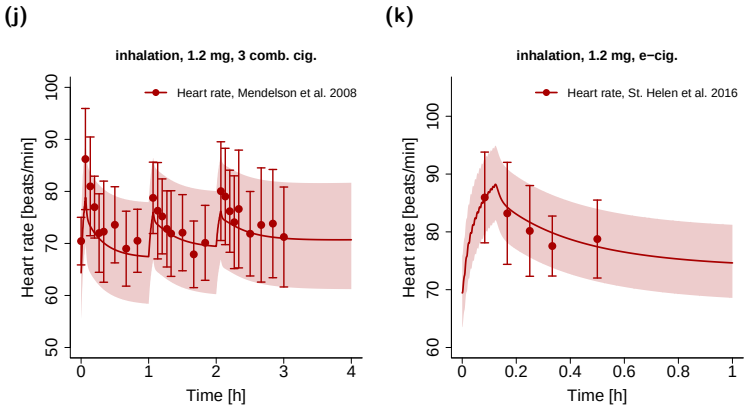

Figure S3.11.1: Heart rate profiles after intravenous, oral and pulmonary administration of nicotine. Observed data are shown as circles (•), if available ± standard deviation (SD). Population simulation (n=100) geometric means are shown as lines (–); the shaded areas represent the predicted population geometric SD. References with numbers in parentheses link to a specific observed dataset described in the study table with detailed information about dosing regimens (Tables S2.6.3 and S2.8.2). **comb. cig.**, combustible cigarette; **e-cig.**, e-cigarette; **iv**, intravenous; **m.d.**, multiple dose.(continued)

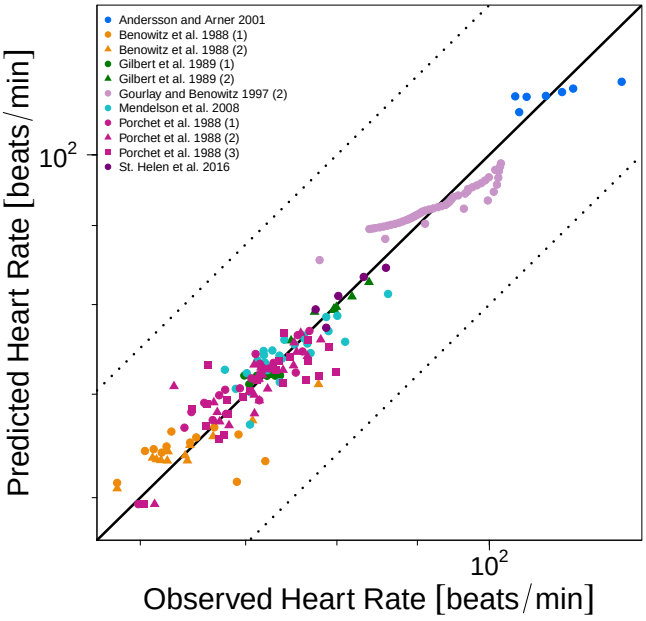

Figure S3.11.2: Predicted versus observed heart rates after nicotine intake. The black solid (——) line marks the line of identity, black dotted lines (·····) indicate 1.25-fold deviation.

3.12 Heart rate simulations

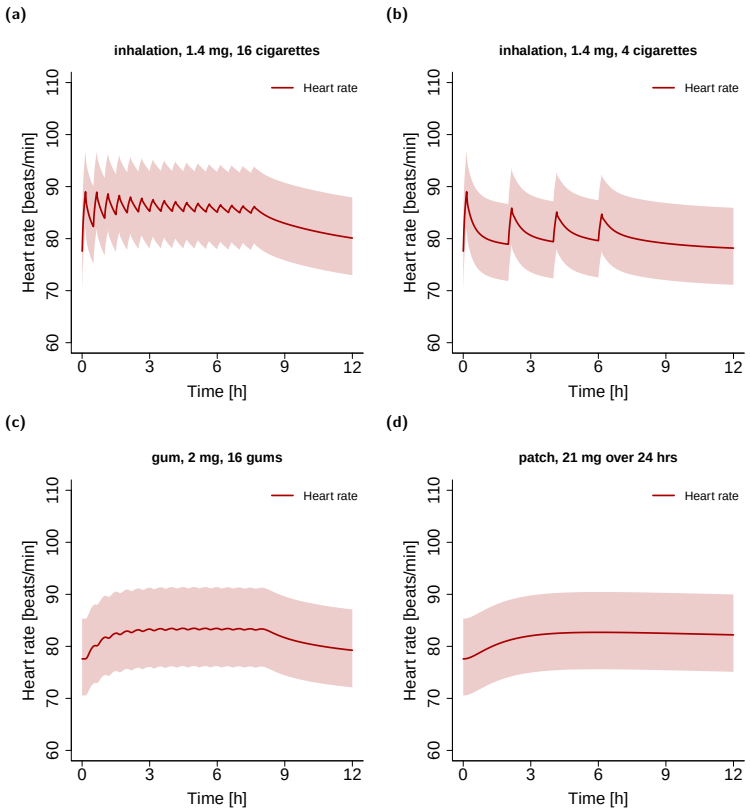

Figure S3.12.1: Simulations of heart rate profiles after pulmonary (16 cigarettes and 4 cigarettes, respectively), oral (16 gums) and transdermal (1 patch) nicotine administration. Population simulation geometric means are shown as lines (–); the shaded areas represent the predicted population geometric SD. Detailed information about dosing regimens, study populations and model input parameters is given in Tables S2.6.3, S2.8.1 and S2.8.3. **patch**, transdermal therapeutic system (nicotine patch).

References

[1] Benowitz NL, Jacob P (1994) Metabolism of nicotine to cotinine studied by a dual stable isotope method. Clinical Pharmacology & Therapeutics 56(5):483–493

[2] Hukkanen J, Jacob P, Benowitz NL (2005) Metabolism and disposition kinetics of nicotine. Pharmacological reviews 57(1):79–115

[3] Tega Y, Yamazaki Y, Akanuma Si, Kubo Y, Hosoya Ki (2018) Impact of Nicotine Transport across the Blood-Brain Barrier: Carrier-Mediated Transport of Nicotine and Interaction with Central Nervous System Drugs. Biological & pharmaceutical bulletin 41(9):1330–1336

[4] De Schepper PJ, Van Hecken A, Daenens P, Van Rossum JM (1987) Kinetics of cotinine after oral and intravenous administration to man. European Journal of Clinical Pharmacology 31(5):583–588

[5] Xu C, Rao YS, Xu B, Hoffmann E, Jones J, Sellers EM, Tyndale RF (2002) An in vivo pilot study characterizing the new CYP2A6*7, *8, and *10 alleles. Biochemical and biophysical research communications 290(1):318–324

[6] Meyer M, Schneckener S, Ludewig B, Kuepfer L, Lippert J (2012) Using Expression Data for Quantification of Active Processes in PBPK Modeling. Drug Metab Dispos 40(5):892–901

[7] Schmidt T, Samaras P, Frejno M, Gessulat S, Barnert M, Kienegger H, Krcmar H, Schlegl J, Ehrlich HC, Aiche S, Kuster B, Wilhelm M (2018) ProteomicsDB. Nucleic acids research 46(D1):D1271–D1281

[8] Yamazaki H, Inoue K, Hashimoto M, Shimada T (1999) Roles of CYP2A6 and CYP2B6 in nicotine C-oxidation by human liver microsomes. Archives of Toxicology 73(2):65–70

[9] Fukami T, Nakajima M, Yoshida R, Tsuchiya Y, Fujiki Y, Katoh M, McLeod HL, Yokoi T (2004) A novel polymorphism of human CYP2A6 gene CYP2A6*17 has an amino acid substitution (V365M) that decreases enzymatic activity in vitro and in vivo. Clinical Pharmacology and Therapeutics 76(6):519–527

[10] Hosono H, Kumondai M, Maekawa M, Yamaguchi H, Mano N, Oda A, Hirasawa N, Hiratsuka M (2017) Functional Characterization of 34 CYP2A6 Allelic Variants by Assessment of Nicotine C -Oxidation and Coumarin 7-Hydroxylation Activities. Drug Metabolism and Disposition 45(3):279–285

[11] Murphy SE, Raulinaitis V, Brown KM (2005) Nicotine 5'-oxidation and methyl oxidation by P450 2A enzymes. Drug Metabolism and Disposition 33(8):1166–1173

[12] Benowitz NL, Jacob P (1993) Nicotine and cotinine elimination pharmacokinetics in smokers and nonsmokers. Clinical pharmacology and therapeutics 53(3):316–323

[13] Rose JE, Mukhin AG, Lokitz SJ, Turkington TG, Herskovic J, Behm FM, Garg S, Garg PK (2010) Kinetics of brain nicotine accumulation in dependent and nondependent smokers assessed with PET and cigarettes containing 11C-nicotine. Proceedings of the National Academy of Sciences of the United States of America 107(11):5190–5195

[14] Morjaria Y, Irwin WJ, Barnett PX, Chan RS, Conway BR (2004) In vitro release of nicotine from chewing gum formulations. Dissolution Technologies 11(2):12–15

[15] Davies M, Pendlington RU, Page L, Roper CS, Sanders DJ, Bourner C, Pease CK, MacKay C (2011) Determining Epidermal Disposition Kinetics for Use in an Integrated Nonanimal Approach to Skin Sensitization Risk Assessment. Toxicological Sciences 119(2):308–318

[16] McCarley KD, Bunge AL (2001) Pharmacokinetic models of dermal absorption. Journal of Pharmaceutical Sciences 90(11):1699–1719

[17] Selzer D, Hahn T, Naegel A, Heisig M, Kostka K, Lehr C, Neumann D, Schaefer U, Wittum G (2013) Finite dose skin mass balance including the lateral part: Comparison between experiment, pharmacokinetic modeling and diffusion models. Journal of Controlled Release 165(2):119–128

[18] Houseman TH (1973) Studies of Cigarette Smoke Transfer Using Radioisotopically Labelled Tobacco Constituents Part II: The Transference of Radioisotopically Labelled Nicotine to Cigarette Smoke. Beitrage zur Tabakforschung International/ Contributions to Tobacco Research 7(3):142–147

[19] Hammond D, Fong GT, Cummings KM, O'Connor RJ, Giovino GA, McNeill A (2006) Cigarette yields and human exposure: A comparison of alternative testing regimens. Cancer Epidemiology Biomarkers and Prevention 15(8):1495–1501

[20] Simon DL, Iglauer A (1960) The acute effect of chewing tobacco and smoking in habitual users*. Annals of the New York Academy of Sciences 90(1):119–132

[21] Benowitz NL, Porchet H, Sheiner L, Jacob P (1988) Nicotine absorption and cardiovascular effects with smokeless tobacco use: comparison with cigarettes and nicotine gum. Clinical pharmacology and therapeutics 44(1):23–28

[22] Lott D, Lehr T, Dingemanse J, Krause A (2018) Modeling Tolerance Development for the Effect on Heart Rate of the Selective S1P1 Receptor Modulator Ponesimod. Clinical pharmacology and therapeutics 103(6):1083–1092

[23] Porchet HC, Benowitz NL, Sheiner LB (1988) Pharmacodynamic model of tolerance: application to nicotine. The Journal of pharmacology and experimental therapeutics 244(1):231–236

[24] Gill A, Hoogwerf BJ, Burger J, Bruce S, Macconell L, Yan P, Braun D, Giaconia J, Malone J (2010) Vasular Effect of exenatide on heart rate and blood pressure in subjects with type 2 diabetes randomized pilot study. Cardiovascular Diabetology 9:1–7

[25] Vandewalle G, Middleton B, Rajaratnam SMW, Stone BM, Thorleifsdottir B, Arendt J, Dijk DJ (2007) Robust circadian rhythm in heart rate and its variability: influence of exogenous melatonin and photoperiod. Journal of Sleep Research 16(2):148–155

[26] Umetani K, Singer DH, McCraty R, Atkinson M (1998) Twenty-four hour time domain heart rate variability and heart rate: Relations to age and gender over nine decades. Journal of the American College of Cardiology 31(3):593–601

[27] Andersson K, Arner P (2001) Systemic nicotine stimulates human adipose tissue lipolysis through local cholinergic and catecholaminergic receptors. International Journal of Obesity 25(8):1225–1232

[28] Benowitz NL, Chan K, Denaro CP, Jacob P (1991) Stable isotope method for studying transdermal drug absorption: the nicotine patch. Clinical pharmacology and therapeutics 50(3):286–293

[29] Benowitz NL, Jacob P, Fong I, Gupta S (1994) Nicotine metabolic profile in man: comparison of cigarette smoking and transdermal nicotine. The Journal of pharmacology and experimental therapeutics 268(1):296–303

[30] Feyerabend C, Ings RM, Russel MA (1985) Nicotine pharmacokinetics and its application to intake from smoking. British journal of clinical pharmacology 19(2):239–247

[31] Gourlay SG, Benowitz NL (1997) Arteriovenous differences in plasma concentration of nicotine and catecholamines and related cardiovascular effects after smoking, nicotine nasal spray, and intravenous nicotine. Clinical Pharmacology and Therapeutics 62(4):453–463

[32] Molander L, Hansson A, Lunell E (2001) Pharmacokinetics of nicotine in healthy elderly people. Clinical Pharmacology and Therapeutics 69(1):57–65

[33] Zevin S, Jacob P, Benowitz N (1997) Cotinine effects on nicotine metabolism. Clinical Pharmacology and Therapeutics 61(6):649–654

[34] Benowitz NL, Jacob P, Denaro C, Jenkins R (1991) Stable isotope studies of nicotine kinetics and bioavailability. Clinical pharmacology and therapeutics 49(3):270–277

[35] Benowitz NL, Dains KM, Dempsey D, Yu L, Jacob P (2010) Estimation of nicotine dose after low-level exposure using plasma and urine nicotine metabolites. Cancer Epidemiology and Prevention Biomarkers 19(5):1160–1166,

[36] Green JT, Evans BK, Rhodes J, Thomas GA, Ranshaw C, Feyerabend C, Russell MA (1999) An oral formulation of nicotine for release and absorption in the colon: its development and pharmacokinetics. British journal of clinical pharmacology 48(4):485–493

[37] Jarvis MJ, Russell MAH, Benowitz NL, Feyerabend C (1988) Elimination of cotinine from body fluids: Implications for noninvasive measurement of tobacco smoke exposure. American Journal of Public Health 78(6):696–698

[38] Choi JH, Dresler CM, Norton MR, Strahs KR (2003) Pharmacokinetics of a nicotine polacrilex lozenge. Nicotine & Tobacco Research 5(5):635–644,

[39] Dautzenberg B, Nides M, Kienzler JL, Callens A (2007) Pharmacokinetics, safety and efficacy from randomized controlled trials of 1 and 2 mg nicotine bitartrate lozenges (Nicotinell). BMC clinical pharmacology 7:11

[40] Du D (2018) A Single-Dose, Crossover-Design Bioequivalence Study Comparing Two Nicotine Gum Formulations in Healthy Subjects. Advances in therapy 35(8):1169–1180

[41] Hansson A, Rasmussen T, Kraiczi H (2017) Single-Dose and Multiple-Dose Pharmacokinetics of Nicotine 6 mg Gum. Nicotine & Tobacco Research 19(4):477–483

[42] Bannon YB, Corish J, Corrigan OI, Devane JG, Kavanagh M, Mulligan S (1989) Transdermal delivery of nicotine in normal human volunteers: a single dose and multiple dose study. European journal of clinical pharmacology 37(3):285–290

[43] Fant RV, Henningfield JE, Shiffman S, Strahs KR, Reitberg DP (2000) A pharmacokinetic crossover study to compare the absorption characteristics of three transdermal nicotine patches. Pharmacology, biochemistry, and behavior 67(3):479–482

[44] Gupta SK, Benowitz NL, Jacob P, Rolf CN, Gorsline J (1993) Bioavailability and absorption kinetics of nicotine following application of a transdermal system. British journal of clinical pharmacology 36(3):221–227

[45] Armitage AK, Dollery CT, George CF, Houseman TH, Lewis PJ, Turner DM (1975) Absorption and metabolism of nicotine from cigarettes. British medical journal 4(5992):313–316

[46] Benowitz NL, Kuyt F, Jacob P (1982) Circadian blood nicotine concentrations during cigarette smoking. Clinical pharmacology and therapeutics 32(6):758–764

[47] Fearon IM, Eldridge A, Gale N, Shepperd CJ, McEwan M, Camacho OM, Nides M, McAdam K, Proctor CJ (2017) E-cigarette Nicotine Delivery: Data and Learnings from Pharmacokinetic Studies. American journal of health behavior 41(1):16–32

[48] Mendelson JH, Goletiani N, Sholar MB, Siegel AJ, Mello NK (2008) Effects of smoking successive low- and high-nicotine cigarettes on hypothalamic-pituitary-adrenal axis hormones and mood in men. Neuropsychopharmacology 33(4):749–760

[49] Russell MA, Jarvis MJ, Feyerabend C, Fernö O (1983) Nasal nicotine solution: a potential aid to giving up smoking? British medical journal (Clinical research ed) 286(6366):683–684

[50] St Helen G, Havel C, Dempsey DA, Jacob III P, Benowitz NL (2016) Nicotine delivery, retention and pharmacokinetics from various electronic cigarettes. Addiction 111(3):535–544,

[51] St Helen G, Nardone N, Addo N, Dempsey D, Havel C, Jacob P, Benowitz N (in press 2019) Differences in nicotine intake and effects from electronic and combustible cigarettes among dual users. Addiction

[52] Curvall M, Elwin CE, Kazemi-Vala E, Warholm C, Enzell CR (1990) The pharmacokinetics of cotinine in plasma and saliva from non-smoking healthy volunteers. European Journal of Clinical Pharmacology 38(3):281–287

[53] Gilbert DG, Robinson JH, Chamberlin CL, Spielberger CD (1989) Effects of smoking/nicotine on anxiety, heart rate, and lateralization of EEG during a stressful movie. Psychophysiology 26(3):311–320

[54] Wishart DS, Knox C, Guo AC, Shrivastava S, Hassanali M, Stothard P, Chang Z, Woolsey J (2006) DrugBank: a comprehensive resource for in silico drug discovery and exploration. Nucleic Acids Research 34(Supplement 1):D668–D672,

[55] Nielsen HM, Rassing MR (2002) Nicotine permeability across the buccal TR146 cell culture model and porcine buccal mucosa in vitro: Effect of pH and concentration. European Journal of Pharmaceutical Sciences 16(3):151–157

[56] Alharbi O, Xu Y, Goodacre R (2014) Simultaneous multiplexed quantification of nicotine and its metabolites using surface enhanced Raman scattering. Analyst 139(19):4820–4827

[57] Zissimos AM, Abraham MH, Barker MC, Box KJ, Tam KY (2002) Calculation of Abraham descriptors from solvent–water partition coefficients in four different systems; evaluation of different methods of calculation. Journal of the Chemical Society, Perkin Transactions 2 pp 470–477

[58] Svensson CK (1987) Clinical Pharmacokinetics of Nicotine. Clinical Pharmacokinetics 12(1):30–40

[59] Benowitz NL, Kuyt F, Jacob P, Jones RT, Osman AL (1983) Cotinine disposition and effects. Clinical pharmacology and therapeutics 34(5):604–611

[60] Dicke KE, Skrlin SM, Murphy SE (2005) Nicotine and 4-(methylnitrosamino)-1-(3-pyridyl)-butanone metabolism by cytochrome P450 2B6. Drug metabolism and disposition: the biological fate of chemicals 33(12):1760–1764

[61] Open Systems Pharmacology Suite Community (2018) Open Systems Pharmacology Suite Manual

[62] Rodgers T, Rowland M (2006) Physiologically based pharmacokinetic modelling 2: Predicting the tissue distribution of acids, very weak bases, neutrals and zwitterions. Journal of Pharmaceutical Sciences 95(6):1238 – 1257

[63] Rodgers T, Leahy D, Rowland M (2005) Physiologically based pharmacokinetic modeling 1: Predicting the tissue distribution of moderate-to-strong bases. Journal of Pharmaceutical Sciences 94(6):1259 – 1276

[64] Rodgers T, Rowland M (2007) Mechanistic approaches to volume of distribution predictions: understanding the processes. Pharmaceutical research 24(5):918–933

[65] Rodrigues AD (1999) Integrated cytochrome P450 reaction phenotyping: attempting to bridge the gap between cDNA-expressed cytochromes P450 and native human liver microsomes. Biochemical pharmacology 57(5):465–480

[66] Nishimura M, Yaguti H, Yoshitsugu H, Naito S, Satoh T (2003) Tissue distribution of mRNA expression of human cytochrome P450 isoforms assessed by high-sensitivity real-time reverse transcription PCR. Yakugaku zasshi : Journal of the Pharmaceutical Society of Japan 123(5):369–75

[67] Valentin J (2002) Basic anatomical and physiological data for use in radiological protection: reference values. Annals of the ICRP 32(3-4):1–277

[68] Edginton AN, Schmitt W, Willmann S (2006) Development and evaluation of a generic physiologically based pharmacokinetic model for children. Clinical pharmacokinetics 45(10):1013–1034